Uncertainty in Macroeconomic Models

Dissertation

Tobias Kranz

University of Trier, Faculty IV

Submission: November 15, 2019

Disputation: January 16, 2020

Most forecasters are . . .
going round in circles while . . .
chasing their own tails.

— ORIGIN UNCERTAIN

Preface

This doctoral thesis is cumulative, containing two published peer-reviewed articles, both in the same journal, *Review of Economics*. The unpublished third paper was written as a co-authorship with Marc-Patrick Adolph, him being responsible for the calibration part. In these three articles, all topics are interlinked and form a reasonable structure, which will be explained in detail.

The main work progress was made in the years 2017 to 2019 at the University of Trier, simultaneously working as a research and teaching assistant at the chair of Empirical Economics (Prof. Matthias Neuenkirch). In 2018, an additional article, together with Hamza Bennani and Matthias Neuenkirch, was published in the *Journal of Macroeconomics*. Thematically too different, it is not included herein.

For the dissertation, ideas were developed and executed on my own and subsequently discussed with the supervisors. Ultimately, my doctorate studies have been accomplished under excellent working conditions.

Trier, November 2019

Table of Contents

Motivation

Macroeconomists are interested in economic factors on a large scale, and therefore they study the interactions between labor, capital, goods, and money from a country-level point of view. Since the early circular flow diagrams, which were developed by Richard Cantillon around 1730, economists have systematically tried to analyze the links between these economic aggregates. His work was partly based on John Locke's quantity theory of money, but Cantillon, in turn, influenced François Quesnay, who was famous for his *Tableau Économique*, published in 1758. Early work in macroeconomics started out by studying concrete market prices and quantities. However, in his *Essai sur la Nature du Commerce in Général*, Cantillon also provided the foundations for a theory of uncertainty.[1] Almost 200 years later, economists like John Maynard Keynes and Frank Knight revisited these same thoughts.

Generally in economic research, the term *uncertainty* occurs in three different contexts: model input, model output, and unknown probabilities. First, the usage of uncertainty as a *model input* is reflected in the model's projection, i.e., the point estimate of the output. In principle, when uncertainty is high, the estimation should be more conservative. In the three articles that follow, this is the single view we consider. Nevertheless, insight can be gained by exploring the other two contexts. Second, as a complementary approach to the first utilization, uncertainty concerning the *model's output* is reflected in confidence intervals around the point estimates. Of course, risky statistical assumptions are sometimes needed to end up with plain probabilities. In this type of work, in order to provide a variety of certain outcomes and to further compare these results, model assumptions are slightly adjusted and parameter values are widely changed. Third, Knightian uncertainty, in contrast to quantifiable risk, means there are *unknown probabilities* assigned to possible events. Surely, this is the vaguest concept, at best, placing the likelihood of events in a certain order.

Uncertainty in macroeconomic models is an issue that was not being considered mathematically when formal modeling was in its infancy. Keynes extensively described qualitative relationships, while Joseph A. Schumpeter, in the later chapters of his last book *History of Economic Analysis*, collected and discussed the macroeconomic formulas, which are still being taught in both introductory and intermediate

[1] Cantillon (1755) addresses this topic inter alia in chapter 13 ("The circulation and exchange of goods, as well as the production of goods and of merchandise, are carried out in Europe by entrepreneurs in conditions of risk.") He writes: "Master craftsmen [...] live under [...] uncertainty since their customers may leave them from one day to the next. Self-employed entrepreneurs in the arts and science [...] practice under the same uncertainty."

economics courses in the 21st century.[2] Back in the first half of the 20th century, a major breakthrough occurred when statements were formulated about (i) the qualitative relationship (positive or negative) between two economic factors, and (ii) how strong this relation is. For example, when people receive more income, they consume more. And, as a next step, how much more will they consume with the additional income? It is conceivable that people would consume, say, half of the income gained, while the rest could be used to increase their savings. This was one of the questions, Keynes was interest in.

But when uncertainty comes into play, how are these stated relationships affected? In 1738, Daniel Bernoulli published an article explaining, for the first time, why an expected (subjective) outcome under uncertainty should be lower.[3] In his work, he already wrote about the principle of non-linear utility. Translated to macroeconomics, this can also explain precautionary savings. Generally speaking, the prospect of a variable outcome diminishes the subjective future outcome, which can be illustrated by a few brief examples in modern times. First, in Mario Draghi's "whatever it takes"-speech about the Euro in 2012, he tried to make the situation more reliable or certain. Second, in cases of uncertainty about credit bubbles, macroprudential regulation has to come into play or has to be more rigorous. As a contrary approach, given the variability, there is the effect that one's action have to be more severe when considering lower outcomes. Therefore, third, in turbulent recessionary periods, the central bank's main financing rate should be lower when considering uncertainty. Forth, as a non-economic example, doubts about the reliability of temperature measures—concerning climate change—require us to take this issue even more seriously when accounting for the effect of uncertainty. All this scales down to our inherent risk-aversion, at least at the macro level, i.e., for the society as a whole.

In the modeling context, non-linearities and uncertainty go hand in hand. In fact, the utility function's curvature determines the degree of risk-aversion. This concept is exploited in the first article of this thesis, which incorporates uncertainty into a small-scale DSGE model. More specifically, this is done by a second-order approximation, while carrying out the derivation in great detail and carefully discussing the more formal aspects. Moreover, the consequences of this method are discussed when calibrating the equilibrium condition. The second article of the thesis considers the es-

[2]Keynes (1936, 249) starts chapter 20 by "Those who (rightly) dislike algebra will lose little by omitting the first section of this chapter." Schumpeter (1954, 1184) writes in the last paragraph of his posthumously published (unfinished) manuscripts: "Keynes gave a mighty impulse [...]—almost all work in macrodynamics now starts from a 'dynamized' form of his model."

[3]A hundred years before the first widely recognized contributions to the field of microeconomics, Bernoulli (1738) put forth the *expected utility hypothesis*.

sential model part of the first paper and focuses on the (forward-looking) data needed to meet the model's requirements. A large number of uncertainty measures are utilized to explain a possible approximation bias. The last article keeps to the same topic but uses statistical distributions instead of actual data. In addition, theoretical (model) and calibrated (data) parameters are used to produce more general statements. In this way, several relationships are revealed with regard to a biased interpretation of this class of models. In the following paragraphs, the respective approaches are explained in more detail and also how they build on each other. Consequently, this dissertation, consisting of three research papers, is divided in part one, two, and three.

Part 1: Quadratic Approximation

The first article takes up the method of higher-order approximation and derives a New Keynesian model (as part of the DSGE family) in full detail. In general, when linearizing the derived equations, a loss of information will be partly compensated by an easier interpretation. However, from the start, the basic concepts and assumptions are carefully explained with a focus on the parameters. Thus, the article is mainly theoretical but uses numerical simulations to compare the purely linearized model with the one containing uncertainty (i.e., variance) as a model variable. The calibration is done following an extensive literature review to quantify possible values or ranges for all parameters. These are used to identify the equilibrium condition and, in turn, to obtain the differences when comparing the models. Summarizing the results, nominal interest rates are generally lower, taking uncertainty into account. The intuition behind this result is relatively simple. The concavity of the aggregate utility function ensures risk-averse households. The degree is determined by the elasticity of intertemporal substitution, which plays a key role throughout the entire thesis. In times of great uncertainty, households need compensation for the resulting disutility. In this simple New Keynesian model, the nominal interest takes on this role.

Part 2: Internal and External Uncertainty

Part two narrows in on deriving the forward-looking IS curve (as part of the New Keynesian model), taking it to a different direction by avoiding any Taylor expansion. Furthermore, any changes that are made to the originally-derived model equations are labeled *approximation bias*. In this context, this occurs by extracting parameters from the expectation values (Jensen's inequality) as it is common practice in the literature. In order to be consistent within the respective articles, the derivation of the Euler equation is very similar to that in the first article. However, there are some differences. The discount parameter is now time-varying, allowing for the conversion into a non-constant real interest rate. The reason for this is to identify the Euler equation with possibly no (external) parameters but using interest rate data (real and nominal) and forward-looking growth rates (Consensus Forecasts surveys) for the macroeconomic indicators. At a later point, also the second parameter—the inverse of the elasticity of intertemporal substitution—is potentially time-varying to allow for a structural break. This parameter is determined by an own, maximum likelihood-type approach. For the econometrics section, the difference of two versions, one with the mean forecasts and one with the individual forecasts—used as a distribution to avoid any approximation—is regressed on a variety of internal and external uncertainty measures. It is interesting that some of these measures can be verified to have a significant impact on the *approximation bias*. However, when using data on major economies with admittedly small variation, the bias amounts to only ten basis points.

Part 3: The Extent of Jensen's Inequality

Finally, the third article focuses on the same issue, asking the question: How large (in basis points) can this difference become when converting the influencing factors into parameters and testing a wide range of values—similar to the first article. This is a more comprehensive approach to derive general results. The model setting is slightly altered such that the resulting difference can be interpreted as growth rate differences. By assuming log-normally distributed growth rates, an analytical solution is derived, which describes the *approximation bias* depending on the second moment (i.e., uncertainty) and the function's curvature (i.e., the elasticity of intertemporal substitution). To control for the variability, instead of inserting potential data points, the Consensus Forecasts survey is utilized to calibrate a distribution of growth rates, further used for Monte Carlo experiments. Augmenting the model by increasing the number of variables gives an idea of how the bias reproduces in large-scale models. Finally, to close the connection to part one, the last article is placed in the context of DSGE models, explaining their importance after the 2007–2008 financial crisis and their future applications.

The central idea is that the *approximation* of a model's equations suppresses uncertainty as an input and, therefore, biases the results. Going beyond the content of this thesis, this connects to the inherent question of whether "simple" macroeconomic models can predict crisis scenarios. Additionally, using forward-looking data, there are two possible problems: forecasts being mutually harmonized and recessionary events being underrepresented. Therefore, economic crises are difficult to predict since the forecasts are designed in a way that, for example, the possibility of a stock market crash is not reflected in (diminished) expected growth rates.

Altogether macroeconomists build macroeconomic models, they teach and talk about these, but they also bring attention to the possible caveats these models contain, showing that they are probably right around the (curved) corner.

Notational Remarks

(1) The original titles of the articles are too long as section names. These are now in quotes at the beginning of each article directly under the new section title.

(2) The personal pronoun "We" (instead of "I") is used throughout the articles for consistency reasons since the third article is a collaboration and as a matter of taste.

(3) "$\log(x)$" always denotes the natural logarithm. "$]0,1[$" always denotes an open interval (instead of "$(0,1)$").

(4) For the conditional expectation, either $\mathrm{E}_t x_{t+1}$ or $\mathrm{E}_t[x_{t+1}]$ is used. The latter case arises when a better overview is needed.

(5) Only in the second article, "Std.Dev." is used in this abbreviated form since it takes an essential role and is frequently mentioned.

(6) On a few occasions, defined acronyms are spelled out to underpin the importance at this point.

(7) Some acronyms are defined more than once since every article is considered to be independent.

(8) The assignment of symbols is adjusted throughout the dissertation to minimize the parallel usage of the same letter (e.g., i can be an index or the nominal interest rate). Even then, the distinction is mostly ensured by subindices.

(9) **References:** To refer to an online-source, the DOI (Digital Object Identifier) is preferred since it uniquely assigns the respective piece of literature to a string of numbers. This works analogously to the ISBN. When this not possible (in case of a corrupted number or an older book), JSTOR or Google Books is used. Other than that, there are only a few exceptions (e.g., referring to the publisher's website).

1 Quadratic Approximation

"Calibrating the Equilibrium Condition of a New Keynesian Model with Uncertainty"

Abstract

This paper presents a theoretical analysis of the simulated impact of uncertainty in a New Keynesian model. In order to incorporate uncertainty, the basic three-equation framework is modified by higher-order approximation resulting in a non-linear (dynamic) IS curve. Using impulse response analyses to examine the behavior of the model after a cost shock, we find interest rates in the version with uncertainty to be lower in contrast to the case under certainty.

1.1 Introduction

For the last 20 years, the New Keynesian framework has been one of the workhorses of macroeconomic analysis. The framework combines market frictions with optimization behavior by the model's agents, and, in its original construction, assumes perfect foresight. However, the treatment of uncertainty is an important issue since its effect can fundamentally change the prediction of these models.

This paper examines possible effects of uncertainty in a simple New Keynesian model (NKM) augmented with stochastic terms and non-linearity that enters the model through a second-order Taylor approximation regarding the IS curve. In line with the literature (see, among others, the textbooks by Galí 2015 and Walsh 2010), cost shock and demand shock are utilized for the New Keynesian Phillips curve (NKPC) and the forward-looking IS curve, respectively. Schmitt-Grohé and Uribe (2004) use second-order approximation in neoclassical growth models. Bauer and Neuenkirch (2017) were the first to use such a framework in the context of a NKM and found empirical evidence that central banks, indeed, take the resulting uncertainty into account. Moreover, their paper provides strong arguments that linear macroeconomic models found in monetary policy literature are less than optimal (see also Boneva et al 2016 and Fernández-Villaverde et al 2011). The main contribution this paper offers is the analysis of how the economy evolves after cost shocks, and the extent to which persistence plays a role.

In order to extend the NKM, we include a quadratic approximation in all derived equations. First, in the analytical part, demand and supply side (including monopolistic competition and price rigidity), where firms use second-order approximation when setting the prices, yields the NKPC. Second, the forward-looking IS curve with uncertainty follows from the households' Euler equation. This method differs fundamentally from standard approaches. Finally, to close the model, a (standard) targeting rule is derived by the central bank's optimization under discretion.

After adding AR(1) processes to the derived equations, conditional expectations and variances can be substituted by solving forward. Next, parameter values are selected for the resulting equilibrium condition (or instrument rule) with the focus on persistence and shock strength. A numerical simulation analyzes differences to the basic model. Finally, to examine the adjustment of macro variables in the medium term, impulse responses are carried out and contrasted with the linear counterpart.[1] In the same vein, but without an explicit derivation of the uncertainty, De Paoli and Zabczyk (2013) compare linear and non-linear models.

The remainder of this paper is organized as follows. Section 1.2 derives a basic version of the NKM augmented with a quadratic IS curve. Section 1.3 expands this model with shocks and discusses the resulting equilibrium condition. Section 1.4 carries out the numerical simulation of both the static equilibrium condition and the dynamic view of an impulse response analysis. Section 1.5 concludes.

[1] To keep the framework easily understandable, government, investments, money supply, and labor markets are omitted. Consequently, neither money holdings nor working hours (or leisure time) will enter the households' utility function.

1.2 New Keynesian Model with Uncertainty

1.2.1 New Keynesian Phillips Curve

For deriving the NKPC, two optimization problems involving private households and firms are employed, leading to aggregated demand and supply. Furthermore, price rigidity is modeled using the method introduced by Calvo (1983).[2] From the Calvo Pricing section on, the time index t is used because it is needed to make a distinction between the different periods.

Demand and Supply Side

Consumers

On the demand side, the representative consumer can choose from a variety of goods C_φ which results in an aggregate consumption of C. Usually, the CES function is used to model monopolistic competition, one of the two market frictions incorporated into the NKPC:[3]

$$C = \left(\int_0^1 C_\varphi^{\frac{\varepsilon-1}{\varepsilon}} \, d\varphi \right)^{\frac{\varepsilon}{\varepsilon-1}}. \tag{1.1}$$

Here, $\varphi \in [0,1]$ can be viewed as a continuum of firms from 0 to 100%. The exponent is a measure for the substitutability between the goods C_φ, where ε represents the elasticity of substitution.

A Hicksian-like optimization helps to solve for the demand curve by means of the Lagrangian function:

$$\mathscr{L}(C_\varphi, \lambda) = \int_0^1 P_\varphi \cdot C_\varphi \, d\varphi - \lambda \left(\left(\int_0^1 C_\varphi^{\frac{\varepsilon-1}{\varepsilon}} \, d\varphi \right)^{\frac{\varepsilon}{\varepsilon-1}} - C \right). \tag{1.2}$$

Since firms have pricing power, the representative consumer takes prices P_φ as given. Minimizing expenditures $\int P_\varphi C_\varphi$ with the constraint of a certain consumption level C requires the following first-order conditions:[4]

$$\frac{\partial \mathscr{L}}{\partial C_\tau} = P_\tau - \lambda C_\tau^{-\frac{1}{\varepsilon}} \left(\int_0^1 C_\varphi^{\frac{\varepsilon-1}{\varepsilon}} \, d\varphi \right)^{\frac{1}{\varepsilon-1}} = 0. \tag{1.3}$$

[2]This paper focuses on the standard approach. For non-linear versions of the Phillips curve see the articles by Collard and Juillard (2001), Dolado et al (2005), and Schaling (2004).

[3]Dixit and Stiglitz (1977) developed this approach. Although they used a discrete sum and no integral, they received the same results.

[4]Note that τ denotes a continuum of derivatives.

Differentiating with respect to λ provides the constraint, Eq.(1.1). Rearranging condition (1.3) and defining $\lambda \equiv P$ as the aggregated price level yields

$$C_\tau = \left(\frac{P}{P_\tau}\right)^{\varepsilon} C, \tag{1.4}$$

the demand for good τ.[5] The aggregated price level can be described by substituting this in Eq.(1.1). Rearranging the formula gives us:

$$P = \left(\int_0^1 P_\varphi^{1-\varepsilon}\, d\varphi\right)^{\frac{1}{1-\varepsilon}}. \tag{1.5}$$

The lack of investment and governmental spendings in this model leads to $Y_\tau = C_\tau$. Each firms' production Y_τ will be consumed completely by private households and hence $Y = C$.

Firms

Because any single firm is too small to directly influence other prices or productions, each firm takes the aggregated demand function and the aggregated price level P as given. It chooses its own price P_τ and faces the typical (real) profit maximization problem

$$\max_{P_\tau, Y_\tau} \left\{\frac{P_\tau Y_\tau}{P} - K(Y_\tau)\right\} \tag{1.6}$$

with the cost function $K(.)$. Using Eq.(1.4), the first-order condition is straightforward and leads to

$$P_\tau^* = \left(\frac{\varepsilon}{\varepsilon - 1}\right) K'(Y_\tau) \cdot P, \tag{1.7}$$

an important result that states that the optimal price P_τ^* equals the nominal marginal costs and a mark-up bigger than one for all $\varepsilon > 1$.[6] Log-linearizing and using the fact that the long-run marginal costs equal the multiplicative inverse of the firms' mark-up ($K_{ss} = 1 - \varepsilon^{-1}$) yields

$$p_\tau^* - p = \psi y_\tau, \tag{1.8}$$

[5]When the consumption constraint is relaxed by one unit, total consumption expenditures (see Galí 2015, 53) will increase to $(C+1)P = CP + P$, where P is the amount by which the optimum will change. This is exactly the information the Lagrange multiplier λ contains. See Appendix A.1 for the missing steps in this paragraph.

[6]See Appendix A.2 for the missing steps.

where ψ is a parameter for the long-run cost elasticity and, therefore, log deviations of marginal costs from their long-run trend are assumed to be linear.[7] Inserting the log-version of Eq.(1.4) gives

$$p_\tau^* - p = \left(\frac{\psi}{1+\psi\varepsilon}\right) y. \tag{1.9}$$

Making use of $\widehat{y}$, the GDP growth rate around the steady state, as an approximation for y and using $\chi_\psi \in [0,1[$ as a summarizing parameter, Eq.(1.9) yields

$$p_\tau^* - p = \chi_\psi \widehat{y}, \tag{1.10}$$

a description of the steady state output growth rate, depending on price level growth and microeconomic behavior. The next section introduces a non-optimal price setting scheme which replicates the actual observed economic patterns.[8]

Calvo Pricing

Nominal rigidities, the second market friction in the basic NKM, are implemented through the assumption that the firms' infrequent price adjustment follows an exogenous Poisson process.[9] This implies that all firms have a constant probability (ϕ) of being unable to update their price in each period with $\phi \in [0,1[$ (i.e., $\phi = 0$ in the absence of price rigidity). It is crucial that price setters do not know how long the nominal price will remain in place. Only the expected value is known due to probabilities that are all equal and constant for all firms and periods. This implies a probability of ϕ^j for having today's same price in j periods, so the average expected duration between price changes will be $1/(1-\phi)$.

From this point forward, the time index t will be used because more than one period is being considered. Simultaneously, the firm index τ is no longer important since it is sufficient to calculate with a share of firms ϕ (or $1-\phi$). Hence, $p_\tau^* \equiv p_t^*$ and $p \equiv p_t$. When q_t is the price that firms set in period t (provided they are able to do so), the following applies:

$$q_t = \frac{p_t - \phi p_{t-1}}{1-\phi} \quad \Rightarrow \quad \mathrm{E}_t q_{t+1} = \frac{\mathrm{E}_t p_{t+1} - \phi p_t}{1-\phi}. \tag{1.11}$$

[7]Note that lower case letters denote the log value of a variable in capital letters minus their long-run log value, e.g., $y = \log(Y) - \log(Y_{ss})$. See Appendix A.3 for the missing steps.

[8]See the survey by Taylor (1999), that came to abundant evidence. See also Galí (2015, 7–8) for a literature overview.

[9]Calvo (1983) originally wrote his article in continuous time. However, using discrete periods immensely helps the clearness and is more realistic with regard to how firms actually operate. Moreover, Calvo (1983, 396–397) shows the equivalence of both approaches.

Because firms act on the probability of not being able to adjust prices in future periods, they attempt to establish a price q_t that is not necessarily the optimal price p_t^*, derived in the previous section. Also, in the presence of price rigidities, $q_t \neq p_t^*$ generally holds.

To reveal the mechanics behind the staggered price setting, it is convenient to verbally treat p_t and q_t as level variables. Strictly speaking, firms set price growth paths in the following optimization problem rather than maximizing a discounted profit as the difference between revenue and costs.[10] In the following, the optimal reset price, determined by the discounted sum of future profits, is derived through a quadratic approximation of the per-period deviation from maximum-possible profit with $\varrho \in [0,1[$, the discount factor over an infinite planning horizon. Therefore, firms minimize their loss function, the discounted deviations from p_t^* over all t:

$$\min_{q_t} \left\{ \mathrm{E}_t \left[k \sum_{j=0}^{\infty} \varrho^j \phi^j \left(q_t - p_{t+j}^* \right)^2 \right] \right\}. \tag{1.12}$$

The parameter $k > 0$ enters the loss function multiplicatively and indicates all exogenous factors that will influence the costs of not setting the optimal price in each period.[11] The first-order condition is

$$\frac{\partial}{\partial q_t} = \mathrm{E}_t \left[2k \sum_{j=0}^{\infty} (\varrho\phi)^j (q_t - p_{t+j}^*) \right] = 0. \tag{1.13}$$

After rearranging and expressing q through p with Eq.(1.11), it follows that

$$p_t - \phi p_{t-1} = \varrho\phi(\mathrm{E}_t p_{t+1} - \phi p_t) + (1-\phi)(1-\varrho\phi)p_t^* \tag{1.14}$$

only contains parameters and variants of the variable p.[12] Expressing p through π,[13] as well as isolating $(p_t^* - p_t)$ and replacing it with the result in Eq.(1.10), gives

$$\pi_t = \varrho \mathrm{E}_t \pi_{t+1} + \frac{\chi_\psi (1-\phi)(1-\varrho\phi)}{\phi} \widehat{y_t}. \tag{1.15}$$

[10]See Walsh (2010, 241–242) for the use of level variables in Calvo pricing.

[11]Note that it can also come up as an additive term or any other positive monotonic transformation and does not alter the results.

[12]See Appendix A.4 for the missing steps.

[13]
$$p_t - p_{t-1} = \log P_t - \log P_{ss} - (\log P_{t-1} - \log P_{ss}) = \log\left(\frac{P_t}{P_{t-1}}\right) = \log(1+\pi_t) \approx \pi_t.$$

In a final step, a summarizing parameter $\kappa > 0$ for all parameters, multiplied with $\widehat{y_t}$, will be defined. This yields the NKPC:[14]

$$\pi_t = \varrho \mathrm{E}_t \pi_{t+1} + \kappa \widehat{y_t}. \tag{1.16}$$

Both the expected inflation rate $\mathrm{E}_t \pi_{t+1}$ and the GDP growth rate around the steady state $\widehat{y_t}$ (or output gap) have a positive impact on π_t since $\varrho, \kappa > 0$. Moreover, the slope of the NKPC (κ), depends on all four parameters ($\varrho, \psi, \varepsilon$, and ϕ) of this section.[15]

1.2.2 The Quadratic IS Curve

'The objective' is to derive an Euler equation via maximizing utility with a dynamic budget constraint. Initially, it is not necessary to formulate an explicit utility function. On the contrary, the general marginal utility provides a better insight into the intertemporal mechanics. The only specific assumption is not taking money, working hours or any other possible utility-gainer into consideration. The utility function solely relies on consumption, thus, households maximize their intertemporal discounted utility

$$\max_{C_t} \left\{ \mathrm{E}_t \left[\sum_{s=t}^{\infty} \varrho^{s-t} U(C_s) \right] \right\}. \tag{1.17}$$

Taking into account an intertemporal budget constraint with prices and the interest rate i_t, the maximization problem leads to the Euler equation

$$U'(C_t) = \varrho \cdot (1 + i_t) \cdot \mathrm{E}_t \left[\frac{P_t \cdot U'(C_{t+1})}{P_{t+1}} \right], \tag{1.18}$$

revealing the intertemporal relationship of the marginal utility out of consumption.[16] Marginal utility in period t equals the counterpart in $t+1$, corrected by discount factor, nominal interest rate, and the ratio of current and expected future price level. Assuming i_t rises, marginal utility in t would also rise relative to period $t+1$. Given the diminishing marginal utility property and, therefore, concavity, consumption will be higher in the future.[17]

[14]In contrast to the IS curve discussed in the next section, the NKPC is still linear. Simulations in MATLAB show that the effect of a non-linear NKPC is rather small. That is why our focus on uncertainty relies on the IS curve.

[15]Depending on the exact model, the slope of the NKPC can have a slightly different meaning, e.g., Walsh (2010, 336) uses a measure for the firm's real marginal costs instead of the output gap.

[16]See Appendix A.5 for the missing steps.

[17]Note that present consumption could also increase because of the income effect.

One convenient formulation for such a function is $U(C_t) = (1-\gamma)^{-1} \cdot (C_t^{1-\gamma} - 1)$ with $\gamma > 0$ implying $1/\gamma$ as the intertemporal elasticity of substitution (EIS). Substituting this in the Euler equation gives

$$Y_t^{-\gamma} = \varrho \cdot (1 + i_t) \cdot \mathrm{E}_t \left[\frac{P_t \cdot Y_{t+1}^{-\gamma}}{P_{t+1}} \right], \tag{1.19}$$

when recalling the market clearing condition $Y = C$. The long-run real interest rate r enters the equation through ϱ since it equals $1/\varrho - 1$.[18]

Quadratic Approximation

Eq.(1.19) can be prepared for quadratic approximation by inserting $1/(1+r)$ for ϱ, treating t-measurable variables as constants for the conditional expectation, rearranging, and taking logs:

$$\log\left(\frac{1+r}{1+i_t}\right) = \log \mathrm{E}_t \left[\left(\frac{Y_{t+1}}{Y_t} \right)^{-\gamma} \right] - \log \mathrm{E}_t \left[\frac{P_{t+1}}{P_t} \right]. \tag{1.20}$$

Ignoring Jensen's inequality is equivalent to first-order Taylor series expansions of both logarithm and exponential function. Furthermore, the right side of Eq.(1.20) can be written as

$$\gtrapprox \mathrm{E}_t \left[\log\left(\left(\frac{Y_{t+1}}{Y_t} \right)^{-\gamma} \right) \right] - \mathrm{E}_t \left[\log\left(\frac{P_{t+1}}{P_t} \right) \right] \tag{1.21}$$

and thereby be expressed in growth rates:[19,20]

$$\mathrm{E}_t[-\gamma \log(1 + \widetilde{y_{t+1}})] - \mathrm{E}_t[\log(1 + \pi_{t+1})]. \tag{1.22}$$

Instead of linearizing, the logarithm will be represented by a second-degree polynomial:[21]

$$\approx \mathrm{E}_t \left[-\gamma \left(\widetilde{y_{t+1}} - \frac{1}{2} \widetilde{y_{t+1}}^2 \right) \right] - \mathrm{E}_t \left[\pi_{t+1} - \frac{1}{2} \pi_{t+1}^2 \right] \tag{1.23.1}$$

$$= -\gamma \mathrm{E}_t \widetilde{y_{t+1}} + \frac{\gamma}{2} \mathrm{E}_t \widetilde{y_{t+1}}^2 - \mathrm{E}_t \pi_{t+1} + \frac{1}{2} \mathrm{E}_t \pi_{t+1}^2 \tag{1.23.2}$$

$$= \gamma \widehat{y_t} - \gamma \mathrm{E}_t \widehat{y_{t+1}} + \frac{\gamma}{2} \mathrm{E}_t \widetilde{y_{t+1}}^2 - \mathrm{E}_t \pi_{t+1} + \frac{1}{2} \mathrm{E}_t \pi_{t+1}^2. \tag{1.23.3}$$

[18] The relation follows from the steady state Euler equation. See Galí (2015, 132) for a more complex definition of the long-term real interest rate.

[19] See Appendix A.6 for the missing steps.

[20] Note that the use of the actual GDP growth rate $\widetilde{y_{t+1}}$ in Eq.(1.22) is merely for clarity. The relationship between $\widetilde{y_{t+1}}$ and $\widehat{y_{t+1}}$ is: $\widehat{y_{t+1}} \approx \widetilde{y_{t+1}} + \widehat{y_t}$.

[21] See Appendix A.7 for more detail.

Bringing together the linearized form of the left side in Eq.(1.20) yields the quadratic IS curve:

$$\widehat{y_t} = \mathrm{E}_t\widehat{y_{t+1}} - \frac{1}{\gamma}(i_t - r - \mathrm{E}_t\pi_{t+1}) - \frac{1}{2\gamma}\mathrm{E}_t\pi_{t+1}^2 - \frac{1}{2}\mathrm{E}_t\widetilde{y_{t+1}}^2. \tag{1.24}$$

Referring to the original graphical IS relation (in the $\widehat{y}/i$–space), the curve shifts to the right if the long-term real interest rate r, the output gap expectations $\mathrm{E}_t\widehat{y_{t+1}}$ or the inflation expectations $\mathrm{E}_t\pi_{t+1}$ rise. However, the slope will rise and the curve becomes flatter if the intertemporal elasticity of substitution $(1/\gamma)$ rises. The second-order terms have a negative effect on $\widehat{y_t}$. However, Eq.(1.24) is not in reduced form since the last term still contains $\widehat{y_t}$. The formula for the conditional variance, can be utilized to show the second moments' influence in detail:[22]

$$\begin{aligned}\widehat{y_t} = {} & \mathrm{E}_t\widehat{y_{t+1}} - \frac{1}{\gamma}(i_t - r - \mathrm{E}_t\pi_{t+1}) - \frac{1}{2\gamma}\mathrm{Var}_t\pi_{t+1} - \frac{1}{2}\mathrm{Var}_t\widetilde{y_{t+1}} \\ & - \frac{1}{2\gamma}(\mathrm{E}_t\pi_{t+1})^2 - \frac{1}{2}(\mathrm{E}_t\widetilde{y_{t+1}})^2. \end{aligned} \tag{1.25}$$

In a first step, looking only at the variances and solving for the interest rate yields

$$i_t = -\gamma\widehat{y_t} + r + \mathrm{E}_t\pi_{t+1} + \gamma\mathrm{E}_t\widehat{y_{t+1}} - \frac{1}{2}\mathrm{Var}_t\pi_{t+1} - \frac{\gamma}{2}\mathrm{Var}_t\widehat{y_{t+1}} - \ldots, \tag{1.26}$$

which states that uncertainty would shift the curve to the left compared to the original IS curve.[23] Considering the second moment, there are two additional effects namely expected output gap growth affects the slope and a variation of the curve's shape. That is because the last term of Eq.(1.25) contains $\widehat{y_t}$ and $\widehat{y_t}^2$:

$$-\frac{1}{2}(\mathrm{E}_t\widehat{y_{t+1}} - \widehat{y_t})^2 = -\frac{1}{2}(\mathrm{E}_t\widehat{y_{t+1}})^2 + \mathrm{E}_t\widehat{y_{t+1}} \cdot \widehat{y_t} - \frac{1}{2}\widehat{y_t}^2. \tag{1.27}$$

Larger values for $\mathrm{E}_t\widehat{y_{t+1}}$ result in a (slightly) flatter IS curve and vice versa. Figure 1.1 illustrates the shift, the different slope, and the quadratic form.

[22]The following applies for a random variable z:

$$\mathrm{Var}_t z_{t+1} = \mathrm{E}_t z_{t+1}^2 - (\mathrm{E}_t z_{t+1})^2 \;\Leftrightarrow\; \mathrm{E}_t z_{t+1}^2 = (\mathrm{E}_t z_{t+1})^2 + \mathrm{Var}_t z_{t+1}.$$

[23]Note that $\mathrm{Var}_t\widetilde{y_{t+1}} \approx \mathrm{Var}_t(\widehat{y_{t+1}} - \widehat{y_t}) = \mathrm{Var}_t\widehat{y_{t+1}}$ because $\widehat{y_t}$ is t-measurable and constants (in period t) do not affect Var_t.

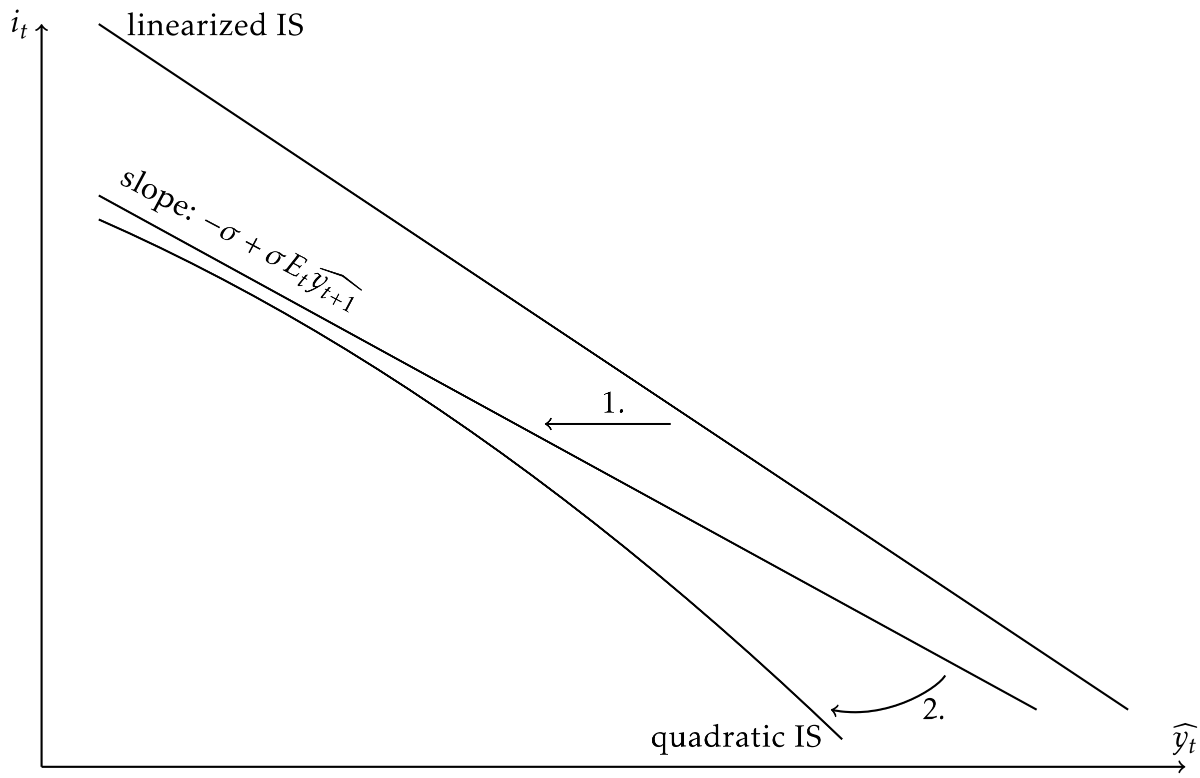

Figure 1.1: 1. Shift of the locus and a change in the slope (for $\mathrm{E}_t\widehat{y_{t+1}} > 0$). 2. The quadratic form.

Inserting everything in Eq.(1.26) gives

$$\begin{aligned} i_t =& -\frac{\gamma}{2}\widehat{y_t}^2 + (\gamma \mathrm{E}_t\widehat{y_{t+1}} - \gamma)\widehat{y_t} + r + \mathrm{E}_t\pi_{t+1} + \gamma\mathrm{E}_t\widehat{y_{t+1}} - \frac{1}{2}\mathrm{Var}_t\pi_{t+1} - \frac{\gamma}{2}\mathrm{Var}_t\widehat{y_{t+1}} \\ & - \frac{1}{2}(\mathrm{E}_t\pi_{t+1})^2 - \frac{\gamma}{2}(\mathrm{E}_t\widehat{y_{t+1}})^2. \end{aligned} \tag{1.28}$$

In the quadratic IS formula, γ is the only parameter besides r. When examining the effects of a variation in γ on the derived curve, it is useful to recapitulate the meaning of $1/\gamma$. The EIS measures the strength of the relationship between i_t and $\widehat{y_{t+1}}/\widehat{y_t}$ (also y_{t+1}/y_t and C_{t+1}/C_t). A positive EIS implies a positive relationship. Also, if i_t rises, there is a negative effect on $\widehat{y_t}$ due to the substitution effect. If the EIS increases (decreases) the relationship gets stronger (weaker) and the IS curve's slope should be flatter (steeper). Hence, increasing γ should lead to a steeper IS curve. The effect is indeed a more concave and steeper curve. Additionally, it shifts to the left (right) if uncertainty is relatively high (low) in comparison to the expected values.

1.2.3 Targeting Rule under Discretion

The central bank takes Phillips and IS curves as given and seeks to optimally set the interest rate for period t. Therefore, the central bank's targeting rule will be derived by minimizing the discounted loss function over all periods[24]

$$\min_{\pi,\, \widehat{y}} \left\{ \mathrm{E}_t \left[\sum_{s=t}^{\infty} \rho^{s-t} \left((\pi_s - \pi^*)^2 + \delta \widehat{y_s}^2 \right) \right] \right\} \tag{1.29}$$

resulting in the standard targeting rule under discretion:[25]

$$\delta \widehat{y_t} = -\kappa \pi_t \quad \Leftrightarrow \quad \widehat{y_t} = -\frac{\kappa}{\delta} \pi_t. \tag{1.30}$$

Every difference between the inflation rate and the central bank's target π^* results in a loss.[26] Also, every output gap leads to a loss but is reduced by a weighting factor δ, normally smaller than one. Squaring ensures that higher deviations yield disproportionately higher losses and the optimized variables will not vanish in the derivatives. Moreover, it makes the loss function symmetrical.[27]

Although the optimal interest rate is not explicitly given, all relationships between the macroeconomic variables are derived. The process is as follows: the nominal interest rate has an effect on the output gap (IS curve), which, in consequence, affects the inflation rate (NKPC). Furthermore, Eq.(1.30), the "leaning against the wind" condition, implies a countercyclical monetary policy intended to stabilize prices and eventually contract the economy. The degree of this contraction increases in κ and decreases in δ, the weight on output stabilization.

Finally, Eqs.(1.16), (1.25), and (1.30) can lead to a forward-looking Taylor type rule (with uncertainty added). Plugging Eq.(1.30) into Eq.(1.16) gives

$$-\frac{\delta}{\kappa} \widehat{y_t} = \rho \mathrm{E}_t \pi_{t+1} + \kappa \widehat{y_t} \quad \Leftrightarrow \quad \widehat{y_t} = -\frac{\kappa}{\delta + \kappa^2} \cdot \rho \mathrm{E}_t \pi_{t+1}, \tag{1.31}$$

[24]The loss function can be derived by a second-order approximation of the households' welfare loss, first introduced by Rotemberg and Woodford (1999, 54–61). It can also be found in the textbooks by Galí (2015), Walsh (2010), and Woodford (2003b). In a similar vein, Kim et al (2008, 3410) argue that utility-based welfare effects of monetary policy should include second-order or even higher-order terms.

[25]See Appendix A.8 for the missing steps.

[26]Note that $\pi^* = 0$ as it does not change the essential findings.

[27]See Nobay and Peel (2003, 661) for an asymmetric loss function (Linex form) that becomes quadratic in a special case.

which can be utilized for Eq.(1.25):

$$i_t = r + \left(1 + \frac{\rho\kappa\gamma}{\delta + \kappa^2}\right)\mathrm{E}_t\pi_{t+1} + \gamma\mathrm{E}_t\widehat{y_{t+1}} - \frac{1}{2}\mathrm{Var}_t\pi_{t+1} - \frac{\gamma}{2}\mathrm{Var}_t\widehat{y_{t+1}}$$
$$- \frac{1}{2}(\mathrm{E}_t\pi_{t+1})^2 - \frac{\gamma}{2}(\mathrm{E}_t\widehat{y_{t+1}} - \widehat{y_t})^2. \tag{1.32}$$

When examining the coefficients on first and second moments, the parameters γ, δ, κ, and ρ have to be taken into account. Larger values for κ and ρ increase the weight on expected inflation, whereas larger values for γ increase not only the weight on expected inflation, but on expectation and uncertainty concerning the output gap growth, as well.[28] Following Bauer and Neuenkirch (2017), the squared expected inflation rate and the squared expected output gap growth rate should not be over-interpreted here, as it takes very small values for advanced economies.

Ultimately, the difference between this approach and the conventionally derived Taylor rules lies in the negative variance term that Bauer and Neuenkirch (2017, 105–107) empirically confirmed for uncertainty in future inflation rates where central banks lower the interest rate for higher values of $\mathrm{Var}_t\pi_{t+1}$. Branch (2014, 1042–1044) also adds variances in an empirical model for a Taylor rule. He estimates negative coefficients with a more significant (and more negative) value for the coefficient on the inflation variance.

The NKPC, the IS curve, and the targeting rule were all derived by second-order approximations. However, this implements uncertainty only in the IS curve since P_{t+1} and Y_{t+1} are non-t-measurable. Thus, besides the quadratic terms of the IS curve, all derivations follow standard approaches.

[28]The increasing relationship holds for $\delta = 0.25$ (independent of ρ and γ) if $\kappa < 0.5$, which can be assumed (see Appendix A.11).

1.3 Persistent Shocks and Equilibrium Condition

This section adds stochastic terms to the derived curves and solves these forward to a reduced form solution for the nominal interest rate.

1.3.1 Adding Persistent Stochastic Shocks

Given the possibility that unforeseen events might interrupt the normal economic process (e.g., inventions, cold winters, higher oil prices, wars), stochastic shocks (in reduced-form) will be added to the existing relationships. The realistic feature of a certain duration of the event that will dwindle over time can be modeled by means of stationary AR(1) processes:[29]

$$e_t = \xi e_{t-1} + \zeta_t, \tag{1.33.1}$$

$$u_t = \nu u_{t-1} + \epsilon_t. \tag{1.33.2}$$

The coefficients of the shocks in period $(t-1)$, $\xi, \nu \in]0,1[$, declare the percentage impact of shocks that carries over to the subsequent period. Additional assumptions are normally distributed error terms with an expected value equal to zero, that is, $\zeta_t \sim \mathcal{N}(0, \sigma_e^2)$ and $\epsilon_t \sim \mathcal{N}(0, \sigma_u^2)$, which are also serially uncorrelated.

Adding Eq.(1.33.1) to the NKPC, Eq.(1.16), can be described as a cost shock, a cost-push shock or an inflation shock and adding Eq.(1.33.2) to the IS curve, Eq.(1.25), indicates a taste shock, a demand shock or fluctuations in the flexible-price equilibrium output level (Walsh 2010, 352):[30]

$$\pi_t = \rho \mathrm{E}_t \pi_{t+1} + \kappa \widehat{y_t} + e_t, \tag{1.34.1}$$

$$\widehat{y_t} = \mathrm{E}_t \widehat{y_{t+1}} - \frac{1}{\gamma}(i_t - r - \mathrm{E}_t \pi_{t+1}) - \frac{1}{2\gamma}\mathrm{E}_t \pi_{t+1}^2 - \frac{1}{2}\mathrm{E}_t \widetilde{y_{t+1}}^2 + u_t. \tag{1.34.2}$$

1.3.2 Equilibrium Condition

A standard approach is chosen to substitute expectations through forward solving. Inserting the targeting rule (1.30) into the stochastic NKPC yields

$$\pi_t = \rho \mathrm{E}_t \pi_{t+1} - \frac{\kappa^2}{\delta}\pi_t + e_t \quad \Leftrightarrow \quad \pi_t = \frac{\rho\delta}{\delta + \kappa^2}\mathrm{E}_t \pi_{t+1} + \frac{\delta}{\delta + \kappa^2} e_t. \tag{1.35}$$

[29] For instance, Clarida et al (2000, 170) are also assuming a stationary AR(1) process in the context of a NKM.

[30] See Galí (2015, 128) for a further discussion of cost shocks, the type that will be most important throughout the remainder of the paper.

Devising the same formula for $t+1$ and substituting π_{t+1} gives

$$\pi_t = \frac{\rho\delta}{\delta+\kappa^2}\mathrm{E}_t\left[\frac{\rho\delta}{\delta+\kappa^2}E_{t+1}[\pi_{t+2}] + \frac{\delta}{\delta+\kappa^2}e_{t+1}\right] + \frac{\delta}{\delta+\kappa^2}e_t. \tag{1.36}$$

With $\mathrm{E}_t[E_{t+n}[\pi]] = \mathrm{E}_t[\pi]$ and $\mathrm{E}_t[e_{t+n}] = \xi^n e_t$, future expectations and shocks will leave the equation:

$$\pi_t = \left(\frac{\rho\delta}{\delta+\kappa^2}\right)^2 \mathrm{E}_t[\pi_{t+2}] + \frac{\rho\delta\xi}{\delta+\kappa^2}\cdot\frac{\delta}{\delta+\kappa^2}e_t + \frac{\delta}{\delta+\kappa^2}e_t. \tag{1.37}$$

After $(n-1)$ iterations, the equation converts to

$$\pi_t = \left(\frac{\rho\delta}{\delta+\kappa^2}\right)^n \mathrm{E}_t[\pi_{t+n}] + \frac{\delta}{\delta+\kappa^2}e_t\sum_{j=0}^{n-1}\left(\frac{\rho\delta\xi}{\delta+\kappa^2}\right)^j. \tag{1.38}$$

Developing n towards infinity, and making use of the formula for the infinite geometric series, leaves only parameters and the cost shock:

$$\pi_t = \frac{\delta}{\delta+\kappa^2}e_t\cdot\frac{\delta+\kappa^2}{\delta+\kappa^2-\rho\delta\xi}. \tag{1.39}$$

Rearranging and setting $\theta = (\kappa^2 + (1-\rho\xi)\delta)^{-1}$ as an auxiliary parameter results in the equilibrium conditions for π_t and $\widehat{y_t}$:[31]

$$\pi_t = \frac{\delta}{\kappa^2+(1-\rho\xi)\delta}\cdot e_t \;= \delta\theta e_t \tag{1.40.1}$$

$$\text{and}\quad \widehat{y_t} = \frac{-\kappa}{\kappa^2+(1-\rho\xi)\delta}\cdot e_t \;= -\kappa\theta e_t. \tag{1.40.2}$$

Determine the expectation values analogously:[32]

$$\mathrm{E}_t\pi_{t+1} = \delta\theta\mathrm{E}_t e_{t+1} = \delta\xi\theta e_t \tag{1.41.1}$$

$$\text{and}\quad \mathrm{E}_t\widehat{y_{t+1}} = -\kappa\theta\mathrm{E}_t e_{t+1} = -\kappa\xi\theta e_t. \tag{1.41.2}$$

Solution without Uncertainty

In a first step, we solve for the target interest rate

$$i_t = r - \gamma\widehat{y_t} + \gamma\mathrm{E}_t\widehat{y_{t+1}} + \mathrm{E}_t\pi_{t+1} + \gamma u_t, \tag{1.42}$$

[31] See also Clarida et al (1999, 1680) for a comparison of these results to those under commitment.

[32] $\mathrm{E}_t e_{t+1} = \mathrm{E}_t\left[\xi e_t + \zeta_{t+1}\right] = \xi\mathrm{E}_t e_t + \underbrace{\mathrm{E}_t\zeta_{t+1}}_{=0} = \xi e_t.$

which can be rewritten with the equilibrium conditions (1.40.2), (1.41.1), and (1.41.2):

$$i_t = r + \gamma\kappa\theta e_t - \gamma\kappa\xi\theta e_t + \delta\xi\theta e_t + \gamma u_t. \tag{1.43}$$

Simplifying results in

$$i_t = r + ((1-\xi)\gamma\kappa + \xi\delta)\theta e_t + \gamma u_t \tag{1.44}$$

and finally setting $\chi_\xi > 0$ as a summarizing parameter gives

$$i_t = r + \chi_\xi e_t + \gamma u_t, \tag{1.45}$$

a reduced-form solution for the nominal interest rate that describes the static equilibrium behavior under optimal discretion. The central bank's optimized interest rate in period t can be expressed through the long-run real interest rate and both shocks, which are weighted by a composition of parameters. Since these coefficients are positive, larger shocks correspond to higher interest rates.[33] Galí (2015, 133–134) refers to this equation type as instrument rule. In contrast to targeting rules (see Eq.(1.30), "practical guides for monetary policy"), Eq.(1.45) is not easy to implement.[34] It requires real-time observation of variations in the cost-push shock and knowledge of the model's parameters, including the efficient interest rate r.

Model with Uncertainty

After including the second-order terms, however, Eq.(1.45) will be examined theoretically in order to understand how shocks and persistence correspond to i_t in the equilibrium.

The basic procedure is to solve the IS curve for the interest rate and replace all variables with shocks. The difference between this approach and standard approaches is the quadratic terms, thus lower interest rates should be expected. Beginning with the expected value of the squared inflation ($\mathrm{E}_t\pi_{t+1}^2$), Eq.(1.40.1) in period $t+1$ gives

$$\pi_{t+1} = \delta\theta e_{t+1} = \delta\theta\,(\xi e_t + \zeta_{t+1}), \tag{1.46}$$

by using the former shock definition with persistence and a normally distributed error term. Therefore,

$$\mathrm{E}_t\pi_{t+1}^2 = \mathrm{E}_t\left[(\delta\theta)^2\,(\xi e_t + \zeta_{t+1})^2\right] = (\delta\theta)^2\mathrm{E}_t\left[\xi^2 e_t^2 + 2\xi e_t\zeta_{t+1} + \zeta_{t+1}^2\right], \tag{1.47}$$

[33] See also Walsh (2010, 364) for a more detailed discussion.

[34] The paper by Svensson and Woodford (2005) discusses the "targeting" vs. "instrument" topic in more detail.

where the middle term equals zero, since e_t can be treated as a constant in E_t and $\mathrm{E}_t\zeta_{t+1} = 0$. Inserting the variance, again with Eq.(22), yields

$$(\delta\theta\xi)^2 e_t^2 + (\delta\theta)^2 \left(\mathrm{Var}_t\zeta_{t+1} + (\mathrm{E}_t\zeta_{t+1})^2\right). \tag{1.48}$$

The variance is defined as σ_e^2 and hence,

$$\mathrm{E}_t\pi_{t+1}^2 = (\delta\theta)^2 \left(\xi^2 e_t^2 + \sigma_e^2\right). \tag{1.49}$$

Doing the same for the expected value of the squared output growth rate ($\mathrm{E}_t\widetilde{y_{t+1}}^2 = \mathrm{E}_t(\widehat{y_{t+1}} - \widehat{y_t})^2$),[35] Eq.(1.40.2) in period $t+1$ gives

$$\widehat{y_{t+1}} = -\kappa\theta e_{t+1} = -\kappa\theta\left(\xi e_t + \zeta_{t+1}\right) \tag{1.50}$$

and therefore,

$$\mathrm{E}_t(\widehat{y_{t+1}} - \widehat{y_t})^2 = (\kappa\theta)^2 \left((1-\xi)^2 e_t^2 + \sigma_e^2\right). \tag{1.51}$$

The equilibrium condition under uncertainty is now

$$i_t = r + \chi_\xi e_t - \frac{1}{2}\left(\left((1-\xi)^2\gamma\kappa^2 + \xi^2\delta^2\right)\theta^2 e_t^2 + \left(\gamma\kappa^2 + \delta^2\right)\theta^2\sigma_e^2\right) + \gamma u_t \tag{1.52}$$

and finally setting $\chi_e > 0$ and $\chi_\gamma > 0$ as summarizing parameters gives

$$i_t = r + \chi_\xi e_t - \frac{1}{2}\left(\chi_e e_t^2 + \chi_\gamma\sigma_e^2\right) + \gamma u_t, \tag{1.53}$$

a reduced-form solution for the nominal interest rate that describes the static equilibrium behavior under uncertainty.[36] Compared to the approach in Clarida et al (1999), a negative term and an additional parameter $\left(\sigma_e^2\right)$ enters the condition. The term entails a generally lower interest rate level. Moreover, a larger cost shock variance also corresponds to lower values for i_t, an essential result.[37]

[35]Note that the output gap can also be replaced by the inflation rate with the standard targeting rule (1.30) to obtain the same results. See Appendix A.10 for the missing steps.

[36]Going one step further, e_t and u_t could be replaced by the error terms:

$$i_t = r + \chi_\xi \sum_{k=0}^{\infty} \xi^k \zeta_{t-k} - \frac{1}{2}\left(\chi_e\left(\sum_{k=0}^{\infty}\xi^k\zeta_{t-k}\right)^2 + \chi_\gamma\sigma_e^2\right) + \gamma\sum_{k=0}^{\infty}\nu^k\epsilon_{t-k}.$$

This visualizes the past (known) shocks that are discounted by ξ and ν.

[37]The equation in its static form does not directly contain ν and σ_u^2. This is due to the simplified targeting rule and the resulting assumption that $\widehat{y}$ and π can be represented only through cost shocks.

1.4 Numerical Simulation

Table 1.1 shows the baseline (BL) values and the overall range used when taking all simulations into account.[38] Every value is assumed to be obtained on a quarterly basis. In order to cover even extreme scenarios, e_t initially ranges from -0.5% to 2.5%.

Parameter	BL Calibration	Applied Range	Description
ρ	0.99	0.99	Discount factor
κ	0.04	0.01 - 0.25	Slope of the NKPC
γ	1	0.5 - 5	Reciprocal value of the EIS
δ	0.25	0.25	Weight on output fluc.
ξ	0.6 - 0.8	0.6 - 0.85	Cost shock persistence
σ_e^2	10^{-4}	$5 \cdot 10^{-5}$ - $5 \cdot 10^{-4}$	Cost shock variance
e_t	-0.005 - 0.025	-0.005 - 0.025	Cost shock

Table 1.1: Overview of all Parameters

1.4.1 Equilibrium Condition

In the baseline calibration, shown in Table 1.1, $\rho = 0.99$, $\kappa = 0.04$, $\gamma = 1$, $\delta = 0.25$, $\sigma_e^2 = 10^{-4}$, ξ reaches from 0.6 to 0.8 and e_t from -0.5% to 2%. Since ν and σ_u^2 play no role when the central bank acts under discretion, u_t is assumed to be zero. The optimal interest rate would react one-to-one and there would be no gain of further insights.

Figure 1.2 shows the results of the model with uncertainty using a variety of persistence and cost shock combinations. The interest rate takes values from -1.1% to 10.2%. It is assumed that negative interest rates are possible and that the zero lower bound does not represent an obstacle. Indeed, central banks can raise a tax on deposits made by commercial banks.[39] When the model calibrates negative values for i_t, it could also be interpreted as an unconventional policy (i.e., quantitative easing) by the monetary authorities.[40] The lowest interest rates occur hand-in-hand with highly persistent negative cost shocks, a fairly extreme scenario since the only major developed country to have faced deflationary tendencies over a prolonged period of time is Japan. But even in the latter case, the negative cost shocks were closer to zero. As expected, the highest

[38]See Appendix A.11 for parameter discussion and literature review.

[39]The concise paper by Bassetto (2004) derives a framework in which the central bank commits to negative nominal interest rates and discusses the equilibrium condition in such a situation.

[40]The Wu and Xia (2016) shadow rate does exactly that and is negative since mid-2009 for the federal funds rate.

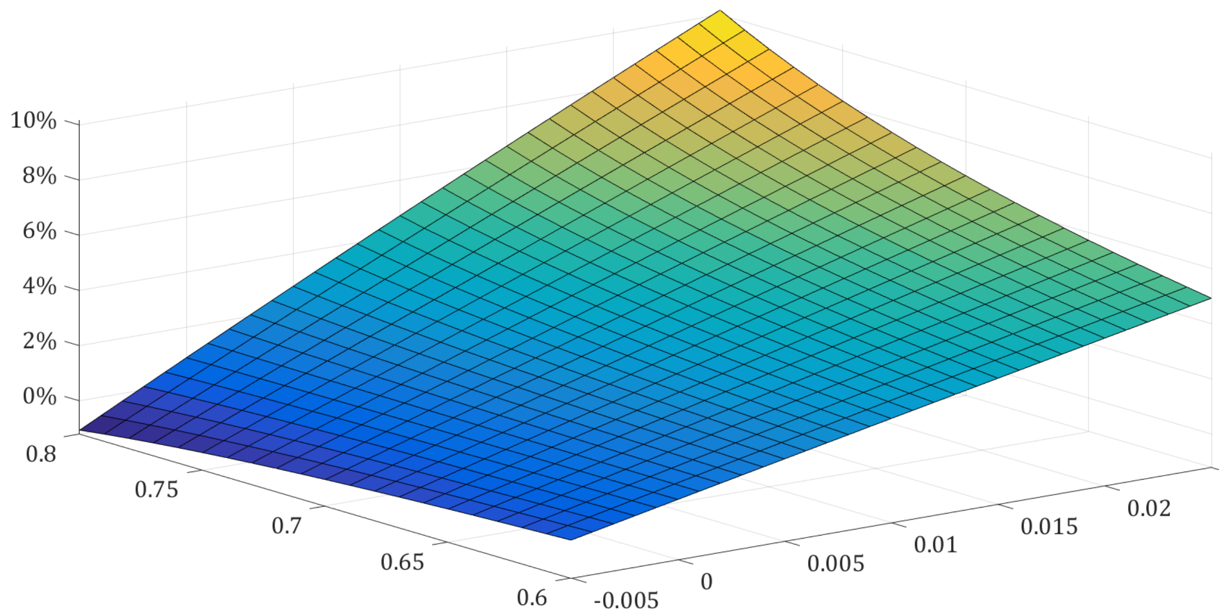

Figure 1.2: Corresponding interest rate in the equilibrium condition. Horizontal axes: Persistence ξ and cost shock e_t. Vertical axis: Interest rate i_t.

values come with large cost shocks. For a low persistence, regardless of the shocks, the resulting interest rate varies very little.

Model Comparison

To isolate the partial effect of the parameters, the interest rate differences after subtracting the values with (see Figure 1.2) and without uncertainty are shown, whereas values for i_t are always higher in the latter case. Due to small interest rate differences, the vertical axis in Figures 1.3 to 1.6 is scaled in basis points (100 basis points = one percentage point).

Figure 1.3 gives a broad overview on the effect of uncertainty. There is a significant amount of persistence/shock combinations that support the estimations by Bauer and Neuenkirch (2017). In particular, highly persistent shocks affect the interest rate outcome in the equilibrium behavior. In this case, the interest rate difference reaches from 10 to 60 basis points. Figure 1.4 can be understood as a cross section of Figure 1.3 with $\xi = 0.8$, a realistic assumption when reviewing the literature, such as Smets and Wouters (2003). It reveals, as one of the main findings from a theoretical point of view, that accounting for uncertainty results in lower policy rates, even during tranquil times. A black line is drawn at 25 basis points to roughly show the empirical conclusion by Bauer and Neuenkirch (2017, 109).[41]

[41]Note that Bauer and Neuenkirch (2017) have no assumption regarding the level of shock persistence.

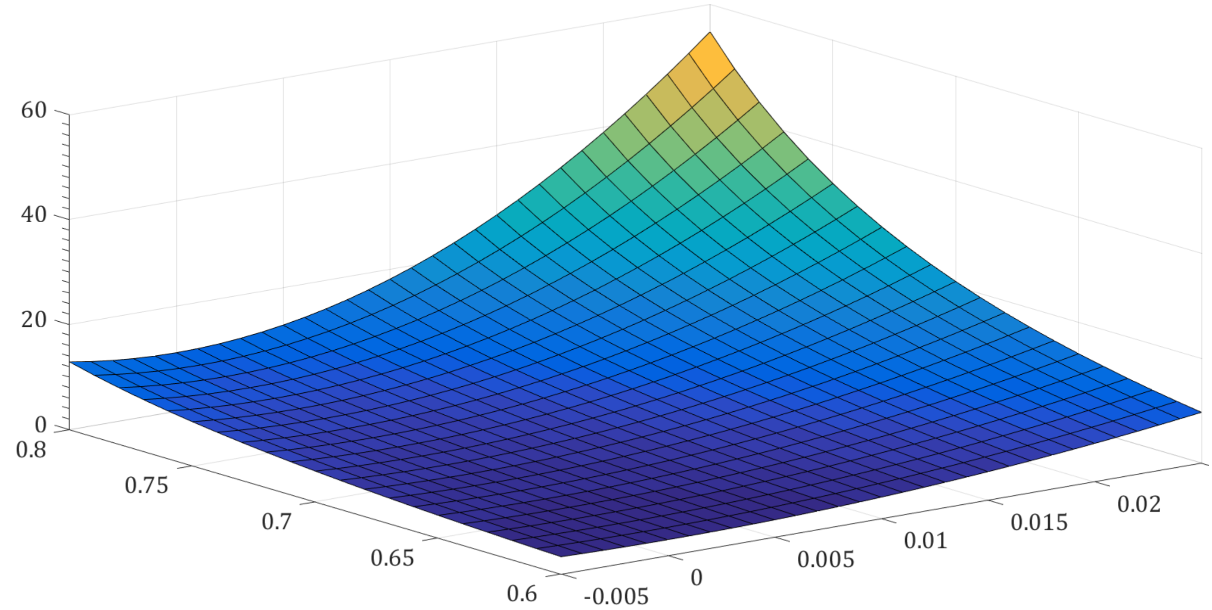

Figure 1.3: Differences between both cases (with and without uncertainty) in the equilibrium condition. Horizontal axes: Persistence ξ and cost shock e_t. Vertical axis: Difference of interest rate i_t in basis points.

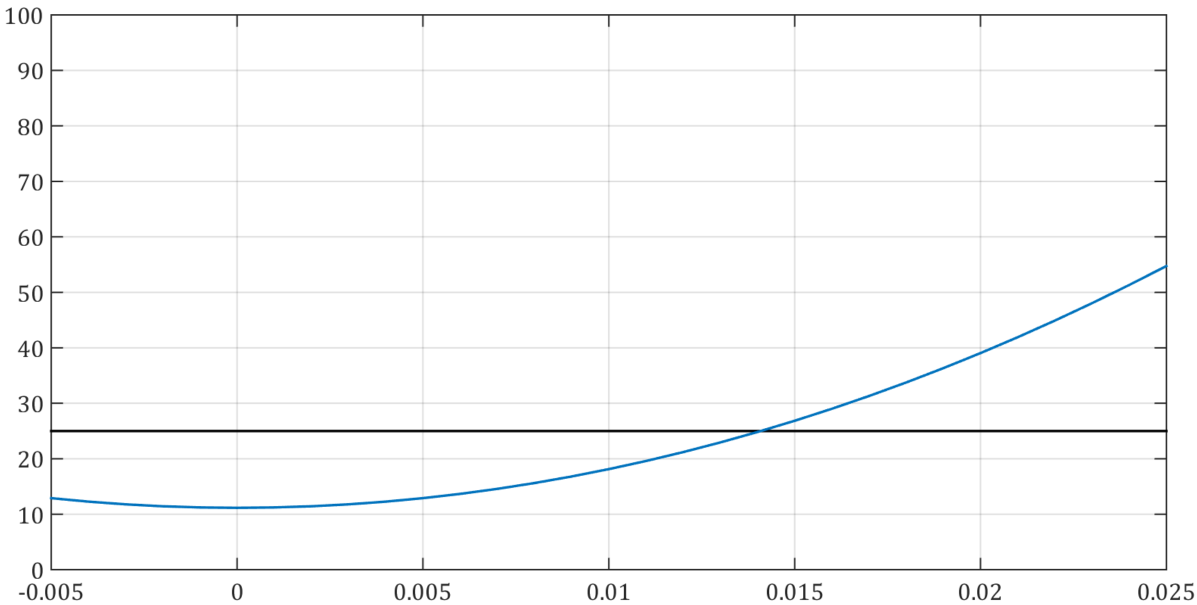

Figure 1.4: Differences between both cases (with and without uncertainty) in the equilibrium condition ($\xi = 0.8$). Horizontal axis: Cost shock e_t. Vertical axis: Difference of interest rate i_t in basis points.

1.4.2 Impulse Response Analysis

First, we examine the macro variables' short- and medium-term adjustments in the newly derived framework. In a subsequent step, the latter will be compared to the basic NKM.

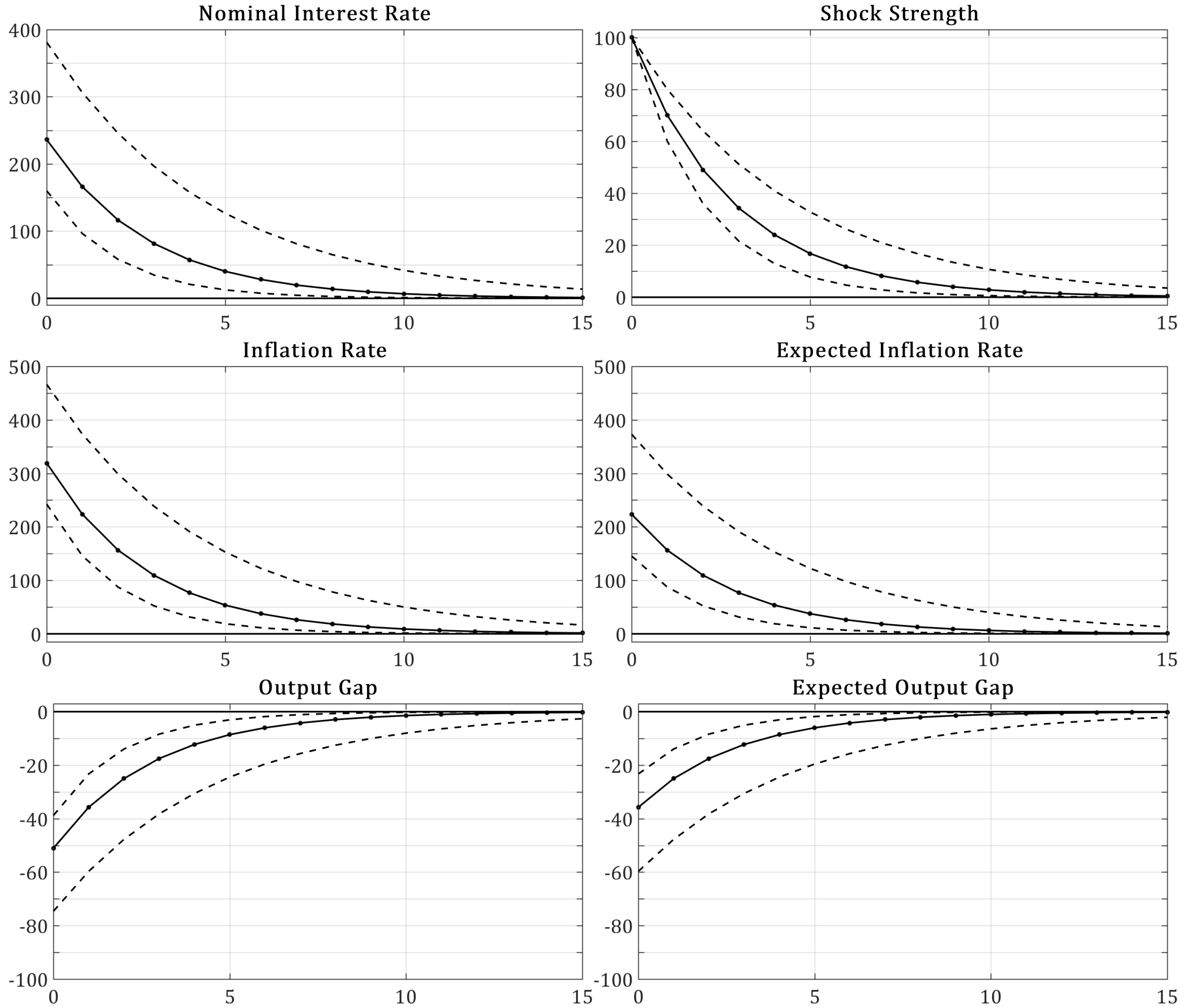

Figure 1.5: Dynamic responses to a cost shock by 100 basis points. Horizontal axes: Timeline in quarters. Vertical axes: Responses of i_t, e_t, π_t, $\mathrm{E}_t\pi_{t+1}$, $\widehat{y_t}$, and $\mathrm{E}_t\widehat{y_{t+1}}$ for $\xi \in \{0.6, 0.7, 0.8\}$ in basis points.

Figure 1.5 shows the adjustment over time to the steady state in the baseline case (see Table 1.1). The dashed lines indicate the scenarios of (relatively) high and low persistent shocks. In these scenarios, the upper (lower) course corresponds to the high (low) persistence for the nominal interest rate, the shock strength, and the (expected) inflation rate. The opposite is the case with regard to the (expected) output gap. All values adjust normally, but with quantitative differences if the level of persistence is varied. In the median case, the nominal interest rate has to be raised by almost 2.5% and should then sluggishly adjust to the steady state (depending on the real interest rate). The inflation rate and output gap follow their respective expectation values. The initial inflation rate is ranged between 2.5% and 5%, and the output gap starts at around -0.5%.

Model Comparison

Similar to Section 1.4.1 the following graphics show the "gap" in i_t when accounting for uncertainty.

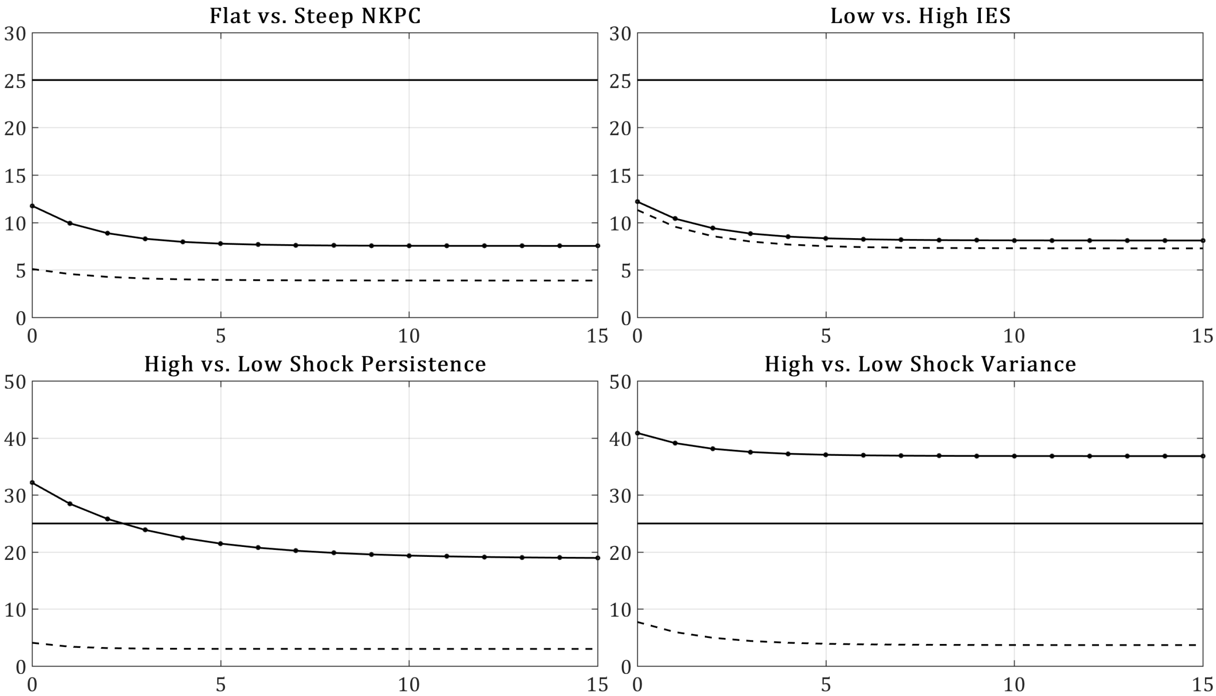

Figure 1.6: Comparing dynamic responses to a cost shock by 100 basis points with $\xi = 0.75$. Horizontal axes: Timeline in quarters. Vertical axes: Difference of interest rate i_t (with and without uncertainty) in basis points.

Figure 1.6 compares the NKM with and without uncertainty and shows the resulting differences of the nominal interest rate in each case. In addition, different scenarios are positioned opposite each other: Slope of the NKPC with 0.01 (black dotted) and 0.25 (dashed), EIS with 0.5 (black dotted) and 5 (dashed), shock persistence with 0.85 (black dotted) and 0.6 (dashed), shock variance with $5 \cdot 10^{-4}$ (black dotted) and $5 \cdot 10^{-5}$ (dashed). The cases with high shock persistence and high shock variance play a very important role showing a difference of up to 30 and 40 basis points, respectively. Also, with a very flat Phillips curve (in contrast to a steep NKPC) an effect comes to light (around 10 basis points). Comparable effects can be observed in the different EIS cases, but variations in elasticity play a negligible role. Although these examples indicate that there is no obligatory difference between the model with uncertainty and without uncertainty, (highly) persistent shocks and, in particular, increasing levels of uncertainty show distinctive variations.

1.5 Conclusions

This theoretical paper explores a variety of situations in which uncertainty is incorporated in the New Keynesian framework. The analysis focuses on how the equilibrium behaves when confronted with a wide range of parameter values. Our analysis reveals several points of interest. First, interest rates are generally lower when taking uncertainty into account. Under reasonable assumptions, accounting for uncertainty leads to lower interest rates of roughly 25 basis points. Second, when there is a higher degree of cost shocks (positive or negative) and shocks are more persistent, this difference in interest rates increases. We also show that a steeper NKPC decreases the impact of uncertainty. Third, over time, the impact of uncertainty on the nominal interest rate decreases and the adjustment critically depends on the degree of persistence. Our theoretical analysis also confirms the results found in the empirical literature.

There are some open avenues left for future research. First, a targeting rule derived under commitment could be taken into account. Second, due to the negative interest rate in the equilibrium and because of the more prominent role of unconventional monetary policy in recent years, the model could include a zero lower bound when considering this type of policy. Third, calibrating the shock variance and the underlying distribution, which is essential for the resulting uncertainty, might also be considered as an additional topic to explore.

Appendix A

Table of Contents

A.1 Consumers – Calculation Steps

$\partial\mathscr{L}/\partial C_\tau$ can be obtained by using the chain rule:

$$P_\tau - \lambda\frac{\varepsilon}{\varepsilon-1}\left(\int_0^1 C_\varphi^{\frac{\varepsilon-1}{\varepsilon}}\,d\varphi\right)^{\frac{\varepsilon}{\varepsilon-1}-1}\cdot\underbrace{\frac{\varepsilon-1}{\varepsilon}C_\tau^{\frac{\varepsilon-1}{\varepsilon}-1}}_{\text{derivative of sub-function}} = 0 \tag{A1.1}$$

$$\Leftrightarrow\qquad P_\tau - \lambda\left(\int_0^1 C_\varphi^{\frac{\varepsilon-1}{\varepsilon}}\,d\varphi\right)^{\frac{1}{\varepsilon-1}}\cdot C_\tau^{-\frac{1}{\varepsilon}} = 0. \tag{A1.2}$$

First, exponentiate the integral with ε and $1/\varepsilon$ for rearranging the first-order condition. Then insert C from the constraint. It follows that

$$P_\tau = \lambda C_\tau^{-\frac{1}{\varepsilon}}C^{\frac{1}{\varepsilon}} \quad\Leftrightarrow\quad P_\tau = \lambda\left(\frac{C}{C_\tau}\right)^{\frac{1}{\varepsilon}} \tag{A2.1}$$

$$\Leftrightarrow\quad \frac{P_\tau}{\lambda} = \left(\frac{C_\tau}{C}\right)^{-\frac{1}{\varepsilon}} \quad\Leftrightarrow\quad \left(\frac{P_\tau}{\lambda}\right)^{-\varepsilon} = \frac{C_\tau}{C}. \tag{A2.2}$$

To obtain Eq.(1.5), solve Eq.(1.4) for C_τ and insert the result for all firms in the constraint, Eq.(1.1):

$$C = \left(\int_0^1\left(\left(\frac{P_\varphi}{P}\right)^{-\varepsilon}C\right)^{\frac{\varepsilon-1}{\varepsilon}}d\varphi\right)^{\frac{\varepsilon}{\varepsilon-1}} \Leftrightarrow\ C = \left(\frac{1}{P}\right)^{-\varepsilon}C\left(\int_0^1 P_\varphi^{1-\varepsilon}\,d\varphi\right)^{\frac{\varepsilon}{\varepsilon-1}} \tag{A3.1}$$

$$\Leftrightarrow \quad P^{-\varepsilon} = \left(\int_0^1 P_\varphi^{1-\varepsilon}\, d\varphi\right)^{\frac{\varepsilon}{\varepsilon-1}} \qquad \Leftrightarrow \; P = \left(\int_0^1 P_\varphi^{1-\varepsilon}\, d\varphi\right)^{\frac{1}{1-\varepsilon}}. \tag{A3.2}$$

A.2 Firms – Calculation Steps

Eq.(1.6) can be written in more detail. Using Eq.(1.4) with Y and rearranging leads to

$$\max_{P_\tau}\left\{\left(\frac{P_\tau}{P}\right)^{1-\varepsilon} Y - K\left(\left(\frac{P_\tau}{P}\right)^{-\varepsilon} Y\right)\right\}. \tag{A4}$$

The first-order condition is now straightforward, using the chain rule:

$$\frac{\partial}{\partial P_\tau} = (1-\varepsilon)\left(\frac{P_\tau}{P}\right)^{-\varepsilon} \cdot \frac{Y}{P} - K'(Y_\tau)\cdot(-\varepsilon)\left(\frac{P_\tau}{P}\right)^{-\varepsilon-1} \cdot \frac{Y}{P} = 0. \tag{A5}$$

Simplifying and denoting the optimal price with P_τ^* yields

$$(\varepsilon-1)\left(\frac{P_\tau^*}{P}\right)^{-\varepsilon} = K'(Y_\tau)\cdot\varepsilon\left(\frac{P_\tau^*}{P}\right)^{-\varepsilon-1} \tag{A6.1}$$

$$\Leftrightarrow \qquad 1 = \left(\frac{\varepsilon}{\varepsilon-1}\right)K'(Y_\tau)\left(\frac{P_\tau^*}{P}\right)^{-1} \tag{A6.2}$$

$$\Leftrightarrow \qquad P_\tau^* = \left(\frac{\varepsilon}{\varepsilon-1}\right)K'(Y_\tau)\cdot P. \tag{A6.3}$$

However, perfect substitutes let the monopolistic structure vanish and show the typical polypolistic result:

$$\lim_{\varepsilon\to\infty}\left(\frac{\varepsilon}{\varepsilon-1}\right)K'(Y_\tau)\cdot P = K'(Y_\tau)\cdot P = P_\tau^*. \tag{A7}$$

Now, with a cost function in real terms of quantities Y_τ defined as

$$K(Y_\tau) = \frac{c_{var}}{\psi+1} Y_\tau^{\psi+1} + c_{fix}, \tag{A8}$$

where c_{fix} are the fix costs, c_{var} is a measure for the variable costs and ψ represents the elasticity of marginal costs, Eq.(1.7) becomes a micro-funded AS curve that takes the form of a power function:

$$P_\tau^* = \left(\frac{\varepsilon}{\varepsilon-1}\right)c_{var} Y_\tau^{\psi}\cdot P. \tag{A9}$$

A.3 Log-Linearization

It is convenient to use log-linearized variables instead of level variables in order to solve the model analytically. Also, some interpretations of the results, in terms of elasticity and growth rates, become quite useful. So both Eq.(1.4) and Eq.(A9) can be approximated through log-linearization around the steady state. Thus, the approximation becomes more precise with small growth rates. However, some preparation is necessary. Let $\mathcal{Z}$ be a state variable that can change over time and $\mathcal{Z}_{ss}$ its long-term value. When defining

$$z \equiv \log \mathcal{Z} - \log \mathcal{Z}_{ss}, \tag{A10}$$

z becomes a good approximation of $\widehat{z}$, the growth rate around the steady state. Also, a first-order Taylor approximation "in reverse" shows the relationship between z and $\widehat{z}$:

$$\widehat{z} \approx \log(1+\widehat{z}) = \log\left(1 + \frac{\mathcal{Z} - \mathcal{Z}_{ss}}{\mathcal{Z}_{ss}}\right) = \log \mathcal{Z} - \log \mathcal{Z}_{ss}. \tag{A11}$$

Furthermore, in the steady state, long-term values for individual variables are by definition the same as for those on aggregated level, thus $\mathcal{Z}_{\tau ss} = \mathcal{Z}_{ss}$. The state would otherwise include endogenous forces. And finally, the long-run marginal costs equal the multiplicative inverse of the firms' mark-up:[42]

$$c_{var} Y_{ss}^{\psi} = \frac{\varepsilon - 1}{\varepsilon}. \tag{A12}$$

An explanation is the long-run version of Eq.(A9) and hence $P_{\tau ss} = P_{ss}$. Now this can be applied to the previous results. First, Eq.(1.4), the AD curve will be log-linearized. Taking logs, expanding with the log long-term values, and using (A10) gives

$$\begin{aligned}
& & \log Y_\tau &= \log Y + \varepsilon(\log P - \log P_\tau) && \text{(A13.1)}\\
&\Leftrightarrow & \log Y_\tau - \log Y &= -\varepsilon(\log P_\tau - \log P) && \text{(A13.2)}\\
&\Leftrightarrow & \log Y_\tau - \log Y_{ss} - (\log Y - \log Y_{ss}) &= -\varepsilon(\log P_\tau - \log P_{ss} - (\log P - \log P_{ss})) && \text{(A13.3)}\\
&\Leftrightarrow & y_\tau - y &= -\varepsilon(p_\tau - p) && \text{(A13.4)}\\
&\Leftrightarrow & y_\tau &= -\varepsilon p_\tau + \varepsilon p + y, && \text{(A13.5)}
\end{aligned}$$

a linearized AD curve in terms of growth rates with the slope of $-1/\varepsilon$. A higher elasticity of substitution would result in a flatter curve, so a change in the firm's price growth p_τ would have a stronger effect on production growth y_τ.

Next, with the use of (A12), the AS curve type Eq.(A9), can be rewritten in a similar way:

$$\log P_\tau^* = \log\left(\frac{\varepsilon}{\varepsilon - 1}\right) + \log c_{var} + \psi \log Y_\tau + \log P \tag{A14.1}$$

[42] Other authors simply define this property, see e.g., Galí (2015, 57).

$$\Leftrightarrow \quad \log P_\tau^* - \log P = \log\left(\frac{\varepsilon}{\varepsilon - 1}\right) + \log c_{var} + \psi\left(\log Y_\tau - \log Y_{ss} + \log Y_{ss}\right) \tag{A14.2}$$

$$\Leftrightarrow \quad p_\tau^* - p = \psi y_\tau + \log\left(\frac{\varepsilon}{\varepsilon - 1}\right) + \log c_{var} + \psi \log Y_{ss} \tag{A14.3}$$

$$\Leftrightarrow \quad p_\tau^* - p = \psi y_\tau + \log\left(c_{var} Y_{ss}^{\psi}\right) - \log\left(\frac{\varepsilon - 1}{\varepsilon}\right) \tag{A14.4}$$

$$\Leftrightarrow \quad p_\tau^* - p = \psi y_\tau + \underbrace{\log\left(\frac{c_{var} Y_{ss}^{\psi}}{(\varepsilon - 1)/\varepsilon}\right)}_{=0}. \tag{A14.5}$$

The latter expression shows the assumption that the log deviations of marginal costs from their long-run trend values are linear in the amount of ψ. When the firm's optimized price growth p_τ^* is equal to the aggregated price growth p, then there is no growth in the firm's production.

Having log-linearized both demand and supply side, Figure A1 sums up.

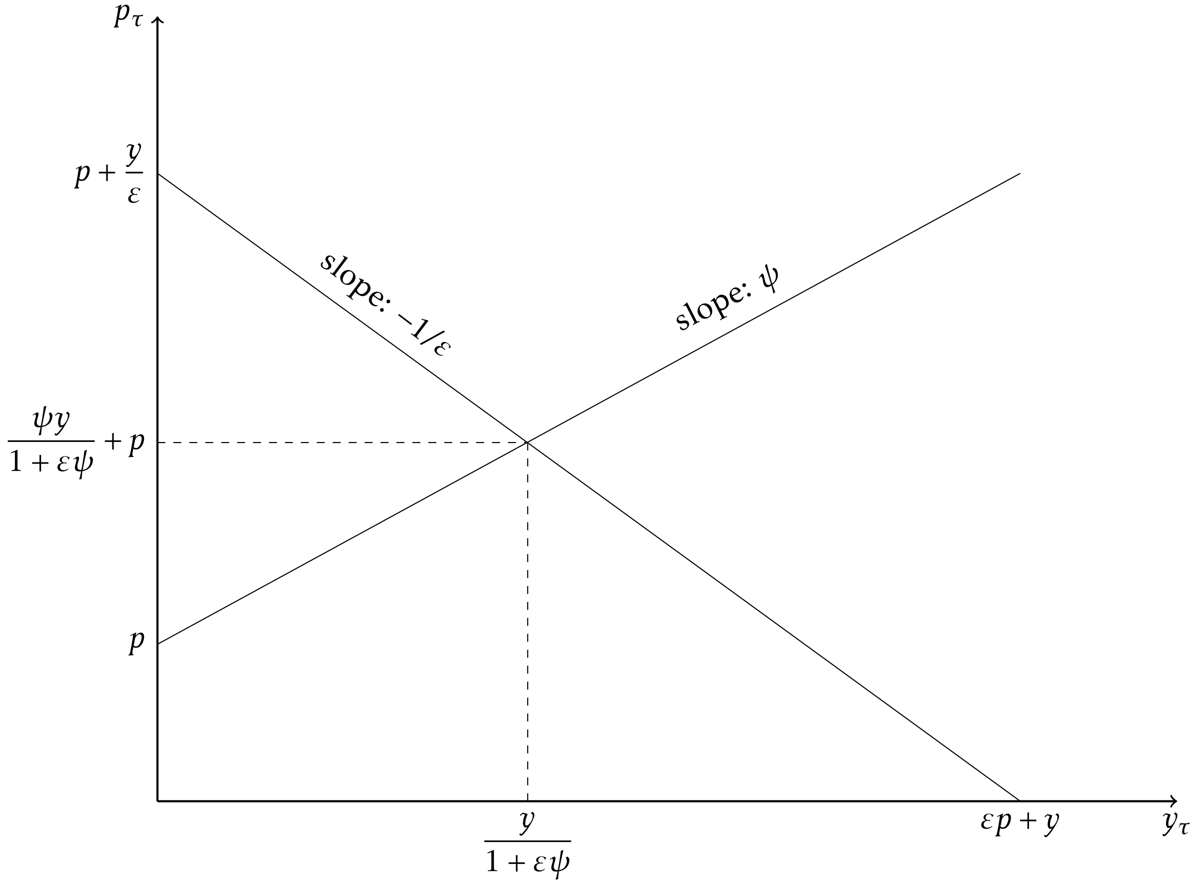

Figure A1: Graphical results of households' and firms' static optimization.

Finally, inserting (A13.5) in (A14.5) combines all the results and gives

$$p_\tau^* - p = \psi(-\varepsilon p_\tau^* + \varepsilon p + y) \tag{A15.1}$$

$$\Leftrightarrow \qquad p^*_\tau - p = -\psi\varepsilon(p^*_\tau - p) + \psi y \tag{A15.2}$$

$$\Leftrightarrow \qquad (1+\psi\varepsilon)(p^*_\tau - p) = \psi y \tag{A15.3}$$

$$\Leftrightarrow \qquad p^*_\tau - p = \left(\frac{\psi}{1+\psi\varepsilon}\right) y. \tag{A15.4}$$

A.4 Calvo Pricing – Calculation Steps

Dividing the first-order condition by $2k$, using the fact that q_t is t-measurable, and expanding the sum gives

$$\sum_{j=0}^{\infty} (\rho\phi)^j q_t - \sum_{j=0}^{\infty} (\rho\phi)^j \mathrm{E}_t p^*_{t+j} = 0. \tag{A16}$$

Excluding q_t from the sum, using the formula for an infinite geometric series, and multiplying by $(1-\rho\phi)$ gives

$$q_t = (1-\rho\phi) \sum_{j=0}^{\infty} (\rho\phi)^j \mathrm{E}_t p^*_{t+j}. \tag{A17}$$

Again, using t-measurability ($\mathrm{E}_t p^*_t = p^*_t$) and excluding the first summand provides a sum from $j = 1$ to infinity that can be substituted in a subsequent step:

$$q_t = (1-\rho\phi) \left[\sum_{j=1}^{\infty} (\rho\phi)^j \mathrm{E}_t p^*_{t+j} + p^*_t \right]. \tag{A18}$$

Furthermore, Eq.(A17) can be rewritten for $t+1$ (since firms optimize in each period),

$$\mathrm{E}_t q_{t+1} = (1-\rho\phi) \sum_{j=1}^{\infty} (\rho\phi)^{j-1} \mathrm{E}_t p^*_{t+j} \tag{A19.1}$$

$$\Leftrightarrow \qquad \rho\phi \mathrm{E}_t q_{t+1} = (1-\rho\phi) \sum_{j=1}^{\infty} (\rho\phi)^j \mathrm{E}_t p^*_{t+j}, \tag{A19.2}$$

for eliminating the sum in (A18):

$$q_t = \rho\phi \mathrm{E}_t q_{t+1} + (1-\rho\phi) p^*_t. \tag{A20}$$

Inserting condition (1.11) leads to the expression

$$\frac{p_t - \phi p_{t-1}}{1-\phi} = \rho\phi \frac{\mathrm{E}_t p_{t+1} - \phi p_t}{1-\phi} + (1-\rho\phi) p_t^* \tag{A21.1}$$

$$\Leftrightarrow \quad p_t - \phi p_{t-1} = \rho\phi(\mathrm{E}_t p_{t+1} - \phi p_t) + (1-\phi)(1-\rho\phi) p_t^*, \tag{A21.2}$$

that only contains parameters and variants of the variable p. Then, with the definition of (A10) and first-order Taylor expansion, the inflation rate π can be expressed through differences of p. In the same way, the conditional expectation value for period $t+1$ can be expressed with

$$\mathrm{E}_t p_{t+1} - p_t \approx \mathrm{E}_t \pi_{t+1}. \tag{A22}$$

Since this approximation is sufficiently exact for small values of π, an equality sign will be used for all following calculations. Now (A21.2) can be rearranged to insert approximations π and Eq.(A22):

$$\phi(p_t - p_{t-1}) = \rho\phi(\mathrm{E}_t p_{t+1} - \phi p_t) + (1-\phi)(1-\rho\phi) p_t^* - (1-\phi) p_t \tag{A23.1}$$

$$\Leftrightarrow \quad \pi_t = \rho \mathrm{E}_t \pi_{t+1} + \frac{(1-\phi)(1-\rho\phi)}{\phi} p_t^* - \frac{1-\phi}{\phi} p_t + \rho(1-\phi) p_t. \tag{A23.2}$$

A.5 Intertemporal Optimization – Calculation Steps

The optimization problem has the constraint

$$C_t \cdot P_t + B_{t+1} = W_t + (1 + i_{t-1}) \cdot B_t, \tag{A24}$$

where W_t is the nominal wage and B_t the nominal value of bonds. The latter provides the link between two periods. Depending on the definition of the interest rate, the period can vary. Here it has been chosen in a way so that the interest from period t enters the Euler condition. Dynamic Programming uses the additively separable utility function and the envelope theorem to set up optimality conditions for two consecutive periods. The procedure can be divided into three parts. The first part is to write a value function, the Bellman equation. Under the assumption that the second term of the expanded utility

$$U(C_t) + \mathrm{E}_t \left[\sum_{s=t+1}^{\infty} \rho^{s-t-1} U(C_s) \right] \tag{A25}$$

is maximized in period t, the Bellman equation is

$$V(B_t) \equiv \max_{C_t} \{ U(C_t) + \rho V(B_{t+1}) \}. \tag{A26}$$

The expected value vanishes since B_{t+1} is determined by variables in period t in the constraint. Differentiating with respect to C_t gives the first-order condition

$$\frac{d}{dC_t}U(C_t) + \varrho\frac{d}{dC_t}V(B_{t+1}) = U'(C_t) + \varrho V'(B_{t+1}) \cdot \frac{dB_{t+1}}{dC_t} = 0, \tag{A27}$$

which results in

$$U'(C_t) = P_t \varrho V'(B_{t+1}). \tag{A28}$$

Eq.(A28) relates the marginal utility to the marginal value in the following period, the time preference, and prices in the same period. Therefore, a higher ϱ and P_t results in a lower C_t.

In the next part, the envelope theorem is used to differentiate the value function (by inserting the optimized C_t^*) with respect to the costate variable B_t:

$$V(B_t) = U(C_t^*) + \varrho V(B_{t+1}) \tag{A29.1}$$

$$\Rightarrow \quad \frac{dV}{dB_t} = \varrho V'(B_{t+1}) \cdot \frac{dB_{t+1}}{dB_t} \tag{A29.2}$$

$$\Leftrightarrow \quad V'(B_t) = \varrho V'(B_{t+1}) \cdot (1 + i_{t-1}). \tag{A29.3}$$

Eq.(A29.3) reveals the relationship of the marginal value functions.

In a third and last step, the first-order condition (A28) can be used to replace the value functions in Eq.(A29.3) with the marginal utility in both periods t and $t-1$:

$$\frac{U'(C_{t-1})}{P_{t-1}\varrho} = \varrho \cdot \frac{U'(C_t)}{P_t \varrho} \cdot (1 + i_{t-1}) \tag{A30.1}$$

$$\Rightarrow \quad \frac{U'(C_t)}{P_t} = \varrho \cdot (1 + i_t) \cdot \mathrm{E}_t\left[\frac{U'(C_{t+1})}{P_{t+1}}\right]. \tag{A30.2}$$

The time shift yields the Euler condition.

A.6 Jensen's Inequality – Calculation Steps

$f(EX) \geq E[f(X)]$ holds for concave functions, i.e., the logarithm and Jensen's inequality still holds for the conditional expected value. Since the function's curvature is sufficiently small, the accuracy is comparable to log-linearization for small growth rates. Moreover, the exactness increases for larger values because of $(\log(x))'' \to 0$ for increasing x. However, resulting values will always be underestimated.

$$\log \mathrm{E}_t\left[\frac{\mathcal{Z}_{t+1}}{\mathcal{Z}_t}\right] = \log \mathrm{E}_t\left[\exp\left(\log\left(\frac{\mathcal{Z}_{t+1}}{\mathcal{Z}_t}\right)\right)\right] \approx \log \mathrm{E}_t\left[1 + \log\left(\frac{\mathcal{Z}_{t+1}}{\mathcal{Z}_t}\right)\right] \tag{A31.1}$$

$$= \log\left(1 + \mathrm{E}_t\left[\log\left(\frac{\mathcal{Z}_{t+1}}{\mathcal{Z}_t}\right)\right]\right) \approx \mathrm{E}_t\left[\log\left(\frac{\mathcal{Z}_{t+1}}{\mathcal{Z}_t}\right)\right]. \tag{A31.2}$$

A.7 Second-Order Taylor Approximation

The Taylor series (in $\mathbb{R}$) helps in finding a polynomial to substitute a certain function $f(x)$ (i.e., exponential, logarithm, etc.) around a point x_0. The generalized formula of the degree n in the compact sigma notation is

$$T_n^f(x \mid x_0) = \sum_{j=0}^{n} \frac{f^{(j)}(x_0)}{j!}(x - x_0)^j, \tag{A32}$$

where $f^{(j)}$ denotes the jth derivative with $f^{(0)} = f$ as a special case. Thereby, larger values for n give better approximations of the original function $f(x)$. In (1.23.1), $f(x) = \log(1 + x)$ and $n = 2$. Formula (A32) simplifies to

$$T_2^f(x \mid x_0) = \log(1 + x_0) + \frac{1}{1 + x_0}(x - x_0) - \frac{1}{2(1 + x_0)^2}(x - x_0)^2. \tag{A33}$$

The result in (1.23.1) appears with $x_0 = 0$ and $\widetilde{y_{t+1}}$ (π_{t+1} respectively) as the argument of the function:

$$\log(1 + \widetilde{y_{t+1}}) \approx \widetilde{y_{t+1}} - \frac{1}{2}\widetilde{y_{t+1}}^2. \tag{A34}$$

A.8 Standard Targeting Rule – Calculation Steps

The Lagrangian has to be differentiated with respect to $\widehat{y_t}$, π_t, and i_t, since the central bank sets the nominal interest rate:

$$\begin{aligned}\mathscr{L}(\pi_t, \widehat{y_t}, i_t) = \mathrm{E}_t\Bigg[\sum_{s=t}^{\infty} \varrho^{s-t}\left(\pi_s^2 + \delta\widehat{y_s}^2\right) - \upsilon_s(\pi_s - \varrho\pi_{s+1} - \kappa\widehat{y_s}) \\ -\omega_s\left(\widehat{y_s} - \widehat{y_{s+1}} + \frac{1}{\gamma}(i_s - r - \pi_{s+1}) + \frac{1}{2\gamma}\pi_{s+1}^2 + \frac{1}{2}\widetilde{y_{s+1}}^2\right)\Bigg].\end{aligned} \tag{A35}$$

The first-order conditions are:

$$\frac{\partial \mathscr{L}}{\partial \pi_t} = 2\pi_t - \upsilon_t = 0 \tag{A36.1}$$

$$\frac{\partial \mathscr{L}}{\partial \widehat{y_t}} = 2\delta\widehat{y_t} + \upsilon_t\kappa - \omega_t(1 + \widehat{y_t} - \mathrm{E}_t\widehat{y_{t+1}}) = 0 \tag{A36.2}$$

$$\frac{\partial \mathscr{L}}{\partial i_t} = -\frac{\omega_t}{\gamma} = 0. \tag{A36.3}$$

Condition (A36.2) follows with Eq.(1.27). From condition (A36.3) follows that $\omega_t = 0$, hence the minimized loss will not change if the IS curve shifts, as the central bank can counteract it one by one through resetting the nominal interest rate. Combining (A36.1) and (A36.2), the standard targeting rule under discretion arises.

A.9 Optimal Interest Rate for Positive Inflation Targets

When the Lagrangian attains the "leaning against the wind" condition, it is extended with π^* (as in Eq.(1.29), the loss function). Therefore, the standard targeting rule changes to

$$\pi_t - \pi^* = -\frac{\delta}{\kappa}\widehat{y_t}, \tag{A37}$$

whereby the optimal output gap,

$$\widehat{y_t} = -\frac{\rho\kappa}{\delta + \kappa^2}\mathrm{E}_t\pi_{t+1} + \frac{\pi^*\kappa}{\delta + \kappa^2}, \tag{A38}$$

comprises an additional term. After inserting Eq.(A38) in the IS curve, the interest rule also has an additional (negative) term. This would lead to a generally lower interest level.

A.10 Equilibrium Condition – Calculation Steps

Eqs.(1.51) and (1.52) in more detail:

$$\begin{aligned}
\mathrm{E}_t(\widehat{y_{t+1}} - \widehat{y_t})^2 &= \mathrm{E}_t\left[((-\kappa\theta)(\xi e_t + \zeta_{t+1}) - (-\kappa\theta)e_t)^2\right] && \text{(A39.1)}\\
&= \mathrm{E}_t\left[(-\kappa\theta)^2(\xi e_t + \zeta_{t+1} - e_t)^2\right] && \text{(A39.2)}\\
&= (-\kappa\theta)^2\mathrm{E}_t\left[((\xi - 1)e_t + \zeta_{t+1})^2\right] && \text{(A39.3)}\\
&= ((-\kappa\theta)(\xi - 1))^2 e_t^2 + (-\kappa\theta)^2\left(\mathrm{Var}_t\zeta_{t+1} + (\mathrm{E}_t\zeta_{t+1})^2\right) && \text{(A39.4)}\\
&= \kappa^2\theta^2(\xi - 1)^2 e_t^2 + \kappa^2\theta^2\sigma_e^2 && \text{(A39.5)}\\
&= (\kappa\theta)^2\left((1 - \xi)^2 e_t^2 + \sigma_e^2\right) && \text{(A39.6)}
\end{aligned}$$

and

$$\begin{aligned}
i_t &= r + \chi_\xi e_t - \frac{1}{2}(\delta\theta)^2\left(\xi^2 e_t^2 + \sigma_e^2\right) - \frac{\gamma}{2}(\kappa\theta)^2\left((1 - \xi)^2 e_t^2 + \sigma_e^2\right) + \gamma u_t && \text{(A40.1)}\\
&= r + \chi_\xi e_t - \frac{1}{2}\left((\delta\theta)^2\xi^2 e_t^2 + (\delta\theta)^2\sigma_e^2 + \gamma(\kappa\theta)^2(1 - \xi)^2 e_t^2 + \gamma(\kappa\theta)^2\sigma_e^2\right)\\
&\quad + \gamma u_t && \text{(A40.2)}
\end{aligned}$$

$$= r + \chi_\xi e_t - \frac{1}{2}\left(\left((1-\xi)^2\gamma\kappa^2 + \xi^2\delta^2\right)\theta^2 e_t^2 + \left(\gamma\kappa^2 + \delta^2\right)\theta^2\sigma_e^2\right) + \gamma u_t. \qquad \text{(A40.3)}$$

A.11 Parameter Discussion

Eq.(1.45) includes all parameters of the model.[43] This subsection gives a brief overview over possible values, which are used to graphically depict the equilibrium conditions.

The discount parameter ρ is typically close to unity. Galí (2015, 67) and Rotemberg and Woodford (1997, 321) set ρ equal to 0.99 (quarterly), whereas Jensen (2002, 939) uses this under an annual interpretation. Walsh (2010, 362) also sets it to 0.99. Galí and Gertler (1999, 207) estimate a value of 0.988. To keep the framework close to the actual interest setting of the central bank, all calculations are carried out quarterly and ρ will be set to 0.99.

The slope of the NKPC κ takes values close to zero and usually lower than unity. Roberts (1995, 982) estimates in his original NKPC article $\kappa \approx 0.3$. On a quarterly basis, Walsh (2010, 362) sets 0.05, Galí and Gertler (1999, 13) estimate 0.02, and McCallum and Nelson (2004, 47) suggest $0.01-0.05$. Jensen (2002, 939) calibrates an annual value of 0.142, whereas Clarida et al (2000, 170) set 0.3 (yearly) and give a range of 0.05 to 1.22 in the literature. In the baseline simulation, κ is set to 0.04.[44]

Woodford (2003a, 165) states that a value of 1 is customary in the RBC literature for γ, the multiplicative inverse of the EIS (see, e.g., Clarida et al 2000, 170, Galí 2015, 67, Yun 1996, 359). A slightly larger value (1.5) is set by Jensen (2002, 939) and Smets and Wouters (2003, 1143) estimate 1.4. An insightful metadata study by Havranek et al (2015) estimates a mean EIS of 0.5 ($\gamma = 2$) across all countries. However, they report that more developed countries have a higher EIS (lower γ). Therefore, γ will be set to unity.

The weight on output fluctuations δ is set to 0.25 in almost all the literature (see, e.g., Walsh 2010, 362, McCallum and Nelson 2004, 47, Jensen 2002, 939). The latter reports values from 0.05 to 0.33 in other papers. Thus, $\delta = 0.25$ will also be assumed for the simulation.

Walsh (2003, 275) allows values up to 0.7 for ξ, the cost shock persistence. Clarida et al (2000, 170) set 0.27 (yearly) and Galí and Rabanal (2004, 48) estimate 0.95. Generally, Smets and Wouters (2003, 1142–1143) estimate persistencies of 0.8 and higher, which is confirmed by Smets and Wouters (2007). Thus, ξ will be treated as a variable in the range of $0.6 - 0.85$. The smallest value 0.6 implies 0.1296 on an annual basis.

[43] Note that variances σ_e^2 and σ_u^2 are only indirectly included.

[44] Note that this implies $\kappa = 0.16$ on a yearly basis.

For the standard deviation of a cost shock, Sims (2011, 17) sets 0.01 ($\sigma_e^2 = 10^{-4}$), Jensen (2002, 939) sets 0.015 ($\sigma_e^2 = 2.25 \cdot 10^{-4}$), and Galí and Rabanal (2004, 48) estimate 0.011 ($\sigma_e^2 = 1.21 \cdot 10^{-4}$). McCallum and Nelson (2004, 47) set an annualized standard deviation of 0.02 ($\sigma_e^2 = 4 \cdot 10^{-4}$). The conservative value of 10^{-4} will be taken for the simulation.

2 Internal and External Uncertainty

"Non-Linearities and the Euler Equation: Does Uncertainty have an Effect on the Approximation Quality?"

Abstract

Deriving a forward-looking Euler equation, this paper compares two fully identified non-linear versions. The difference (or bias) between them stems from an approximation by extracting parameters from the expectation values (Jensen's inequality) as it is common practice in the literature. Furthermore, the model is completely identified using Consensus Forecasts data for the expectations, inflation-indexed bonds as a proxy for the long-run real interest rate, and estimates for the elasticity of intertemporal substitution. Regression analyses using data for three major economies reveal that the difference between the two Euler versions can be explained by uncertainty in the data itself and external uncertainty measures. The results confirm a connection between theoretical and empirical higher-order moments in economic models.

2.1 Introduction

Motivated by the shortcomings of economic policies, Lucas (1976) famously criticized modeling approaches at that time for the lack of agents' adaption possibility. This resulted in the implementation of expectations and, therefore, forward-looking behavior. In addition, since the 1980's, macroeconomic models have been obtained by more and more elegant and sophisticated derivations (see the paper by Kydland and Prescott (1982) as a starting point). In many cases, a microeconomic foundation has been used to derive relationships like the Euler equation or the Phillips curve via intertemporal optimization.

However, bringing data to the model as intended by theory is oftentimes a difficult task. For example, log-linearizing level variables to receive growth rates already imply Taylor approximation, which can fundamentally change the derived equations. Schmitt-Grohé and Uribe (2004), for instance, solve dynamic stochastic general equilibrium (DSGE) models up to second-order, showing the result being thereupon robust to volatility, the second moment of exogenous shocks. Zeldes (1989) and Blanchard and Mankiw (1988) examine the deviation of certainty equivalence in the context of consumption models, emphasizing the importance of higher-order moments.

As another approach, since the triumph of rational expectations, expectation values almost always turn into actual values added by an error term. This skips the step of finding appropriate, forward-looking data. However, this technique adds assumptions which risk to dilute the explanatory power of the actual equations when they become in fact backward-looking. In his meta-study, Lovell (1986) challenges the acceptance of the rational expectations hypothesis as "stylized fact" by reviewing empirical evidence and discussing theoretical research. Considering these concerns, two facets are important with regard to applied macroeconomic modeling in general and to our work in particular: (i) preserving the functional form, i.e., no linearization, and (ii) using forecast data for expectations in an economic model.

Nevertheless, when using forecast values in connection with non-linearities, another issue arises: Jensen's inequality (see Jensen 1906). A concave (convex) function evaluated at the mean of possible outcomes is larger (smaller) than the mean of functional values at these possible outcomes. In contrast to our paper, Jensen was not interested in the magnitude of the inequality, but rather describes the difference (of functional values) in a qualitative way.[1] As a new contribution to the literature, we explicitly calculate the difference (from here on called "bias" or "residuals") and explain it by measures for higher-order moments. For this purpose, we utilize the consumption Euler condition, parameterized by the elasticity of intertemporal substitution (EIS), which was subject to a large variety of research. The next paragraph gives an overview in terms of approximation quality.

The first article using the log-linearized Euler equation relating to consumption was written by Hall (1988). Back then, approximating made sense to estimate equations due to limited computational power. Starting around 2000, concerns grew that flattening out higher-order moments would not catch the underlying interdependencies well enough, i.e., precautionary savings (described by the utility function's convexity) and prudence (described by the change in the utility function's curvature). In a more recent paper, Gomes and Paz (2013) discuss the weak instrument problem when estimating the linear form. They partly overcome this issue by using a weighted interest rate scheme. The theoretical paper by Ludvigson and Paxson (2001) reaches the same result, namely, the instrument variable approach cannot completely fix the er-

[1] Behavioral finance (or decision theory) studies a similar question by finding a different value, the certainty equivalent, as the non-linear (utility) function's argument such that the inequality disappears. The well-known work by Pratt (1964) labels this—the difference between mean value and certainty equivalent—risk premium. Hence, the central issue is the change in the function's argument.

ror in linear Euler equations. Attanasio and Low (2004) examine simulated log-linear equations which are significantly biased when discount rates are high.

Taking this into account and concretizing the aforementioned concept regarding expectations, we focus on (i) avoiding approximations and (ii) preserving expectation values.[2] The latter can be achieved using suitable data from the Consensus Forecasts (CF), which provide monthly projections (e.g., GDP growth, inflation, ...) from a variety of economic and financial institutions. This allows to replace the random variables in the model's expectation values by individual forecasts and, further, compare this result with a version using the mean values only. To form a bigger picture, this is done for the United States (US), the United Kingdom (UK), and the Euro Area (EA), separately. For the nominal interest rate, the short-term interbank rates: Effective Federal Funds Rate (EFFR), Sterling Overnight Index Average (SONIA), and Euro Overnight Index Average (EONIA) are utilized for US, UK, and EA, respectively. Inflation-indexed bonds serve as proxy for the long-run real interest rate. To fully identify the model, the (time-varying) EIS parameters are derived by a maximum likelihood-type estimation.

Regarding the combination of Jensen's residuals and uncertainty, Carroll and Kimball (1996) confirm the link between a concave consumption function and income uncertainty. Going one step further, we regress the bias (stemming partly from consumption) on a variety of uncertainty measures, using mostly region-specific covariates since there are three different economies involved. These measures can be divided into uncertainty stemming from the CF data (internal) and from external sources, including stock market and oil price volatility, financial/systematic stress, and uncertainty indices by Baker et al (2016), Jurado et al (2015), and Rossi and Sekhposyan (2015, 2017). Both internal and external uncertainty measures can be consulted to explain the bias, confirming the connection between theoretical and empirical higher-order moments in non-linear, forward-looking models. Yet, the bias' magnitude is relatively small (up to 10 basis points) but closes the gap in the literature that examines this kind of approximation.

The remainder of this paper is organized as follows. Section 2.2 derives the forward-looking Euler equation from scratch and illustrates the consequence when extracting non-linear relationships out of an expectation value. Section 2.3 introduces the data and presents measures for forecasts, interest rates, and uncertainties. Section 2.4 proposes the method to capture the EIS, calculates the Euler equation's bias, regresses this on uncertainty measures, and discusses the results. Section 2.5 concludes.

[2]As a warning example: approximation is already involved when we define the EIS. Elasticities are always %-changes on %-changes. However, in ceteris paribus analysis, we typically change the underlying interest rate by one percentage point. Therefore, the effect that is actually described should be somewhat smaller than the true value for the EIS.

2.2 Derivation: Euler Equation

The derivation follows the standard expected utility framework and is similar to the approach by Attanasio and Weber (1989). Common to the DSGE literature, the Euler equation in the context of a New Keynesian framework can also be found in the book by Galí (2015). To specify the aggregated utility, we do not take money, working hours, or any other possible utility-gainer into consideration. It solely relies on consumption, hence, households maximize their intertemporal discounted utility:

$$\max_{C_t} \left\{ \mathrm{E}_t \left[\sum_{s=t}^{\infty} \rho_s^{s-t} U(C_s) \right] \right\}. \tag{2.1}$$

Taking into account an intertemporal budget constraint with prices and the nominal interest rate i_t, the maximization problem leads to the Euler equation

$$\frac{dU(C_t)}{dC_t} = \rho_t \cdot (1 + i_t) \cdot \mathrm{E}_t \left[\frac{P_t}{P_{t+1}} \frac{dU(C_{t+1})}{dC_{t+1}} \right], \tag{2.2}$$

revealing the intertemporal relationship of the marginal utility depending on consumption.[3] Marginal utility in period t equals the expected counterpart in $t+1$, corrected by a discount factor, nominal interest rate, and the ratio of current and expected future price level. Assuming i_t rises, marginal utility in t would also rise relative to period $t+1$. Given the diminishing marginal utility property and, therefore, concavity, consumption will be higher in the future.[4]

Replacing the households' utility, $U(C_t)$, with the flexible CRRA function provides a constant EIS ($= \gamma^{-1}$).[5] Furthermore, taking the (time-varying) long-run real interest rate as a proxy for the inverse discount factor changes the Euler equation to:

$$C_t^{-\gamma} = \frac{1 + i_t}{1 + r_t} \cdot \mathrm{E}_t \left[\frac{P_t \cdot C_{t+1}^{-\gamma}}{P_{t+1}} \right]. \tag{2.3}$$

Rearranging for both growth rates, π_{t+1} (inflation) and c_{t+1} (consumption growth), yields:

$$1 = (1 + i_t) \cdot (1 + r_t)^{-1} \cdot \mathrm{E}_t \left[(1 + \pi_{t+1})^{-1} \cdot (1 + c_{t+1})^{-\gamma} \right]. \tag{2.4}$$

[3] See Appendix B.1 for the missing steps.

[4] Note that present consumption could also increase because of the income effect.

[5] Another way is to use the more exotic exponential function (CARA) or the recursive Epstein-Zin (1989) preferences, where the current utility depends also on the expected, future utility. However, in the latter case, this link is already closed by means of the interest rates in the Euler condition. Moreover, depending on γ, the CRRA changes to root-, hyperbola-, or log-utility. See Appendix B.2 for more detail.

Solving for the expectation values and converting the equation to a stochastic version, that is, including an error term, provides

$$\varepsilon_t = (1+i_t)\cdot(1+r_t)^{-1}\cdot\left(\left[(1+\mathrm{E}_t[\pi_{t+1}])^{-1}+\Delta_\pi\right]\cdot\left[(1+\mathrm{E}_t[c_{t+1}])^{-\gamma}+\Delta_c\right]+Cov\right), \tag{2.5}$$

with $\varepsilon_t \sim \mathcal{N}(1,\sigma^2)$ and Cov as the covariance of the transformed growth rates regarding inflation and consumption.[6] Δ_π and Δ_c stand for the residuals in Jensen's inequality. Figure 2.1 illustrates these (by means of the inflation expression), that is, the function value with the expectation value as input subtracted by the expected value of the function.

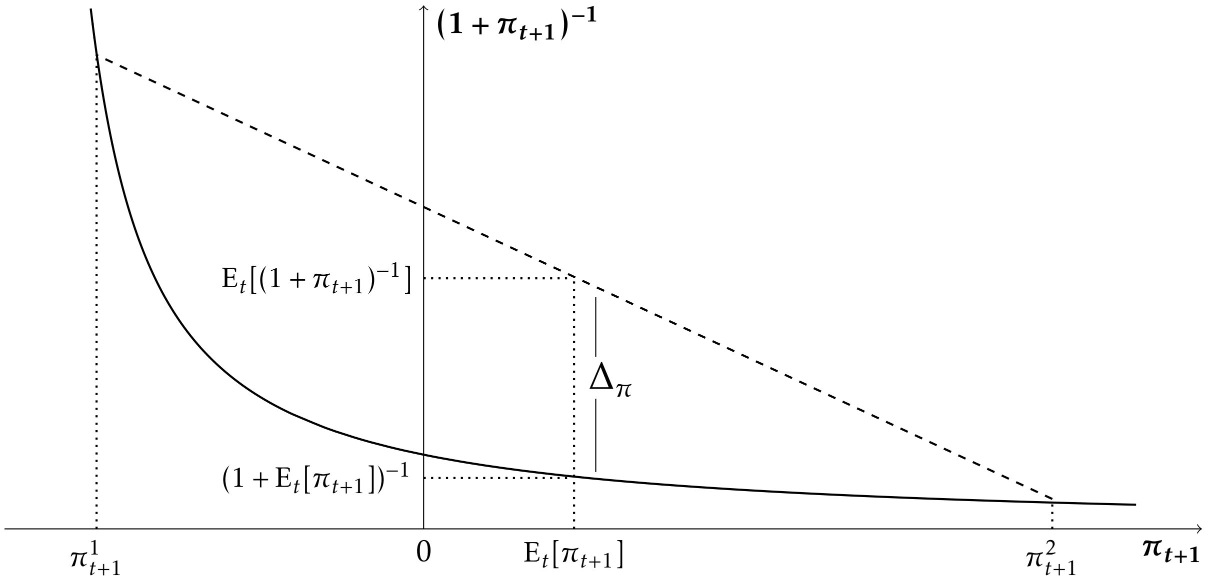

Figure 2.1: The residual in Jensen's inequality (Δ_π) in a case with two observations, π^1_{t+1} and π^2_{t+1}. The solid line shows the derived hyperbola regarding inflation from Eq.(2.4). (The scale is distorted due to illustrative reasons, i.e., Δ_π is relatively small in the data.)

In the following, we will derive measures for Δ_π, Δ_c, and Cov out of the CF data. For this purpose, the random variables c_{t+1} and π_{t+1} are replaced by individual forecasts. This renounces the stochastic component to be able to explicitly calculate the residuals.[7] Thus, these variables coming from a macroeconomic level are met with firm-level expectations.

[6]The normal distribution property is met when assuming the model conditions are satisfied and the relationship is not systematically biased due to omitted variables. Cov corresponds to $\mathrm{Cov}\left[(1+\pi_{t+1})^{-1},(1+c_{t+1})^{-\gamma}\right]$, which arises from the algebraic formula for the variance in terms of the covariance: $\mathrm{Cov}[X,Y]=\mathrm{E}[X\cdot Y]-\mathrm{E}[X]\cdot\mathrm{E}[Y]$.

[7]Implementing proxies that are truly forward-looking by adding an error term, i.e., $\mathrm{E}^i_t[\pi_{t+1}]+error$, would bring forth further questions about the forecast error distribution. See Rossi and Sekhposyan (2015, 2017) for an examination of these forecast errors. Also, the authors built indices out of the distributions, which are used later in this paper.

2.3 Data

2.3.1 Consensus Forecasts

The data for expected consumption growth and inflation stem from the Consensus Forecasts G-7 & Western Europe, which include monthly predictions by economic and financial institutions for both the current and immediately following year using surveys.[8] Therefore, the one-year-ahead forecasts are constructed by the mean values of the individual institutions and a weighting scheme depending on M (month), counting from 1 to 12:

$$\mathrm{E}_t[growth_{t+1}|M] = \frac{13-M}{12} \cdot \mathrm{E}_{t,M}[growth_t] + \frac{M-1}{12} \cdot \mathrm{E}_{t,M}[growth_{t+1}], \qquad (2.6)$$

where $growth_{t+1} \in \{c_{t+1}; \pi_{t+1}\}$.[9] In the country-specific data sets, consumption growth is referred to as the real %-change of personal consumption (US), household consumption (UK), and private consumption (EA). Inflation consists of the %-change of consumer prices (US and EA) and retail prices (UK). To apply these data to the Euler equation but yet avoid any approximation, Δ_π and Δ_c in Eq.(2.5) are calculated using the individual predictions.[10] The covariance of (transformed) inflation and consumption growth, in the same equation, is measured in each period also relying on the individual level.

For the US and UK, the first observations start in 10/1989, whereas the EA data start in 01/1999.[11] The Consensus Forecasts end in 12/2018. Figures 2.2 and 2.3 show expected growth rates over time for all three economies. The graphic containing consumption growth identifies the US' saving and loans crisis in 1991, spilling over to the UK, which was amplified by the subsequent impact of the Lawson Boom (along with high bank rates due to rising inflation). The UK's downturn in 1999 reflected public concerns about New Labour policies at that time. US forecasts in 2000 go along with the dot-com bubble's burst, with an additional sharp decrease shortly after the 9/11 disaster. All countries simultaneously decreased their expectations in 2008 due

[8] In contrast to the IMF's World Economic Outlook (published twice a year) and the ECB's Survey of Professional Forecasters (quarterly data), Consensus Economics publishes its forecasts on a monthly basis, which rapidly increases the number of observations. This counteracts the limited time horizon for EA data and several interest rates (e.g., EONIA) and hence, allows to consider time-varying parameters.

[9] For example, January data sets contribute 100% of the current year forecasts since the publishing dates are at the beginning of the month while the surveys are filled out in the previous month.

[10] There is no additional weighting for single, firm-level forecasts. See Figure 2.1 for the illustration of the Δ's.

[11] However, the interval 01/1999 – 11/2002 is composed of GDP-weighted forecasts for France, Germany, Italy, Netherlands, and Spain. See Appendix B.4 for a detailed discussion of the weighting scheme.

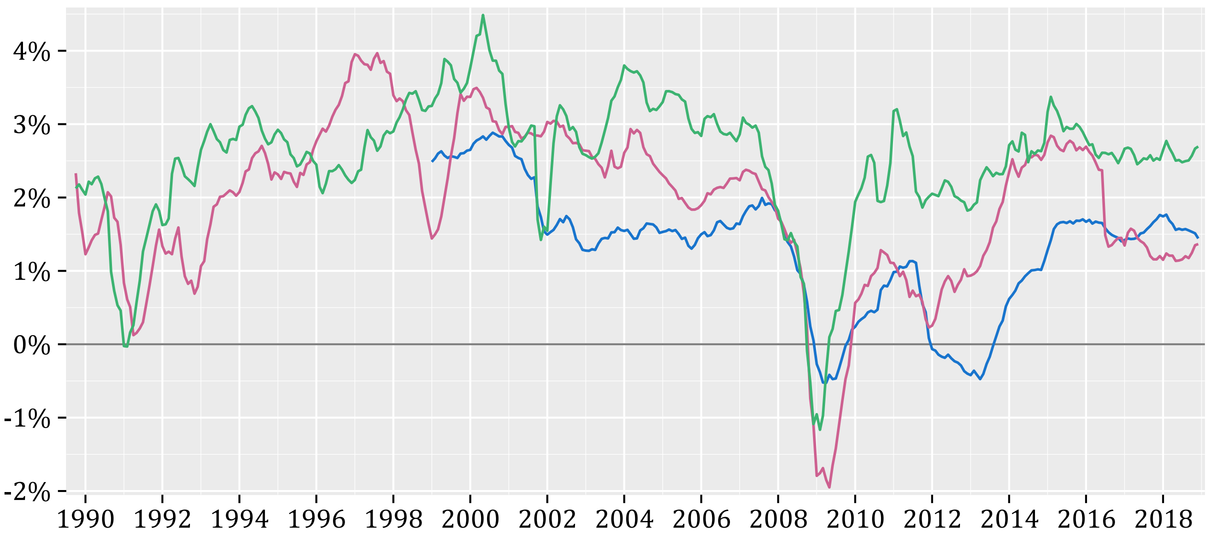

Figure 2.2: One-year ahead consumption growth mean forecasts, $E_t[c_{t+1}]$, for US (green), UK (red), and EA (blue). *Note: EA forecasts start in 01/1999.*

to the financial crisis—the UK even falling down to -2%. The EA experienced a major decline in 2012/13 as part of the euro crisis. However, the rates for all three regions stabilized in recent years.

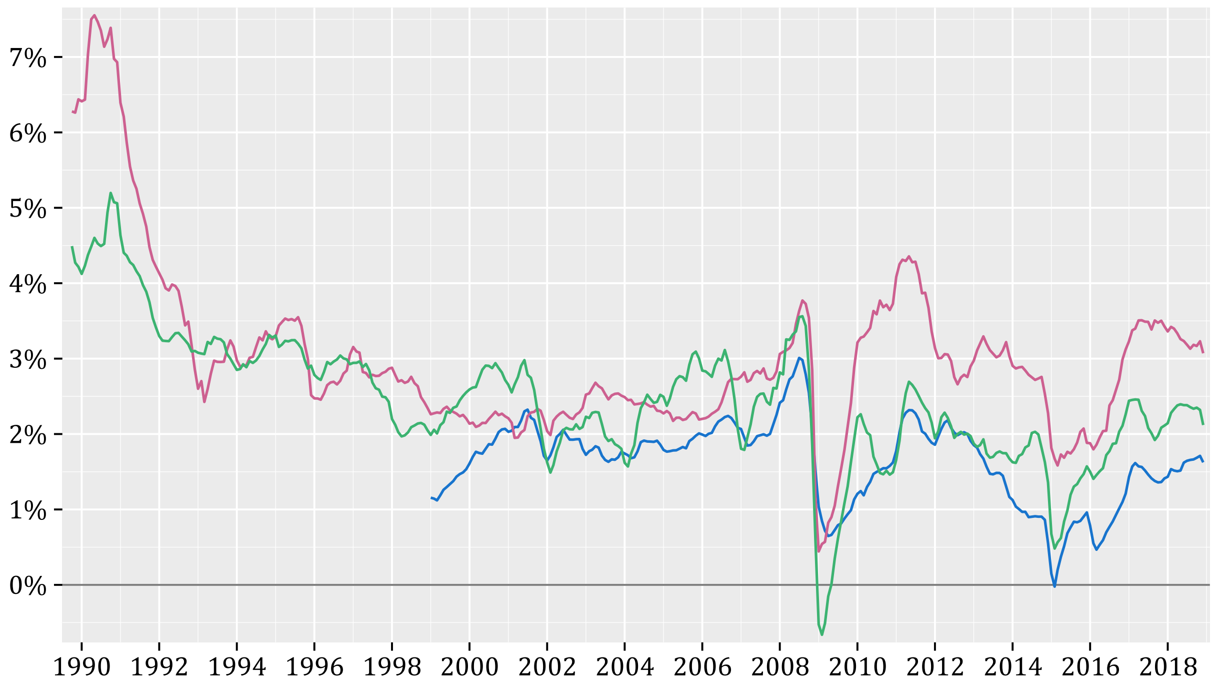

Figure 2.3: One-year ahead inflation mean forecasts, $E_t[\pi_{t+1}]$, for US (green), UK (red), and EA (blue). *Note: EA forecasts start in 01/1999.*

Figure 2.3 shows the UK's rising expected inflation due to the Lawson Boom in 1990 and a decline in the next three years. This is followed by stable rates for all economies around 1.5% to 3%. Two further events caused a simultaneous decrease.

First, in 2008, there was the financial crisis with US firms expecting even negative inflation. Second, at the end of 2014, there was the massive drop in oil prices with the three regions incipiently on different levels of inflation and only the EA expecting deflationary tendencies.

2.3.2 Interest Rates

Nominal interest rates in the model are represented by the overnight interbank rates: the EFFR (US), SONIA (UK), and EONIA (EA). Thus, i_t stands for the effective short-run averaged (or weighted) nominal interest. Since all rates are available on a daily basis, end of month values are taken to match the CF's beginning of the month values. Figure 2.4, showing the nominal rates over time, reveals the initially higher levels

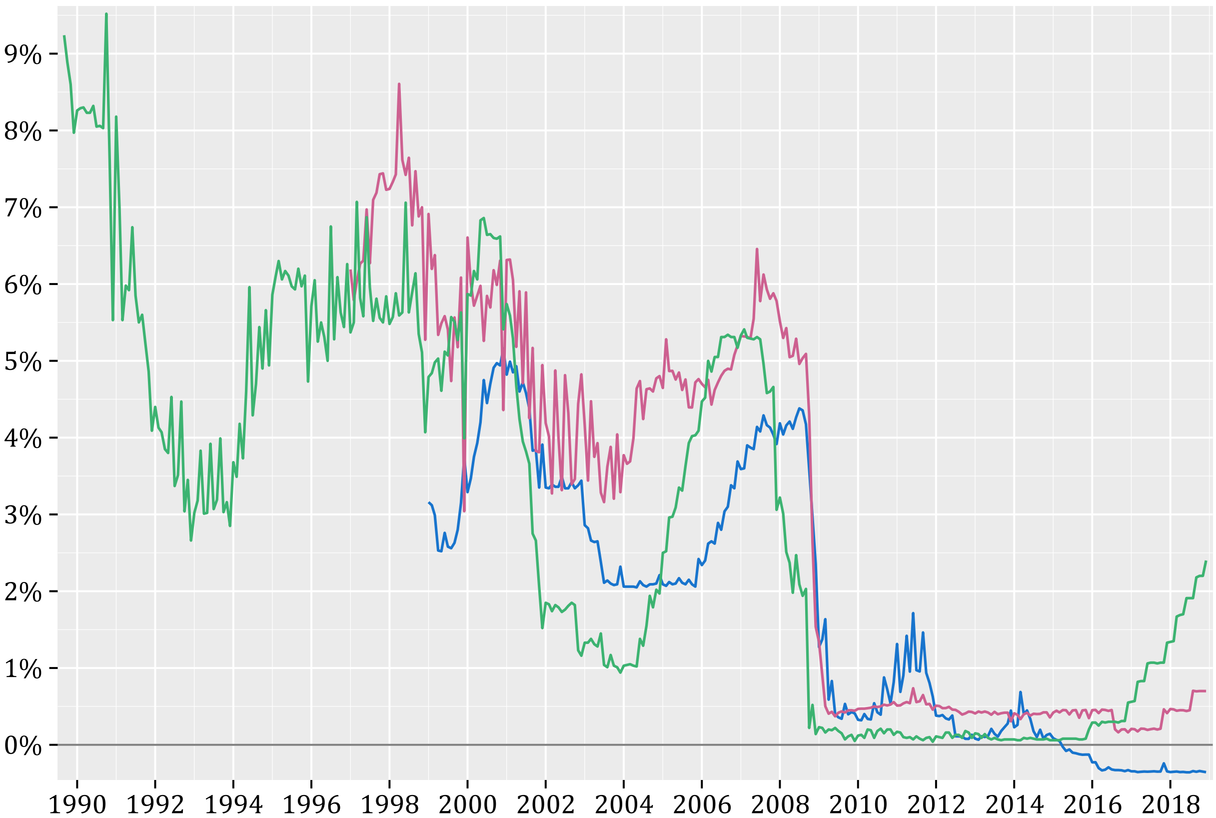

Figure 2.4: Nominal interest rates, i_t, for US (green), UK (red), and EA (blue). *Note: UK (EA) rates start in 01/1997 (01/1999).*

and more pronounced short-term volatility.[12] After a sharp decrease in 2001 (dot-com bubble), the US rate regained its previous level over the next five years. Starting in 2007/08, the consequence of the financial crisis is reflected in all three time series.

[12]The short-term fluctuations (US: until 2000, UK: 2000 – 2004) are also due to the volatile end of month values. Using an average version, however, shows no substantial differences to the results in Section 2.4.2. To be in line with other (uncertainty) measures, we stick to the end of month values.

In the process, the Fed took the leading action whilst central banks around the world aggressively cut rates. Several years near the zero lower bound, the EONIA even goes below 0% starting in 2015.[13] From 2017 on, there is a successive increase in US market rates reflecting the Fed's recent interest rate hiking cycle.

As defined in Eq.(2.3), the time-varying discount parameter, ρ_t, turns into the real interest rate, r_t. Instead of simply using a static expression, as is sometimes done in the literature, e.g., $r = 2\%$, inflation-indexed bonds serve as a proxy for the discount factor, allowing for a change over time.[14] To model a preferably long duration but, at the same time, considering the availability in each country, a ten-year time horizon is chosen. The Federal Reserve and the Bank of England provide the Treasury inflation-indexed securities and gilt-edged securities, respectively, on a daily basis. Again, as for the nominal rates, end of month values or last available values per month are calculated. As an exception, since the ECB only provides their government benchmark bond yields as monthly averages, end of month values cannot be used in this case.[15] Figure 2.5 shows the real interest rates over time. UK and EA rates appear to be downward trending, falling negative in recent years. Similarly, the US passed through a period around 2012/13 where rates dropped below 0%. The most significant increase is represented by the EA's spike in 2009 associated with the sovereign debt crisis.

[13] Market rates started to become negative in mid-2014. However, end of month values remained positive until 2015.

[14] One can interpret the long-run real rate as the Taylor rule's intercept (output equaling its potential while experiencing stable inflation) and thus, it is possible to estimate. However, this can be subject to severe limitations (see Laubach and Williams 2003). When bringing data to the theory, r_t is typically compared to inflation-indexed bonds (see Hamilton et al 2016). Gürkaynak et al (2010) give an insight into how these bonds are constructed for the US.

[15] Note that interpolation is not an option to not violate the model assumptions by including (partly) future values.

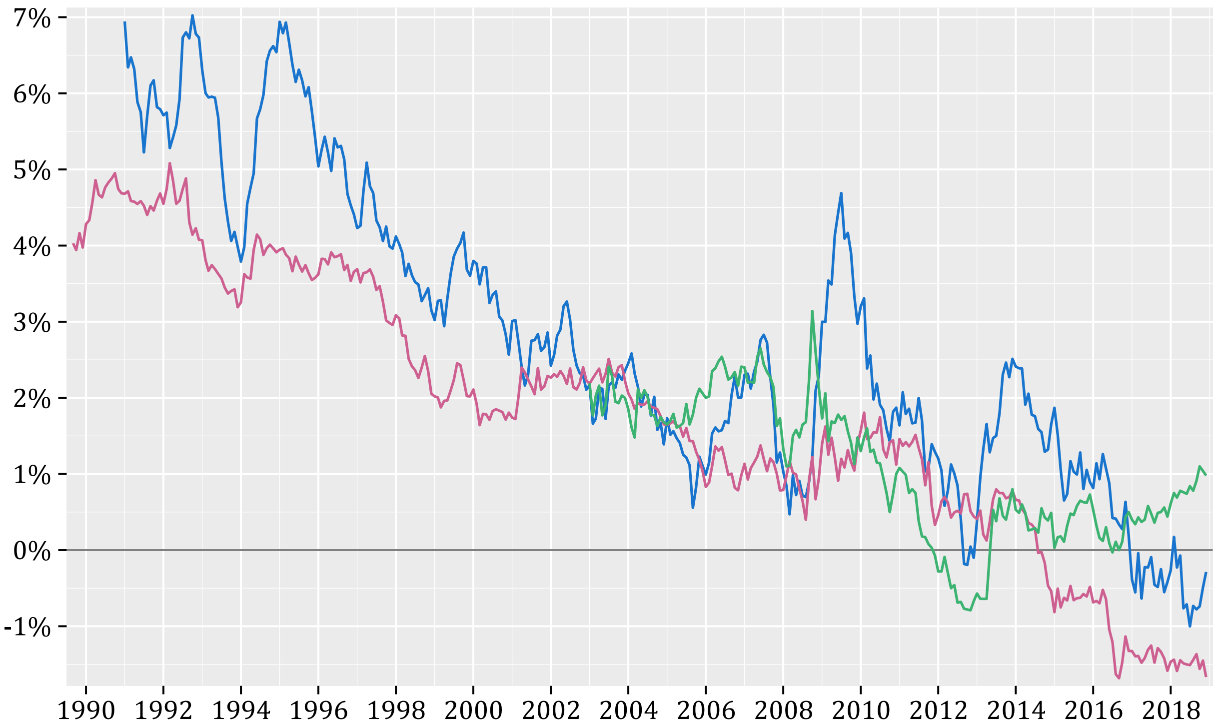

Figure 2.5: Real interest rates, r_t, for US (green), UK (red), and EA (blue). *Note: US (EA) rates start in 01/2003 (01/1991).*

Appendix B.5 lists the descriptive statistics of both CF data and interest rates.

2.3.3 Uncertainty Measures

At a second stage, uncertainty measures are supposed to explain the Euler equation's bias resulting from Jensen's inequality. These measures can be divided into internal (out of the CF data) and external measures. Table 2.1 gives an overview, whereas Tables B3–B6 provide descriptive statistics and correlation matrices.

Some additional notes regarding variable construction are worth mentioning. In the case of daily or weekly availability, end of month values are taken. The stock market's range variable consists of monthly averages but it also enables the capturing of intra-day movement. In general, the weekly St. Louis FSI is normalized. After taking end of month values, the standardization is retained. Only the measures by Rossi and Sekhposyan (2015, 2017) and Ahir et al (2018) are originally constructed on a quarterly basis and hence, are interpolated.[16]

[16]For the forecast uncertainty, values always refer to the first month of the respective quarter. The WUI is based on the Economist Intelligence Unit country reports, typically published at the beginning of the quarter. Therefore, the reference month for Q1 should be December, etc. Cubic splines are used for interpolation.

Description	Availability
Std.Dev. of CF's individual forecasts (GDP, Consumption, Inflation)	US/UK/EA
Std.Dev. of stock market indices (S&P 500, FTSE 100, Euro Stoxx 50)	US/UK/EA
Average daily range of stock market indices in % (S&P 500, FTSE 100, Euro Stoxx 50)	US/UK/EA
Stock market volatility (VIX, VFTSE, VSTOXX)	US/UK/EA
Std.Dev. of oil prices (WTI, Brent)	US/UK/EA
Financial stability indicator (St. Louis FSI, CLIFS)	US/UK/EA
Economic policy uncertainty by Baker et al (2016) (EPU)	US/UK/EA
Monetary policy uncertainty by Baker et al (2016) (MPU)	US
Macroeconomic and financial uncertainty by Jurado et al (2015)	US
Composite indicator of systemic stress by the ECB (CISS)	EA
Forecast uncertainty by Rossi and Sekhposyan (2015, 2017) (GDP, Inflation)	US/EA
World uncertainty index by Ahir et al (2018) (WUI)	US/UK/EA

Table 2.1: CLIFS stands for country-level index of financial stability and is constructed for the EA using a weighting scheme using GDP data. Brent oil is assigned to both the UK and EA, whereas the WUI is a single index, assigned to all regions.

2.4 Econometric Approach and Results

2.4.1 Elasticity of Intertemporal Substitution

Since the first study on Euler equations in economics by Hall (1978), an extensive literature covers how to capture the EIS as one of the parameters in this optimality condition. When quantifying the EIS, Beaudry and van Wincoop (1996) provide evidence that the parameter is smaller, but close to 1.0 for the US. The meta-analysis by Havranek et al (2015) shows a typical value range of 0.5–0.7 across all studies for the US, 0.3–0.5 for the UK, and 0.1–0.3 for the EA. However, in this meta-study, the standard deviation of the estimates (excluding outliers), as reported by the 33 studies published in the top five general interest economics journals, is relatively large, even reaching negative territory.

Most studies use log-linear approximations (see Carroll (2001), who criticizes this in the context of consumption Euler equations), while others prefer generalized methods of moments (GMM) as an estimation method to preserve the non-linearities. Our approach uses simple normality tests, exploiting a grid of γ-values where the parameter can be found. The idea is to utilize and account for the paper's unique setting when estimating the EIS instead of simply taking values the literature suggests.

Consulting Havranek et al (2015) for possible values for the EIS, the grid for γ^{-1} reaches from 0.01 to 10, adjusting the step fineness such that there are 1,000 equidistant steps overall. Out of Eq.(2.5), the residuals in the error term, u_t, are tested for normality for each γ^{-1}. In this maximum likelihood-type approach, the normal distribution property is met when assuming the model conditions are satisfied and the relationships are not systematically biased due to omitted variables. This results in a maximal p-value, which, given that it is large enough to not reject the H_0 of non-normality, indicates a likely value for the EIS. For normality tests, we chose Jarque-Bera for its simplicity and Lilliefors since it is a more complex Kolmogorov-Smirnov test.[17] In addition, we allow for a time-varying γ_τ, choosing the global financial crisis for all regions as the break point, resulting in 71/143/119 (120/120/120) observations in the first (second) sample for US/UK/EA.[18] For inference, bootstrapping is utilized, that is, resampling with replacement by keeping randomly 90% of the original data points for 1000 runs.

[17] In contrast to Jarque-Bera, Kolmogorov-Smirnov is a non-parametric test. As a goodness of fit test, it quantifies the distance between the empirical distribution function and the cumulative distribution function (of the normal distribution).

[18] Rolling window analysis indicates the end of 2008 (as the only structural break for all regions) as a good compromise in terms of complexity and a sufficient amount of observations for each time interval.

As in Table 2.2, both tests cannot reject the H_0 of normality in any of the cases and show substantial differences in the point estimates before and after the financial crisis. Compared to Havranek et al (2015), the pre-crisis results are similarly graded: 0.3–0.5 (US), 0.5–0.7 (UK), and 1.1–1.3 (EA). This implies that a change in interest rates drives the future aggregated consumption somewhat stronger than presumed by most articles. Post-crisis figures reaching above 1 for the UK and up to 3 for the US and the EA, accompanying a decrease in the utility function's curvature in recent years. Furthermore, in most cases, p-values show notable spikes in the indicated EIS-regions, being close to zero otherwise.

	Pre-crisis sample (until 2008)			Post-crisis sample (2009 – 2018)		
Normality Test	EIS	p-value	95% interval	EIS	p-value	95% interval
US						
Jarque-Bera	0.51	0.60	$[0.39, 0.63]$	3.06	0.76	$[2.40, 3.72]$
Lilliefors	0.33	0.72	$[0.09, 0.57]$	2.60	0.19	$[1.77, 3.43]$
UK						
Jarque-Bera	0.70	0.65	$[0.56, 0.85]$	1.87	0.73	$[1.46, 2.28]$
Lilliefors	0.54	0.14	$[0.40, 0.68]$	1.28	0.21	$[1.06, 1.50]$
EA						
Jarque-Bera	1.34	0.47	$[1.15, 1.53]$	3.00	0.87	$[2.25, 3.75]$
Lilliefors	1.11	0.40	$[0.73, 1.49]$	2.95	0.12	$[2.00, 3.90]$

Table 2.2: Results for the US, UK, and EA depending on max. p-values. Inference via bootstrapping (1000 runs) assuming t-distributed point estimates.

To eventually fully identify the Euler equation, and thereupon calculating and examining Jensen's bias in the next section, we choose the average across the normality test estimates for the EIS. However, since a change in γ (or curvature) entails a monotone transformation of the approximation quality, moderately different values do not affect the fundamental results of the main regression.

2.4.2 Approximation Bias

When comparing Euler equations, we do not evaluate the actual error as in the research by Lettau and Ludvigson (2009) but rather using another version by inserting the mean forecast values from Eq.(2.6) directly into the equation

$$\varepsilon_t^J = (1+i_t)\cdot(1+r_t)^{-1}\cdot\left(\left[(1+\mathrm{E}_t[\pi_{t+1}])^{-1}\right]\cdot\left[(1+\mathrm{E}_t[c_{t+1}])^{-\gamma}\right]+Cov\right), \tag{2.7}$$

dropping the Jensen residuals, Δ_π and Δ_c. Subtracting this from Eq.(2.5),

$$bias_t = \varepsilon_t - \varepsilon_t^J > 0, \tag{2.8}$$

results in a variable being strictly positive due to strict convexity in both functions.[19] Lastly, this leads to the main regression equation

$$bias_t = \beta_0 + \beta_1\sigma_t^{CF} + \beta_2 X_{t-1} + \varepsilon_t^{bias}, \tag{2.9}$$

allowing for an intercept which, from a theoretical point of view, should be zero when controlling for higher-order moments. Vectors β_1 and β_2 contain slope parameters regarding CF uncertainty and external uncertainty, respectively.

Tables 2.3–2.5 show the main results for the three regions. Newey and West (1987) standard errors are used across models M1 to M3.[20] For all countries, M3 denotes the full model, M2 is a variant excluding the CF's standard deviation concerning GDP due to the high correlation with its consumption growth counterpart, and M1 is an even smaller model dropping the (insignificant) stock market variables. Starting with the CF measures, the consumption growth Std.Dev. for the US (insignificant in the full model) becomes significant after dropping the GDP Std.Dev. In general, internal uncertainty has a higher impact on the bias than the other variables, usually five to ten times larger. Interestingly, the UK's inflation Std.Dev. is not significant in any model. However, other uncertainty measures out of the CF's data could fill this gap since the GDP Std.Dev is highly significant. The WUI has a positive impact for the US and in most constellations for the EA. Oil price movement is highly significant

[19]Note that the value of γ will determine the *bias*' magnitude. Since γ is closely associated with the curvature of one of the approximated expressions, the following expression necessarily holds:

$$\frac{d\mathrm{E}[bias_t]}{d\gamma} > 0.$$

To not bias the point estimates due to the structural break, we adjust the conditional means which, however, is not germane since we are interested in the variation of the *bias*-variable.

[20]Controlling for autoregressive error terms indicates highly significant serial correlation up to order 2, with other lags occasionally being significant at the 10% level.

US	M1	M2	M3
β_0	−0.00	−0.00	−0.00
	(0.01)	(0.01)	(0.01)
GDP Std.Dev.			0.44**
			(0.21)
Consump. Std.Dev.	0.55**	0.57***	0.34
	(0.24)	(0.20)	(0.22)
Infl. Std.Dev.	0.41***	0.44***	0.40***
	(0.12)	(0.14)	(0.15)
S&P Std.Dev.		0.00	0.00
		(0.00)	(0.00)
S&P Range		0.04	0.05
		(0.07)	(0.07)
VIX		−0.00	−0.00
		(0.00)	(0.00)
WTI Std.Dev.	0.04***	0.04***	0.04***
	(0.01)	(0.01)	(0.01)
STLFSI	0.06*	0.05	0.06
	(0.03)	(0.04)	(0.04)
EPU	0.02	0.02	0.01
	(0.03)	(0.04)	(0.04)
MPU	−0.00	−0.01	−0.00
	(0.02)	(0.03)	(0.03)
Macro	0.13	0.09	0.07
	(0.61)	(0.68)	(0.72)
Finance	−0.41	−0.19	−0.56
	(0.43)	(0.44)	(0.46)
Forecast	−0.03	−0.03	−0.01
	(0.09)	(0.10)	(0.10)
WUI	0.12***	0.12***	0.14***
	(0.03)	(0.03)	(0.03)
$\overline{R}^2$	0.69	0.69	0.69
AIC	−241.72	−238.78	−241.72
BIC	−203.75	−191.31	−191.08
Observations	175	175	175

Table 2.3: The measures by Baker et al (2016) and Ahir et al (2018), namely EPU, MPU, and WUI, are divided by 100 to better fit the scales of the other external uncertainty variables. All covariates are demeaned. AIC: Akaike information criterion; BIC: Bayesian information criterion. ***/**/* denote significance at the 1%/5%/10% level.

for the US, possibly illustrating their dependencies on oil. In the reduced model, the CLIFS' size for the UK is similar to the CF measures since their range is also comparable. Nevertheless, the typical interpretation—an increase by one unit—should not be overemphasized. With the weakly significant WUI for the UK, there is also a puzzling result, not fitting into the narrative. Finally, the forecast uncertainty with respect

UK	M1	M2	M3
β_0	0.00	0.00	0.00
	(0.01)	(0.01)	(0.01)
GDP Std.Dev.			0.42***
			(0.15)
Consump. Std.Dev.	0.98***	0.80***	0.63***
	(0.18)	(0.11)	(0.16)
Infl. Std.Dev.	−0.04	0.04	0.08
	(0.18)	(0.10)	(0.16)
FTSE Std.Dev.		−0.00	−0.00
		(0.00)	(0.00)
FTSE Range		0.10	0.10
		(0.06)	(0.06)
VFTSE		0.00	0.00
		(0.00)	(0.00)
Brent Std.Dev.	0.04	0.03*	0.02
	(0.03)	(0.01)	(0.02)
CLIFS	0.48**	0.16	0.20
	(0.19)	(0.16)	(0.19)
EPU	0.02	0.00	0.00
	(0.02)	(0.02)	(0.01)
WUI	−0.10*	−0.05*	−0.04
	(0.05)	(0.03)	(0.03)
$\overline{R}^2$	0.66	0.71	0.72
AIC	−188.32	−187.15	−198.01
BIC	−160.18	−149.57	−157.02
Observations	249	225	225

Table 2.4: The measures by Baker et al (2016) and Ahir et al (2018), namely EPU and WUI, are divided by 100 to better fit the scales of the other external uncertainty variables. All covariates are demeaned. AIC: Akaike information criterion; BIC: Bayesian information criterion. ***/**/* denote significance at the 1%/5%/10% level.

to GDP is significant for the EA across all specifications, which could partly account for the institutions' priorities when participating in the CF's surveys. However, it is difficult to determine the quantitative impact relative to other variables due to the non-standardized scales.[21]

[21] In order to not exaggerate the interpretation of uncertainty, we refrained from standardizing the covariates in terms of their respective standard deviations.

EA	M1	M2	M3
β_0	−0.00	−0.00	−0.00
	(0.00)	(0.00)	(0.01)
GDP Std.Dev.			−0.21
			(0.22)
Consump. Std.Dev.	0.29***	0.36***	0.49**
	(0.09)	(0.12)	(0.22)
Infl. Std.Dev.	0.50***	0.38***	0.41***
	(0.07)	(0.12)	(0.09)
ESTOXX Std.Dev.		0.00	0.00
		(0.00)	(0.00)
ESTOXX Range		0.04	0.03
		(0.06)	(0.05)
VSTOXX		−0.00	−0.00
		(0.00)	(0.00)
Brent Std.Dev.	−0.01	−0.01	−0.01
	(0.00)	(0.00)	(0.01)
CLIFS	0.05	−0.09	−0.00
	(0.11)	(0.19)	(0.15)
EPU	0.03	0.01	0.01
	(0.02)	(0.02)	(0.02)
CISS	0.04	0.02	0.03
	(0.06)	(0.08)	(0.08)
Forecast Infl.	0.08	0.09	0.11
	(0.07)	(0.08)	(0.08)
Forecast GDP	0.10**	0.12**	0.12*
	(0.04)	(0.05)	(0.06)
WUI	0.07	0.09**	0.09**
	(0.04)	(0.04)	(0.04)
$\overline{R}^2$	0.56	0.57	0.57
AIC	−276.41	−277.44	−277.95
BIC	−240.35	−231.55	−228.77
Observations	196	196	196

Table 2.5: The measures by Baker et al (2016) and Ahir et al (2018), namely EPU and WUI, are divided by 100 to better fit the scales of the other external uncertainty variables. All covariates are demeaned. AIC: Akaike information criterion; BIC: Bayesian information criterion. ***/**/* denote significance at the 1%/5%/10% level.

2.5 Conclusions

In this paper, we derived a forward-looking consumption Euler equation in two, slightly different versions. First, the functional form was completely preserved when bringing data to the theory. This includes the usage of individual forecasts by inserting them into the expectation value without ignoring Jensen's inequality. Second, exactly this concept is ignored while using mean forecasts, replacing all expectation values. Subtracting both Euler versions, the resulting bias was then regressed on a variety of (lagged) uncertainty measures to control for the connection between theoretical and empirical higher-order moments.

Our analysis sheds some light on this kind of approximation. First, uncertainties with respect to inflation forecasts better explain the approximation bias than their counterparts regarding consumption growth. Second, uncertainty stemming from the data itself, the cross-sectional Std.Dev., plays a predominant role, exceeding the explanatory power of the external sources. Third, in the latter group of covariates, the World Uncertainty Index by Ahir et al (2018) and oil price volatility (both for the US), the ECB's financial stability indicator (for the UK), and the forecast uncertainty index regarding GDP by Rossi and Sekhposyan (2017) (EA) show a significant impact, which can also refer to the surveyed institutions' priorities when the Consensus Forecasts were conducted.

As open avenue, implementing the individual forecasts as truly forward-looking by adding an error term was not considered in the current paper. Carrying out research on the distribution of these errors could reflect the model's assumptions more appropriately. The bias in our setting was relatively small, rarely exceeding 10 basis points. Further research, both theoretical and empirical, can investigate the bias' quantity in a variety of models. This brings up a question to address in future research: Ultimately, to what extent does the data structure play a role such that the residuals are significantly large to bias estimated parameters?

Appendix B

Table of Contents

B.1 Euler Equation – Calculation Steps

The optimization problem uses the constraint

$$C_t \cdot P_t + B_{t+1} = W_t + (1 + i_{t-1}) \cdot B_t, \tag{B1}$$

with W_t as the nominal wage and B_t as the nominal value of bonds. The latter provides the link between two periods. Depending on the definition of the interest rate, the horizon can vary. Since the right-hand side of Eq.(B1) represents the disposable income in period t, B_t is the investment by households starting in period $t-1$ by the interest-bearing condition i_{t-1}.

Dynamic Programming uses the additively separable utility function and the envelope theorem to set up optimality conditions for two consecutive periods. The procedure can be divided into three parts. The first part is to write a value function, the Bellman equation. Under the assumption that the second term of the expanded utility

$$U(C_t) + E_t\left[\sum_{s=t+1}^{\infty} \rho_s^{s-t-1} U(C_s)\right] \tag{B2}$$

is maximized in period t, the Bellman equation is

$$V(B_t) \equiv \max_{C_t} \{U(C_t) + \rho_t V(B_{t+1})\}. \tag{B3}$$

The expected value vanishes since B_{t+1} is determined by variables in period t in the constraint. Differentiating with respect to C_t gives the first-order condition

$$\frac{dU(C_t)}{dC_t} + \rho_t \frac{dV(B_{t+1})}{dB_{t+1}} \frac{dB_{t+1}}{dC_t} = 0, \tag{B4}$$

which results, when including Eq.(B1), in

$$\frac{dU(C_t)}{dC_t} = P_t \rho_t \frac{dV(B_{t+1})}{dB_{t+1}}. \tag{B5}$$

Eq.(B5) relates the marginal utility to the marginal value in the following period, the time preference, and prices in the same period. Therefore, a higher ρ_t and P_t results in a lower C_t.

In the next part, the envelope theorem is used to differentiate the value function (by inserting the optimized C_t^*) with respect to the costate variable B_t:

$$V(B_t) = U(C_t^*) + \rho_t V(B_{t+1}) \tag{B6.1}$$

$$\Rightarrow \quad \frac{dV(B_t)}{dB_t} = \rho_t \frac{dV(B_{t+1})}{dB_{t+1}} \cdot \frac{dB_{t+1}}{dB_t} \tag{B6.2}$$

$$\Leftrightarrow \quad \frac{dV(B_t)}{dB_t} = \rho_t \frac{dV(B_{t+1})}{dB_{t+1}} \cdot (1 + i_{t-1}). \tag{B6.3}$$

Eq.(B6.3) reveals the relationship of the marginal value functions.

In a third step, the first-order condition (B5) can be used to replace the value functions in Eq.(B6.3) with the marginal utility in both periods t and $t-1$:

$$\frac{dU(C_{t-1})}{dC_{t-1}} \frac{1}{P_{t-1}\rho_{t-1}} = \rho_t \cdot \frac{dU(C_t)}{dC_t} \frac{1}{P_t \rho_t} \cdot (1 + i_{t-1}) \tag{B7.1}$$

$$\Rightarrow \quad \frac{dU(C_t)}{dC_t} = \rho_t \cdot (1 + i_t) \cdot E_t \left[\frac{P_t}{P_{t+1}} \frac{dU(C_{t+1})}{dC_{t+1}} \right]. \tag{B7.2}$$

The time shift yields the Euler condition.

B.2 Constant Relative Risk Aversion – Utility Function

The CRRA-function,

$$U(C) = \frac{C^{1-\gamma} - 1}{1-\gamma}, \quad \gamma > 0, \tag{B8}$$

transforms into a root-, log-, or inverse hyperbolic-form, depending on the value of γ. For $\gamma \in \,]0,1[$, a root-function appears, for example the square root:

$$U(C \mid \gamma = 0.5) = 2(\sqrt{C} - 1). \tag{B9}$$

Log-utility ($\gamma = 1$) can be considered as a special case since l'Hôpital's rule is needed to reveal the ratio between the limit values in numerator and denominator:

$$U(C \mid \gamma = 1) = \lim_{\gamma \to 1} \frac{C^{1-\gamma} - 1}{1 - \gamma} = \lim_{\gamma \to 1} \frac{\log(C) \cdot C^{1-\gamma} \cdot (-1)}{-1} = \log(C). \tag{B10}$$

Finally, a hyperbolic-form, mirrored at the abscissa, emerges for $\gamma > 1$:

$$U(C \mid \gamma = 2) = \frac{C^{-1} - 1}{-1} = -\frac{1}{C} + 1. \tag{B11}$$

Note that for all cases, a positive utility is only assured if more than one unit is consumed.

B.3 Covariances of Transformed Random Variables

The idea is to show the substantial difference in the correlation after transforming two random variables (RV's). Figure B1 compares the correlation of repeated draws between two (i) normally-distributed and (ii) the inverse of normal-distributed RV's. Inverting the variables as transformation is chosen because it is relatively simple and basically matches the non-linearities in Eq.(2.5). Per repetition, 30 RV's are drawn since this roughly corresponds to the number of observations per cross-section, presented in Section 2.3. We calculate the correlation as standardized covariance, otherwise outliers would distort the density function.

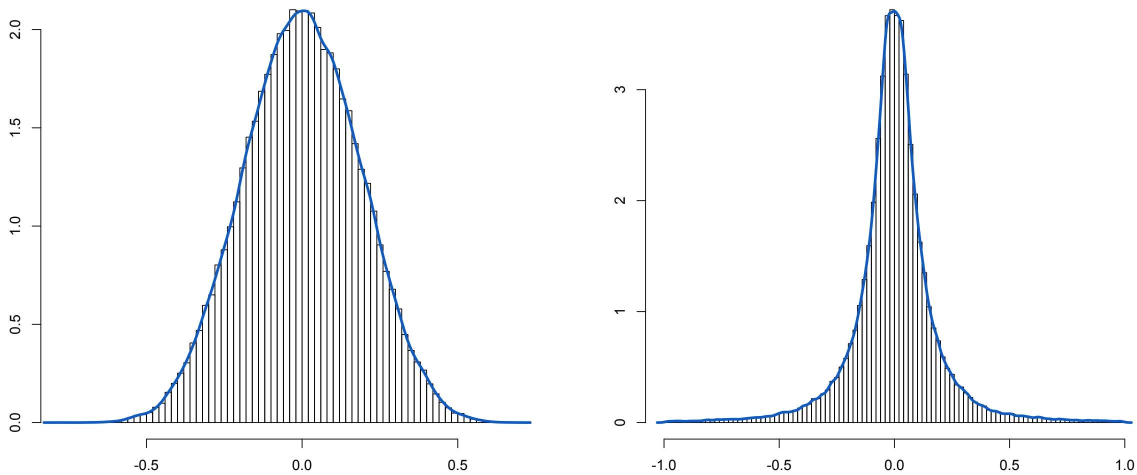

Figure B1: Resulting correlation with 10^5 repetitions, each with 30 draws. Distributions: Standard-Normal (left) and inverted Standard-Normal (right).

While the second moments are equal (Std.Dev. = 0.2), the kurtosis shows a fundamental difference: 2.8 (non-transformed) vs. 8.1 (transformed).

B.4 Euro Area – Weighting Scheme

Weighting of EA countries (France, Germany, Italy, Netherlands, and Spain) is conducted from January 1999 to November 2002. Seasonal- and calendar-adjusted real GDP data from Eurostat show that these five countries contribute around 86% to the EA's GDP. Over time, there is a slight downward trend and a minor structural break in 2001 when Greece joined the euro zone. Quarterly GDP data are converted to a monthly basis via linear interpolation. The weighting scheme is as follows:

$$\mu_{EA} = \sum_{i=1}^{5} \kappa_i E[\mathcal{Y}_i] = E[\lambda \mathcal{Y}], \tag{B12}$$

where κ_i are GDP-weights with $\sum_{i=1}^{5} \kappa_i = 1$ and λ, the firm level weights for each country (depending also on number of firms: $\lambda_i = (N/N_i) \cdot \kappa_i$), is needed to insert the individual forecasts directly into the expectation value, i.e., $E[(1+\lambda\mathcal{Y})^{-\gamma}]$.

Using this method for the period after 11/2002 shows no substantial difference, when comparing with the actual values for the EA.

B.5 Descriptive Statistics

Euler Equation Data	Mean (%)	Std.Dev. (pp)	Min. (%)	Max. (%)
Personal Consumption (US)	2.52	0.87	-1.17	4.49
Household Consumption (UK)	1.92	1.08	-1.95	3.97
Private Consumption (EA)	1.31	0.84	-0.53	2.88
Consumer Prices (US)	2.46	0.87	-0.66	5.2
Retail Prices (UK)	3.01	1.14	0.44	7.55
Consumer Prices (EA)	1.62	0.53	-0.02	3.01
Effective FFR (US)	3.07	2.55	0.04	9.52
SONIA (UK)	3.02	2.53	0.16	8.61
EONIA (EA)	1.7	1.7	-0.36	5.16
Inflation-Indexed Security (US)	1.07	0.89	-0.79	3.14
Inflation-Indexed Bond (UK)	1.82	1.75	-1.68	5.08
Gov. Benchmark Bond Yield (EA)	2.74	1.98	-1	7.02

Table B1: Consumption and price level measures are represented as one-year ahead expected growth rates.

CF Uncertainty	Mean	Std.Dev.	Min.	Max.	CV
GDP Std.Dev. (US)	0.3	0.11	0.13	0.7	0.37
GDP Std.Dev. (UK)	0.37	0.12	0.17	0.76	0.32
GDP Std.Dev. (EA)	0.27	0.14	0.08	0.7	0.51
Consumption Std.Dev. (US)	0.29	0.1	0.11	0.77	0.34
Consumption Std.Dev. (UK)	0.48	0.17	0.18	1.12	0.36
Consumption Std.Dev. (EA)	0.31	0.15	0.12	0.7	0.49
Prices Std.Dev. (US)	0.28	0.1	0.11	0.92	0.35
Prices Std.Dev. (UK)	0.33	0.17	0.1	1.12	0.5
Prices Std.Dev. (EA)	0.24	0.18	0.06	0.77	0.76

Table B2: Consensus Forecasts uncertainty measures are based on the one-year ahead expected growth rates. The last column shows the coefficient of variation.

Uncertainty Measures	Mean	Std.Dev.	Min.	Max.	CV
S&P 500 Std.Dev. (US)	18.85	14.41	1.42	111.41	0.76
FTSE 100 Std.Dev. (UK)	79.76	49.35	11.09	335.78	0.62
Euro Stoxx 50 Std.Dev. (EA)	55.37	40.31	4.75	245.33	0.73
S&P Avg. Daily Range (US)	1.24	0.69	0.37	6.62	0.55
FTSE Avg. Daily Range (UK)	1.28	0.67	0.53	5.95	0.52
EStoxx Avg. Daily Range (EA)	1.69	0.84	0.6	5.88	0.5
VIX (US)	19.29	7.42	9.51	59.89	0.38
VFTSE (UK)	19.19	7.68	9.55	54.15	0.4
VSTOXX (EA)	23.93	8.81	11.99	61.34	0.37
WTI Std.Dev. (US)	1.64	1.35	0.15	11.29	0.82
Brent Std.Dev. (UK/EA)	1.64	1.31	0.16	10.79	0.8
St.Louis FSI (US)	0	1	-1.53	4.71	-
CLIFS (UK)	0.12	0.09	0.01	0.56	0.78
Weighted CLIFS (EA)	0.12	0.08	0.03	0.42	0.66
EPU (US)	113.79	43.05	44.78	284.25	0.38
EPU (UK)	119.66	68.77	24.04	558.22	0.57
EPU (EA)	131.35	61.48	45.3	433.28	0.47
MPU (US)	106.14	50.84	12.8	362.44	0.48
Macro Uncertainty (US)	0.91	0.05	0.85	1.15	0.05
Financial Uncertainty (US)	0.98	0.05	0.91	1.13	0.05
Systemic Stress (EA)	0.18	0.16	0.02	0.8	0.92
Forecast Uncertainty (US)	0.73	0.13	0.49	1.01	0.17
Forecast Inf. Uncertainty (EA)	0.75	0.14	0.45	1.02	0.18
Forecast GDP Uncertainty (EA)	0.75	0.14	0.51	1	0.19
World Uncertainty Index	122.63	37.67	63.76	250.52	0.31

Table B3: The last column shows the coefficient of variation, only differing by a small amount across related variables. CLIFS is an index of financial stability by the ECB. EPU and MPU are the Baker et al (2016) uncertainty measures. Macroeconomic and Financial Uncertainty are the indices by Jurado et al (2015). Systemic Stress is an indicator provided by the ECB. Originally, the Forecast Uncertainty data by Rossi and Sekhposyan (2015, 2017) are standardized such that the maximum is 1. Slightly larger values in our data are due to interpolation. Interestingly, there is no or weak negative correlation between these measures. The correlation between all other related variables across regions is as expected: positive and significant (available on request). The World Uncertainty Index comes from the paper by Ahir et al (2018).

B.6 Correlation – Uncertainty Measures

US	S&P	S&P_R	VIX	WTI	FSI	EPU	MPU	Macro	Fin.	Rossi
S&P	1	-	-	-	-	-	-	-	-	-
S&P_R	**0.6**	1	-	-	-	-	-	-	-	-
VIX	**0.49**	**0.9**	1	-	-	-	-	-	-	-
WTI	**0.45**	**0.45**	**0.37**	1	-	-	-	-	-	-
FSI	0.11	**0.68**	**0.67**	0.08	1	-	-	-	-	-
EPU	**0.45**	**0.39**	**0.39**	**0.32**	-0.04	1	-	-	-	-
MPU	**0.23**	0.07	0.06	-0.04	-0.08	**0.48**	1	-	-	-
Macro	**0.36**	**0.63**	**0.6**	**0.59**	**0.55**	**0.23**	-0.06	1	-	-
Fin.	**0.46**	**0.76**	**0.83**	**0.31**	**0.64**	**0.3**	-0.02	**0.65**	1	-
Rossi	0.03	**0.14**	**0.19**	-0.08	**0.17**	**0.16**	0.05	0.1	**0.18**	1
WUI	**0.13**	**-0.28**	**-0.29**	**0.14**	**-0.62**	**0.44**	**0.37**	**-0.21**	**-0.36**	0.08

Table B4: S&P and WTI are the monthly standard deviations. S&P_R are monthly averages of the daily range in percent (S&P 500). FSI is the St. Louis Financial Stress Index. EPU and MPU are the Baker et al (2016) uncertainty measures. Macro (Macroeconomic Uncertainty) and Fin. (Financial Uncertainty) are the uncertainty measures by Jurado et al (2015). Rossi is the forecast uncertainty by Rossi and Sekhposyan (2015). WUI is the World Uncertainty Index by Ahir et al (2018). Numbers in bold denote significance at the 5% level.

UK	FSTE	$FSTE_R$	VFTSE	Brent	CLIFS	EPU
FSTE	1	-	-	-	-	-
$FSTE_R$	**0.76**	1	-	-	-	-
VFTSE	**0.65**	**0.93**	1	-	-	-
Brent	**0.39**	**0.43**	**0.28**	1	-	-
CLIFS	**0.38**	**0.56**	**0.6**	**0.32**	1	-
EPU	**0.2**	**0.21**	**0.13**	**0.17**	**0.18**	1
WUI	0	-0.11	**-0.26**	**0.18**	**-0.18**	**0.59**

Table B5: FTSE and Brent are the monthly standard deviations. $FSTE_R$ are monthly averages of the daily range in percent (FTSE 100). CLIFS is an index of financial stability by the ECB. EPU is the Baker et al (2016) uncertainty measure. WUI is the World Uncertainty Index by Ahir et al (2018). Numbers in bold denote significance at the 5% level.

EA	EStoxx	EStoxx$_R$	VStoxx	Brent	CLIFS	EPU	CISS	INF	GDP
EStoxx	1	-	-	-	-	-	-	-	-
EStoxx$_R$	**0.7**	1	-	-	-	-	-	-	-
VStoxx	**0.62**	**0.92**	1	-	-	-	-	-	-
Brent	**0.32**	**0.2**	**0.18**	1	-	-	-	-	-
CLIFS	**0.4**	**0.72**	**0.75**	**0.31**	1	-	-	-	-
EPU	**0.15**	**0.15**	**0.13**	**0.29**	**0.14**	1	-	-	-
CISS	**0.37**	**0.59**	**0.61**	**0.48**	**0.79**	**0.15**	1	-	-
INF	-0.12	**-0.21**	**-0.21**	**0.31**	-0.05	0.11	0.06	1	-
GDP	**0.27**	**0.24**	**0.25**	**0.27**	**0.28**	-0.12	**0.36**	-0.1	1
WUI	-0.1	**-0.13**	**-0.14**	**0.18**	**-0.16**	**0.78**	-0.12	**0.18**	**-0.38**

Table B6: EStoxx and Brent are the monthly standard deviations. EStoxx$_R$ are monthly averages of the daily range in percent (ESTOXX 50). CLIFS is an index of financial stability by the ECB. EPU is the Baker et al (2016) uncertainty measure. INF and GDP are forecast error measures by Rossi and Sekhposyan (2017). WUI is the World Uncertainty Index by Ahir et al (2018). Numbers in bold denote significance at the 5% level.

3 The Extent of Jensen's Inequality

"Evaluating the Approximation Bias in Forward-Looking DSGE Models"

Abstract

Occurring in non-linear, forward-looking models, we evaluate a source of error of the type: $\mathrm{E}[f(X)] \approx f(\mathrm{E}[X])$. Since the difference is negligible in typical DSGE models, we explore settings in which this can become a liability. For that purpose, an illustrative model containing growth rates, calibrated via Consensus Forecasts (CF), is utilized in a way that the magnitude of the inequality can be determined in basis points. In a simulation-based analysis, we investigate the accuracy depending on the empirical standard deviation and the function's curvature. Our findings show that the difference is reaching up to 25 or 30 basis points. In addition, we analytically solve for a baseline case, showing that the difference depends on the standard deviation in a quadratic way. Finally, the number of variables and the correlation between them is taken as further influence on the approximation bias. In cases with over five highly-correlated variables, a difference of over 25 basis points can be reached. As a general result, the bias' relation is nearly linear to the data's (co)variance and exponential to both the curvature and the number of variables. Taking this source of error into account, the economist's attention should be on how a model is built and not so much on the data itself. This can be important especially for large-scale models.

3.1 Introduction

In a recent article, Lindé (2018) discusses the usefulness of DSGE models in policy analyses in the aftermath of the 2007–2008 financial crisis. Despite weaknesses in these models, he argues that improved versions will play an important role for a long time to come—at least for smaller policy institutions. He explains that DSGE models are advantageous for smaller entities because more sophisticated models are extremely costly, requiring both advanced human resources and full data access and availability. This usefulness extends to central banks in developing and emerging countries, yet to a lesser degree to central banks in developed countries. Therefore, smaller institutions are reliant upon well-known workhorses in the process of building up their technical analysis apparatus. In the same vein, by discussing challenges when evaluating these models, Fernández-Villaverde et al (2016), Schorfheide (2013), and Christiano et al (2011) highlight their (future) importance. This underpins the potential of further scrutinizing models from the "simpler" DSGE family.

In our work, we add another puzzle piece by examining situations in which forward-looking behavior encircles a non-linear transformation. In the time dimensional context of DSGE models, the conditional expectation usually spans from one period to the next after solving for the first-order conditions. Moving on by log-linearizing, the non-linearities typically resolve and only the function's parameters—multiplied by an expectation value containing growth rates—remain.[1] This method is utilized in many studies, whereby Fernández-Villaverde (2010) and Sbordone et al (2010) provide a good introduction. As a consequence, models obtain the certainty equivalence property. This sophisticates or suppresses the impact of second (and higher) moments like risk, volatility, or uncertainty.[2] These are measures that play an important role in financial crisis scenarios. To fix this, higher-order approximations are a practicable way, but how exactly to incorporate the additional moments can be arbitrary. Avoiding this caveat, in a scenario alike, is equivalent to considering Jensen's inequality.[3] To account for this, we label any changes that are made to the originally derived model equations, *approximation bias*.

To the best of our knowledge, there is no literature dealing with this specific problem. There are, however, a large number of articles dealing with workarounds, e.g., Sargent (1987) and Ljungqvist and Sargent (2012), or sophisticated approximation methods, e.g., Judd (1998) and Aruoba et al (2006).[4] Two main reasons could account for Jensen's inequality being underrepresented in macroeconomics. First, the resulting error (or approximation bias) is very small in the context of DSGE models. Nonetheless, we aim to see the whole picture and examine several scenarios with a wide variety of parameter values. This gives a good impression in which situations caution is advised. Second, it is challenging (or almost impossible) to find a whole distribution of future values to bring the model to the data as originally intended. In this case, we argue that there is no necessity to have raw data at hand. It is sufficient to calibrate certain parameters concerning the data and to translate model assumptions into

[1] E.g., $\mathrm{E}_t[(X_{t+1}/X_t)^\eta] \Rightarrow \log \mathrm{E}_t[(X_{t+1}/X_t)^\eta] \approx \eta \mathrm{E}_t[\widehat{x_{t+1}}]$.

[2] See the technical paper by Straub and Ulbricht (2019) for a discussion on the connection between theoretical and empirical second moments.

[3] Note that ignoring Jensen's inequality as an approximation technique is different from (non-linear) Taylor expansion. We show this in Section 3.2.

[4] Sargent (1987, 32) resolves the future consumption (in the context of the Euler condition) at time $t+1$ into variables in time t, with the interest rate as a stochastic element that can be overcome with the unconditional expectation value. Aruoba et al (2006, 2484) compare several approximation methods for Euler equations, among them perturbation up to order five.

parameters. Therefore, we build a small-sized model that could be part of an Euler condition or a similar intertemporal connection, which can be found in every DSGE model—for instance in Christiano et al (2011, 290) and Schorfheide (2013, 219). In this framework, we derive an analytical solution describing the approximation bias, interpreted in basis points. To assess the variability of the theoretical results we also conduct Monte Carlo (MC) simulations.

Emerging from a slightly altered Jensen's inequality—for a cleaner economic interpretation—the illustrative model consists of two terms of weighted (or transformed) growth rates, $f(\mathrm{E}_t[gr_{t+1}])$ and $\mathrm{E}_t[f(gr_{t+1})]$.[5] The first term simply contains the expected growth rate transformed by a non-linear function. The same function weights the future growth rates in the second term and only afterwards the expectation value is calculated. Subtracting these terms results in the approximation bias measured in basis points. Also, the future growth rates follow a log-normal distribution in our baseline case and an inverted-beta distribution in a robustness check. We will cover this in more detail in the next section. In a final step, we increase the number of variables to emulate large-scale models. Prominent references in this context are the IMF's Global Projection Model (Carabenciov et al 2013) and the ECB-Global (Dieppe et al 2018). The latter contains over 800 parameters.

In our model, the different parameters can be assigned to five categories: (i) first moments of the future growth rates, (ii) second moments of the future growth rates, (iii) the curvature of the non-linear function, (iv) the number of variables or the model size, and (v) the number of possible future states or the number of drawn random variables (RV's) per repetition in the MC simulation. Although the mean plays an important role in the analytical solution, the impact of realistic values is negligible. The second moments, consisting of the standard deviation in a univariate case and the correlation in a multivariate case, show a mixed picture. While the latter plays a minor role, even counteracting the bias for negatively correlated variables, large values for the standard deviation produce a serious approximation bias. The third category, the degree of curvature, can be associated with risk aversion or elasticity measures in an economic context.[6] In our model, for a realistic range of values, the outcome is very similar to the impact of the standard deviation. Augmenting the model in a multiplicative way, we add variables to check the influence of the model's size. By including ten variables when assuming a weak, positive correlation in the data, we find a similar result to that of large values for standard deviation and curvature. Except for the last

[5] Note that the growth rates, gr, will be centered around unity.

[6] See Bollerslev et al (2011), Chetty (2006), and Morin and Suarez (1983) for a discussion of the practical application and estimation of the level of risk aversion.

category (the number of future states), the simulated distributions of the approximation bias draw a similar picture, with a constant increase in their second moment and a weak, right-tail property. Increasing the number of (potential) future states, however, decreases the third moments of the initially heavily skewed distributions toward zero. Also, the distributions contract slowly to ideal values of the analytical solution.

As a general result, the approximation bias' relation is nearly linear to the data's (co)variance and exponential to both the curvature and the number of variables. Moreover, the mean of the simulated distributions converges to the analytical result from below when allowing for more possible future states. In most setups, the bias is smaller than ten basis points, which confirms the insignificant role of this issue in the literature. However, taking up the focus on frontier markets as a cost-efficient usage for DSGE models, some of the discussed parameters can become significantly large and, therefore, justify a closer examination.

The remainder of this paper is organized as follows. Section 3.2 explains Jensen's inequality more carefully and how it is used to establish our illustrative model. In addition, the non-linear function and the utilized distributions are introduced. Section 3.3 derives an analytical solution for the baseline case, subsequently discussing and interpreting the results. Section 3.4 presents the data and the calibration method. Section 3.5 shows the simulation results, depending on uncertainty (standard deviation), the degree of non-linearity (curvature), number of future states (number of drawn RV's), correlation (covariance), and model size (number of variables). Section 3.6 concludes.

3.2 Theoretical Framework

3.2.1 Preliminary Consideration

Apart from the actual, numerical difference, Jensen's inequality is well studied in the sole mathematical context.[7] Shifting into economical terrain, decision theory in particular examines how the expectation value has to be altered such that an equal sign can be applied:

$$\mathrm{E}[f(X)] = f(\mathrm{E}[X] + \tilde{x}), \tag{3.1}$$

where $\tilde{x}$ stands for the risk premium, which can be positive or negative, depending on the curvature of the non-linear function, f. In contrast, we aim to describe the actual degree of the inequality. To account for this difference, we define

$$\begin{aligned} & \mathrm{E}[f(X)] &= f(\mathrm{E}[X]) + \Delta_X \qquad (3.2.1)\\ \Leftrightarrow \quad & \Delta_X &= \mathrm{E}[f(X)] - f(\mathrm{E}[X]), \qquad (3.2.2) \end{aligned}$$

where the LHS of Eq.(3.2.1) shows the actual value and the RHS shows the approximated value plus the bias. When f is convex (concave) the residual Δ is positive (negative).

Considering approximation techniques in general, only first-order Taylor expansion makes Jensen's inequality redundant. The second-order version already leaves a distinction between $\mathrm{E}[f(X)]$ and $f(\mathrm{E}[X])$ for non-linear functions. Although—after a quadratic approximation—both expressions contain a measure for the curvature, the latter is always smaller for convex functions.[8] For this reason, to not dilute the results by other approximations, our model originates from the basic inequality.

Going one step further, a juxtaposition of Jensen and Taylor helps to visualize the methodology. Therefore, Figure 3.1 compares both sources of inaccuracy. Due to graphical clarity, the expectation values are stemming from only two points on the function, respectively. However, taking a (continuous) distribution does not change the basic result. To further depict the difference, one could imagine an additional curve (as the dashed line on the right side) passing through the intersections of the compatible dotted lines, showing a smaller difference the less curved the black line is (left to right). In this example, this holds true even when the range of the x_i increases from left to right. Also, in contrast to the second-order Taylor polynomial (Figure 3.1,

[7] Jensen's inequality for convex functions is: $f(\mathrm{E}[X]) \leq \mathrm{E}[f(X)]$. See, for example, Mitrinović et al (1993) for an examination of continuous and multivariate versions and the connection to other inequalities.

[8] See Appendix C.1 for the proof, taking advantage of the inequality of arithmetic and geometric means (AM-GM).

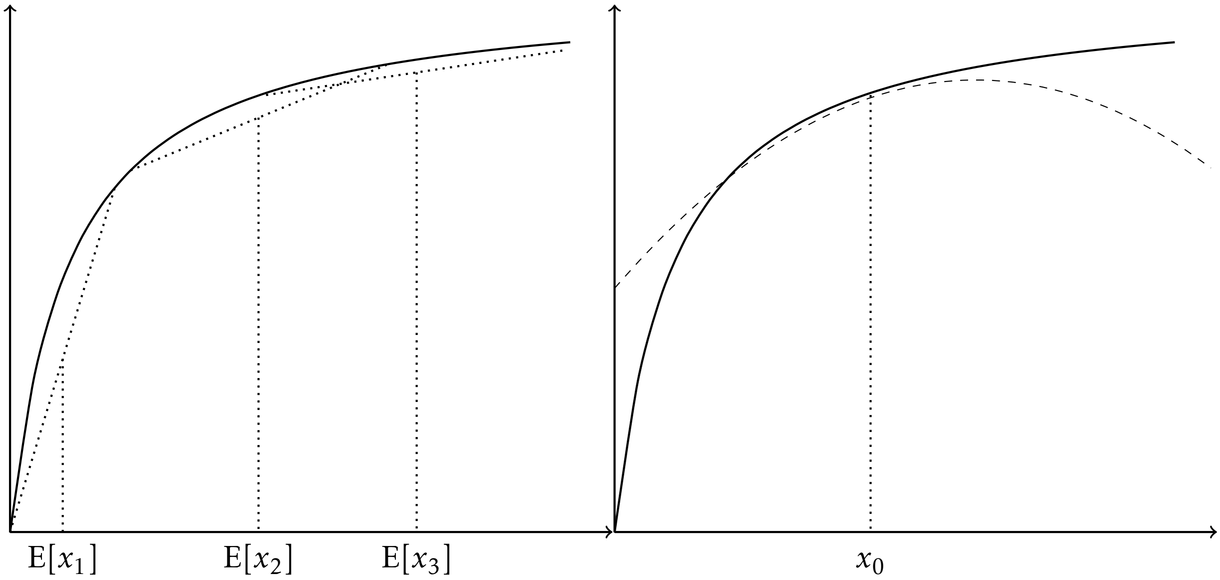

Figure 3.1: On the left side (Jensen), the approximation bias (Δ) is displayed as the vertical difference between the non-linear function (black line) and the intersection of the compatible dotted lines. On the right side (2^{nd}-order Taylor), the difference between the black and dashed line shows the inaccuracy. (The three expectation values and the evaluation point, x_0, are arbitrarily chosen.)

right side, dashed line), the Δ are always negative with the sign depending on the function's concavity. In the Taylor example, the sign of the deviation is ambiguous, having an exact result only around x_0, with equal slope and curvature. On the other hand, in the Jensen case, a rule of thumb for accuracy is more complicated, such as the "small deviation" around the steady state (x_0) or ±5% growth rates when log-linearizing.

3.2.2 An Illustrative Model

As typically found in Euler equations, we isolate the non-linear, forward-looking part and, for the purpose of generality, apply growth rates to it.[9] Also, even when renouncing log-linearization in DSGE models, they can be implemented in a straightforward way.[10] This goes hand in hand with the data availability of future rates from the CF data for the subsequent calibration. Moreover, we assume a log-normal distribution, following the approach by Black and Scholes (1973) and Merton (1973).[11] As an alternative, the inverted beta distribution is used, also being restricted with a lower bound

[9] A simple version, including the marginal utility with respect to consumption and the interest rate as an intertemporal connection is as follows: $\mathrm{d}U/\mathrm{d}C_t = i_t \cdot \mathrm{E}_t[\mathrm{d}U/\mathrm{d}C_{t+1}]$.

[10] E.g., $\mathrm{E}_t[(X_{t+1}/X_t)^\eta] = \mathrm{E}_t[(1+\widehat{x_{t+1}})^\eta]$.

[11] More precisely, the Black-Scholes formula requires log-normally distributed returns to price options in a relatively simple manner. In a similar context, the distribution is first mentioned by Samuelson (1965). The obvious normal distribution is problematic since there is no lower bound (for growth rates) and, defined on $\mathbb{R}$, the expression $\mathrm{E}[X^\eta]$ ($\eta \in \mathbb{N}$) is challenging to solve and requires many cases or complex functions. This is not practical for an analytical solution.

(i.e., being non-symmetric), which is appropriate for the data structure. Notwithstanding the usage of growth rates, the expression $\mathrm{E}[X]$ as the arithmetic mean (instead of the geometric mean) is reasonable since the rates are not consecutive but cross sectional.

In line with most (consumption) Euler conditions, the CRRA utility function provides a flexible functional form for the non-linearities. As a result of this and because the expressions typically stem from first-order conditions, we use the marginal utility for $f(X)$:

$$f(X) = \frac{1}{(1+X)^{\gamma}}, \quad \text{where} \quad F(X) = \frac{1}{1-\gamma} \cdot \left((1+X)^{1-\gamma} - 1\right) + C_0, \quad \gamma > 0. \tag{3.3}$$

The general antiderivative $F(X)$ in Eq.(3.3) is formulated in a way that for $\gamma = 1$ the function collapses to log-utility, a case common to the literature (see, e.g., Clarida et al 2000, 170, Galí 2015, 67, Yun 1996, 359).

Figure 3.2 captures these assumptions in a single coordinate system, showing the approach to evaluate Jensen's inequality. Starting next to the lower bound, the marginal

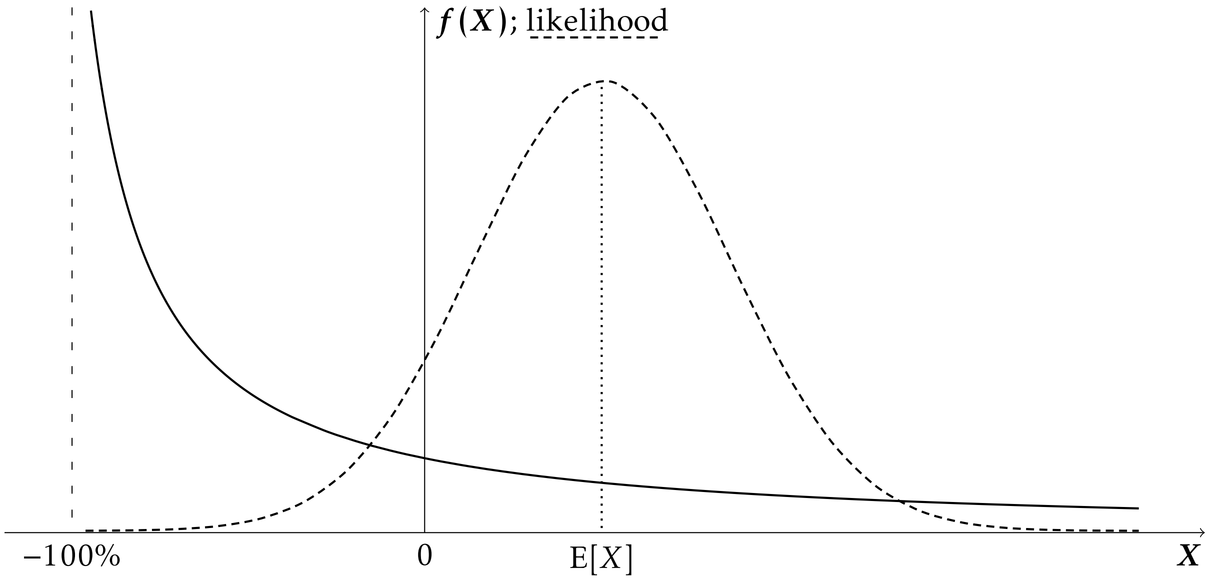

Figure 3.2: The model is tailored to growth rates due to a lower bound. Shown as schematic representation, values are drawn from a distribution (dashed curve) to insert into the non-linear function (black curve), $f(X)$.

utility or revenue from growth rates is the highest, monotonically decreasing for larger values. Not depending on the curvature parameter, the intercept equals the neutral value of one describing a situation without growth. In the following, we refer to the transformation result as weighted, inverse growth rates.[12]

Three of the model's decisive parameters are visualized in the graphics: the curvature in the hyperbola and the mean and variance in the density function. The latter predefines the probability by which values X, the growth rates, are drawn to insert into $f(X)$. Hence, the domain of the density function (support of X) has to be a subset of the inverse image of $f(X)$.

On the basis of Eq.(3.2.2), the plain concept, we change two components for a more intuitive and meaningful economic interpretation. First, this is done by switching the biased and the un-approximated value by changing the order of the difference (or multiplying by -1) and second, by adding a composite function $g(y)$ to obtain a growth rate difference,

$$\Delta_{g(X)} = g \circ f(\mathrm{E}[X]) - g(\mathrm{E}[f(X)]). \tag{3.4}$$

Applied only after the situation in Figure 3.2, $g(y)$ acts as a monotone transformation of Jensen's inequality that flips the unequal sign. Since $f(X)$ is already inverting the growth rates, setting $g(y) = y^{-1}$ produces re-inverse, weighted (γ) growth to counteract the initial transformation. Combining the slight deviations from Eq.(3.2.2) makes $\Delta_{g(X)}$ positive.[13]

Pouring the preceding considerations into one equation results in

$$bias(X) = 10^4 \cdot \left((\mathrm{E}[1+X])^{\gamma} - \mathrm{E}[(1+X)^{-\gamma}]^{-1} \right), \quad (1+X) \sim \log \mathcal{N}\left(\mu, \sigma^2\right), \tag{3.5}$$

the approximation bias measured in basis points when multiplying the RHS of Eq.(3.5) by 10^4. Moreover, $f(X) = (1+X)^{-\gamma}$ is the derivative (marginal utility) of the CRRA (isoelastic) utility function with γ as the curvature and γ^{-1} as the elasticity of intertemporal substitution (EIS). Furthermore, X follows a horizontally shifted log-normal distribution with a lower bound of -1. This meets the characteristics of growth rates with their minimum possible value of -100% and no upper bound. However, the actual parameter constellation concentrates the probability mass relatively tight around their mean value slightly larger than zero. Ultimately, using a continuous distribution enables us to derive simple, analytical results for the approximation bias.

[12] Weighting growth (as a relative number, expressing the change in absolute numbers) by means of an exponent works analogously to weighting absolute numbers multiplicatively with coefficients. Here, the approximate log-transformation can be misleading since growth rates oftentimes appear to have a coefficient or to be addable.

[13] Without $g(y)$, the interpretation as growth rate difference would include first-order Taylor expansion and, thus, would be similar. See Appendix C.2 for the proof and numerical examples.

3.3 Analytical Solution

In this section, we derive a function, depending on the first two moments and the curvature-parameter, which is able to predict the approximation bias. Therefore, we use the framework of Eq.(3.5) with the X now labeled as *growth* to address the economic setting. This distinction is also made to first draw from a standard-normal distribution and subsequently transform into log-normally distributed RV's. The advantage is to keep track of the parameters of the latter distribution. The conditional expectation operator accounts for the time series context. Initially, we specify the expected bias,

$$bias(\mu,\sigma,\gamma) = \mathrm{E}\Big[10^4 \cdot \Big(\underbrace{(1+\mathrm{E}_t[growth_{t+1}])^{\gamma}}_{\text{(1): approximated}} - \underbrace{\mathrm{E}_t\left[(1+growth_{t+1})^{-\gamma}\right]^{-1}}_{\text{(2): unbiased}}\Big)\Big], \tag{3.6}$$

where $growth = \exp(\alpha + \beta Z) - 1$ and $Z \sim \mathcal{N}(0,1)$. This makes *growth*, the growth rates, a log-normally distributed RV with a lower bound of -1 (or -100%). Three notational aspects are worth mentioning. First, we drop the time indices for more clearness. Second, we further simplify by setting $m = 1 + \mu$, defining m as the *centered mean*, thus, centering the growth rates around 1. Third, there is the risk to confound the transformation parameters, α and β, and the targeted moments, μ and σ, since they are approximately the same size.[14] The following formulas show the connection between log-normal parameter and moments:

$$\alpha = \log(m) - \log\left(\sqrt{1+(\sigma/m)^2}\right) \tag{3.7.1}$$

$$\beta = \sqrt{\log\left(1+(\sigma/m)^2\right)} \tag{3.7.2}$$

$$m = \exp(\alpha + \beta^2/2) \tag{3.7.3}$$

$$\sigma^2 = \exp\left(2\alpha+\beta^2\right)\cdot\left[\exp\left(\beta^2\right)-1\right]. \tag{3.7.4}$$

The key step relies on the moment generating function of the normal distribution.[15] By inserting the distribution expression in the approximated (1) and the unbiased (2) terms of Eq.(3.6), the stochastic source Z becomes apparent but immediately cancels out:

$$(1): \mathrm{E}[\exp(\alpha+\beta Z)]^{\gamma} \quad = \exp(\gamma\alpha)\cdot \mathrm{E}[\exp(\beta Z)]^{\gamma} \quad = \exp(\gamma\alpha)\cdot\exp(\gamma\beta^2/2) \tag{3.8.1}$$

[14] Note that the assignment of Greek letters is different from most sources for the reason mentioned above and for being in accordance with the parameter designation of the inverted beta distribution, also used in this article.

[15] $\mathrm{E}\left[e^{tZ}\right] = e^{t^2/2}, t \in \mathbb{R}$ (see Appendix C.3 for the proof).

$$(2): \mathrm{E}[\exp(\alpha+\beta Z)^{-\gamma}]^{-1} = \exp(\gamma\alpha)\cdot \mathrm{E}[\exp(-\gamma\beta Z)]^{-1} = \exp(\gamma\alpha)\cdot\exp(-(\gamma\beta)^2/2). \quad (3.8.2)$$

This replaces all RV's by parameters only and ensures that no stochastic part is remaining. Re-merging the function without inserting μ/m and σ yet using summarizing parameters gives a first impression of the functional form regarding the curvature:

$$bias(\gamma) = 10^4 \cdot A^\gamma \left(B^\gamma - B^{-\gamma^2}\right), \quad (3.9)$$

with $A = \exp(\alpha) \approx 1$ and $B = \exp(\beta^2/2) > 1$. Writing the function in the shape of Eq.(3.6) gives

$$bias(\alpha,\beta,\gamma) = 10^4 \cdot \left(\exp(\alpha+\beta^2/2)^\gamma - \exp(\alpha-\gamma\beta^2/2)^\gamma\right). \quad (3.10)$$

When using Eqs.(3.7) to replace α and β, we can take advantage of the inverse function (exponential and logarithm, square and square root) to arrive at the main function:

$$\begin{aligned} &bias(m,\sigma,\gamma) \\ &\quad = 10^4 \cdot \left(m^\gamma - \exp\left(\log(m) - \log\left(\sqrt{1+(\sigma/m)^2}\right) - \gamma\log\left(\sqrt{1+(\sigma/m)^2}\right)\right)^\gamma\right) && (3.11.1) \\ &\quad = 10^4 \cdot \left(m^\gamma - m^\gamma \cdot \left(\frac{1}{\sqrt{1+(\sigma/m)^2}}\right)^\gamma \cdot \left(\frac{1}{\sqrt{1+(\sigma/m)^2}}\right)^{\gamma^2}\right) && (3.11.2) \\ &\quad = 10^4 \cdot m^\gamma \cdot \left(1 - \left(\frac{m}{\sqrt{m^2+\sigma^2}}\right)^{\gamma(\gamma+1)}\right). && (3.11.3) \end{aligned}$$

Factoring out m^γ, such that the first term in the outer brackets becomes one, focuses on the second term stemming from the unbiased expression. To get more insight, Eq.(3.11.3) can be separately examined from the perspective of both moments and curvature. The *bias* depending on m and σ with $\gamma = 1$ (corresponds to log-utility) heavily reduces the complexity:

$$bias(m,\sigma \mid \gamma=1) = 10^4 \cdot m\left(1 - \frac{m^2}{m^2+\sigma^2}\right) = 10^4 \cdot \frac{m\sigma^2}{m^2+\sigma^2}. \quad (3.12)$$

Eq.(3.12) shows a nearly quadratic relationship with regard to σ (since $m^2 \gg \sigma^2$), corrected by m, the centered mean. This non-trivial result is plausible considering the schematic representation in Figure 3.2. Shifting the distribution to the right (increasing m) decreases the approximation bias since the function becomes less curved. A wider distribution (large σ) spreads the probability mass over the non-linear function in a manner that the approximation bias becomes larger. However, as mentioned above, there is no stochastic element left in the formulas. Finally, an upper bound can be found by applying l'Hôpital's rule, $\lim_{\sigma\to\infty} bias(\sigma \mid m) = 10^4 \cdot m$, revealing a maximum deviation of 100pp, again, corrected by m.

Consulting an economic interpretation, term (1) from Eq.(3.6) stays at the mean value since it does not consider any uncertainty. However, term (2), the inverse of the "marginal utility," converges towards zero. This shows, via a roundabout route, the negative relationship between uncertainty and utility. Moreover, it shows that in an economic model a function's curvature artificially replaces the actual real-world higher-order moments, stemming from the data.

Shifting the focus to γ, Eq.(3.11.3) with $r = \sqrt{m^2 + \sigma^2}$ reveals the fraction as the crucial term, approaching zero when γ is increasing:

$$bias(\gamma) = 10^4 \cdot m^{\gamma} \cdot \Big[1 - (m/r)^{\gamma(\gamma+1)}\Big]. \tag{3.13}$$

Eq.(3.13) has some simple properties. When σ approaches zero then r approaches m and the *bias* vanishes. Also, for positive growth rates, there is no upper bound since $\lim_{\gamma\to\infty} bias(\gamma \mid m > 1)$ does not exist. It is easy to show that $bias(0) = bias(-1) = 0$ and for $\gamma \in]-1, 0[$ the *bias* becomes negative. Although mathematically correct, this would break the models framework ($\gamma > 0$) and dilute the interpretation. Therefore, for a concave version, by multiplying the function by -1 (mirroring on the abscissa), a negative sign can be factored out, such that the *bias*-function stays the same otherwise.[16]

Putting everything together, Figure 3.3 graphically presents the findings concerning the function $bias(\mu, \sigma, \gamma_i)$, with γ as a parameter in levels (i.e., different opacity-levels). Taking the mathematical curvature instead of the EIS highlights the theoretical aspect. The ranges for the parameters are relatively large to show a broader picture. The realistic ranges will be introduced in the next sections.

[16]See Appendix C.4 for additional investigations concerning this function.

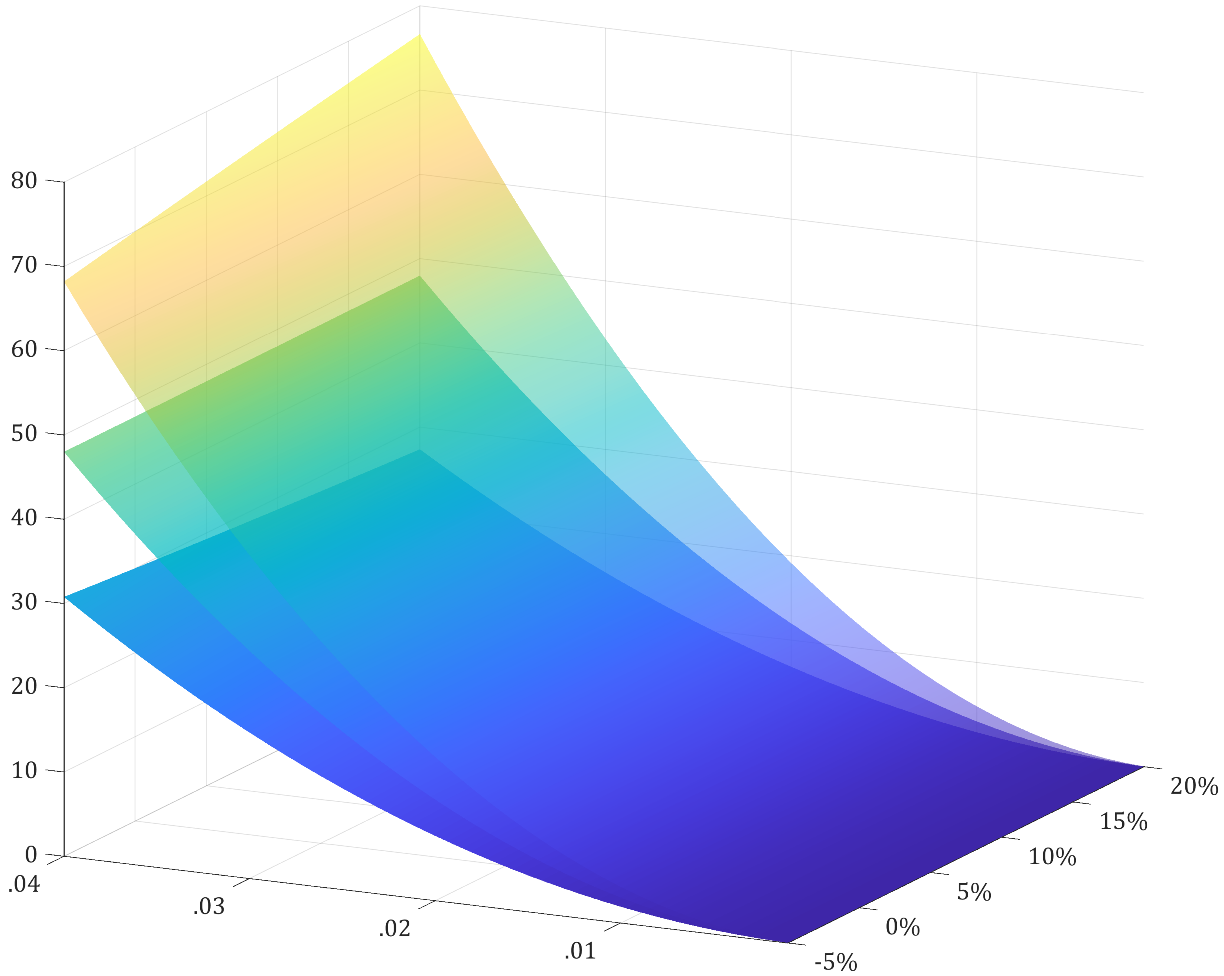

Figure 3.3: Theoretical approximation bias depending on all parameters with $\gamma_i \in \{1, 1.5, 2\}$ represented in the different planes. Horizontal axes: $\sigma \in [0.001, 0.04]$ and $\mu \in [-0.05, 0.2]$. Vertical axis: Growth rate difference in basis points.

Figure 3.3 shows how the impact of m on the *bias* changes with γ. The undermost plane reveals a slightly negative relationship, whereas the intermediate plane constantly remains close to a 50bp difference (max. σ) for all m. In contrast, for $\gamma = 2$ (uppermost plane) the relationship becomes positive. In each case, the absolute effect of m (conditional on large σ and γ) is rather small.

3.4 Data and Calibration

After the analytical solution, the next step is to check whether the assumptions are also fulfilled in the empirical data. This can be done by checking whether the RV's, which is *growth* in the previous section, are log-normally distributed. The final aim is to get a realistic range of parameters/moments to work with when there is no or insufficient raw data available. For the empirical tests, we use CF data from the *Consensus Economics* surveys. They provide projections on a series of macroeconomic indicators (e.g., GDP growth and inflation measures) that are mainly collected from companies in the finance sector. The data sets are issued on a monthly basis and display the forecasts for the current and upcoming year. Originally, the survey started in October 1989, whereas our data reach to June 2019, resulting in a total of 357 months. The observations start with estimations for the G-7 countries. From 1995 on, the number of countries for which there are forecasts available are successively expanded. Therefore, the time horizon for these countries is significantly shorter. The method and calibration results are introduced for US data due to a high availability in the number of observations. For the US, the minimum number of forecast observations per month is 19, the maximum is 33, and on the average is 27 per month.[17] Subsequently, we use existing data for frontier or emerging markets with a sufficient amount of observations (Egypt, Nigeria, and South Africa) to account for the possible application of DSGE models as stated in the introduction.

Since the variables' meaning is changing from month to month due to a varying forecast horizon, the values from the current period and the next year shall be combined into another variable:

$$\mathrm{E}_t[x_{t+1}|M] = \frac{13-M}{12} \cdot \mathrm{E}_{t,M}[x_t] + \frac{M-1}{12} \cdot \mathrm{E}_{t,M}[x_{t+1}]. \tag{3.14}$$

Consequently, a weighting scheme as in Eq.(3.14) is constructed to combine the forecasts. With the weighting scheme, it is also ensured that the viewed future time horizon is always 12 months. The examined variable of the CF data set is the consumer price (%-change) forecast, which is equivalent to an inflation measure.

Several normality tests are run on the adjusted data for consumer price. This is done due to the requirement in Section 3.3 that Z is normally distributed. The observed variables x_t need to be rearranged to

$$z_t = \log(x_t + 1) \tag{3.15}$$

[17] Based on these numbers, N—which represents the number of drawn variables—is initially fixed to 30 in Section 3.5.

and z_t is checked on normality. If the normality test approves the hypotheses and z_t is normally distributed, the observed variables are log-normally distributed.

We use four different tests including Jarque-Bera (J-B), Shapiro-Wilk (S-W), Anderson-Darling (A-D), and Lilliefors (LF). The results can be seen in Table 3.1. In 85% of the observations, the J-B test cannot reject the H_0 of non-normally distributed variables.

Norm. Test	***p*-value** Min	25$^{\text{th}}$centile	Median	75$^{\text{th}}$centile	Max
J-B	0	0.225	0.478	0.718	0.998
S-W	$1.95 \cdot 10^{-5}$	0.126	0.308	0.615	0.989
A-D	$8.06 \cdot 10^{-5}$	0.102	0.290	0.549	0.991
LF	$1.68 \cdot 10^{-4}$	0.089	0.312	0.592	0.999

Table 3.1: Normality test results for inflation forecasts (US).

As the normality tests show sufficient results, the observed variables shall be log-normally distributed. Now, the calibration of the distribution on the weighted observations can be run. We use a non-linear least square model to solve this issue. The drawn variables are shifted by a subtraction of one to fit the observations:

$$x_{\text{shift}} = x_{\text{draw}} - 1, \tag{3.16}$$

where $x_{\text{draw}} \sim \log\mathcal{N}(\mu, \sigma^2)$ are the drawn pseudo-observations from the log-normal distribution. Forecasts can also contain negative values, i.e., negative growth for consumer prices or other macroeconomic indicators, which cannot be drawn in a log-normal distribution. This can be solved by the shift. For this we calculate the mean squared error, MSE, between the observations and the shifted variables by

$$MSE = \frac{1}{N} \cdot (x_{\text{obs}} - x_{\text{shift}})^2, \tag{3.17}$$

where x_{obs} are the observed variables and N is the number of observations. The target is to minimize MSE and to find the optimal parameters μ and σ^2 of the distribution. The start-parameters of the log-normal distribution in the calibration are chosen in respect of μ_{obs} and σ^2_{obs} of the observed variables. From every parameter we go ten predefined equidistant steps in every direction. This builds a grid

$$\mathcal{C}_1 = \{\mu_{1,\text{lower}}, .., \mu_{1,\text{obs}}, .., \mu_{1,\text{upper}}\} \times \{\sigma^2_{1,\text{lower}}, .., \sigma^2_{1,\text{obs}}, .., \sigma^2_{1,\text{upper}}\} \in \mathbb{R}^2, \tag{3.18}$$

where $\mu_{1,\text{lower}} = \mu_{1,\text{obs}} - 10 \cdot \text{step}_1$ and $\mu_{1,\text{upper}} = \mu_{1,\text{obs}} + 10 \cdot \text{step}_1$ and step_1 is the equidistant step. The same calculation is done with the variance, but the step size can differ from the one used for the mean. As a result, there are $21^2 = 441$ possible parameter combinations $(\mu, \sigma^2) \in \mathcal{C}_1$.

At every combination, as many random variables are drawn as observations we have in these respective time periods. The MSE of the drawn and observed variables at every combination point is calculated. The parameter combination with the lowest MSE is chosen as the new optimal point $(\mu_1^*, \sigma_1^{2*}) \in \mathcal{C}_1$.

In the next step, we again go from this optimal point ten equidistant steps in every direction with the difference that the steps are with a factor 10 smaller than before. They can be calculated by the following method:

$$\text{step}_i = \frac{\text{step}_1}{10^{i-1}}. \tag{3.19}$$

The new grid is of the form:

$$\mathcal{C}_2 = \{\mu_{2,\text{lower}}, .., \mu_1^*, .., \mu_{2,\text{upper}}\} \times \{\sigma^2_{2,\text{lower}}, .., \sigma_1^{2*}, .., \sigma^2_{2,\text{upper}}\} \in \mathbb{R}^2. \tag{3.20}$$

So, we assure that the grid is getting finer. The least MSE in this step forms the new optimal point $(\mu_2^*, \sigma_2^{2*}) \in \mathcal{C}_2$. These steps are repeated until we reach a sufficiently predefined small error term and the resulting parameters are $(\mu^*_{\text{opt}}, \sigma^{2*}_{\text{opt}})$. The results are the specific parameters of both distributions, which are transformed to μ and σ^2 using Eqs.(3.7) from Section 3.3 and Eqs.(C16) from Appendix C.6. The calibration results for two distribution functions (log-normal and inverted beta) are displayed in Table 3.2, whereas the calibration method for the inverted beta is nearly the same as for the log-normal distribution. The only difference is the shift of the drawn variables from Eq.(3.16) by 0.01. This ensures that the inverted beta distribution also generates negative values.[18]

[18] Due to the characteristics of the inverted beta distribution a larger shift is not feasible. A significant part of the probability mass is concentrated at the lower bound, which is in this case the shift, and this would mainly result in negative values. The mass can be stretched by changes in the parameters of the distribution but this would deliver an unreasonable large σ.

Para-meter	Min	25$^{\text{th}}$centile	Median	75$^{\text{th}}$centile	Max	Obs. Median	Mean Error
log-norm.							
μ_{opt}	−0.0032	0.0191	0.0246	0.0320	0.0420	0.0239	$1.09 \cdot 10^{-6}$
σ_{opt}	0.0001	0.0001	0.0002	0.0007	0.0060	0.0027	$1.09 \cdot 10^{-6}$
inv. beta							
μ_{opt}	0.0061	0.0233	0.0275	0.0322	0.0556	0.0239	$4.56 \cdot 10^{-5}$
σ_{opt}	0.0011	0.0023	0.0028	0.0036	0.0262	0.0027	$4.56 \cdot 10^{-5}$

Table 3.2: Calibration results (US) when assuming CF data follow a log-normal and inverted beta distribution, respectively. The calibration is run on a monthly basis for the rolling window-adjusted observations on inflation forecasts.

In the first column, the two variables, which are the focus of our calibration, are shown. The following five columns focus on the results of the calibration. It shows descriptive statistics for the 357 months. The next column switches from the calibrated to the observed variables in the CF data set. In each of the 357 months, the mean and the standard deviation of the observed variables are calculated. This delivers 357 empirical values for both moments. The median of the two calculated moments is displayed in the respective row. Consequently, the results for the median of the observed variables are the same for both distribution methods because the viewed data set is the same. The mean error that arises from the calibration can be found in the last column. Focusing on the mean error, the log-normal distribution is clearly better in fitting the observed variables. Regarding the estimation of μ_{opt}, the log-normal distribution gives a better fit than the inverted beta distribution. This is mainly due to the concentration of probability mass at the lower bound of the inverted beta distribution. The picture changes when fitting σ_{opt}. Here the log-normal distribution underestimates the standard deviation whereas the inverted beta distribution gives a better fit. Nonetheless, it is noticeable that the inverted beta distribution sometimes generates relatively large values for the standard deviation.

For comparison purposes and due to a potentially high interest in DSGE models for emerging/frontier markets, we now focus on forecasts of consumer prices for Egypt, Nigeria, and South Africa.[19] Other countries that are classified in these markets are not available in the data set. Due to a low number of forecasts per month—in contrast to developed countries, e.g., the US—quarterly data is used. The observations start in Q1 2008, which results in a time horizon of 46 quarters. The minimum number of

[19]The classification regarding frontier and emerging markets is taken from MSCI. This is a provider of equity market indexes that uses a classification for different markets.

forecast observations per quarter is six for Nigeria in Q1 2008, the maximum is 57 for South Africa in Q4 2016, and the average is 22. The average is built considering all three countries.

The previous adjustment to rearrange all variables on a 12 months time horizon is also done for the monthly variables as mentioned in Eq.(3.14). In the following normality test, the adjusted variables in a whole quarter are checked for normal distribution. The results can be seen in Tables 3.3–3.5. In all countries, the J-B test results support normally distributed random numbers in more than 65% of the cases. In Egypt and Nigeria, normally distributed random numbers are supported in even more cases, amounting to 90%.

Norm. Test	***p*-value** Min	25$^{\text{th}}$centile	Median	75$^{\text{th}}$centile	Max
J-B	$4.62 \cdot 10^{-7}$	0.256	0.449	0.578	0.996
S-W	0	0.037	0.241	0.417	0.843
A-D	0	0.018	0.138	0.328	0.858
LF	0	0.027	0.114	0.300	0.980

Table 3.3: Normality test results for inflation forecasts (Egypt).

Norm. Test	***p*-value** Min	25$^{\text{th}}$centile	Median	75$^{\text{th}}$centile	Max
J-B	$8.21 \cdot 10^{-11}$	0.397	0.562	0.682	0.900
S-W	0	0.053	0.219	0.523	0.951
A-D	0	0.018	0.146	0.344	0.865
LF	$5.32 \cdot 10^{-6}$	0.039	0.151	0.281	0.779

Table 3.4: Normality test results for inflation forecasts (Nigeria).

Norm. Test	***p*-value** Min	25$^{\text{th}}$centile	Median	75$^{\text{th}}$centile	Max
J-B	$7.99 \cdot 10^{-15}$	0.028	0.371	0.648	0.947
S-W	$1.69 \cdot 10^{-5}$	0.004	0.103	0.391	0.756
A-D	$1.05 \cdot 10^{-6}$	0.004	0.087	0.342	0.883
LF	$5.37 \cdot 10^{-6}$	0.003	0.088	0.402	0.851

Table 3.5: Normality test results for inflation forecasts (South Africa).

The normality tests again show sufficient results for the three countries analyzed. So the same calibration can be run for the log-normal distribution and inverted beta is again used as a robustness check. The method of the calibration stays the same. The results can be seen in Tables 3.6–3.7.

Para-meter	Min	25^{th}centile	Median	75^{th}centile	Max	Obs. Median	Mean Error
Egypt							
μ_{opt}	0.0804	0.0965	0.1075	0.1193	0.2033	0.1057	$2.88 \cdot 10^{-4}$
σ_{opt}	0.0054	0.0073	0.0085	0.0106	0.0179	0.0134	$2.88 \cdot 10^{-4}$
Nigeria							
μ_{opt}	0.0591	0.0972	0.1094	0.1224	0.1507	0.1088	$1.30 \cdot 10^{-4}$
σ_{opt}	0.0055	0.0080	0.0106	0.0131	0.0341	0.0096	$1.30 \cdot 10^{-4}$
S. Africa							
μ_{opt}	0.0464	0.0523	0.0576	0.0612	0.0852	0.0571	$4.03 \cdot 10^{-5}$
σ_{opt}	0.0047	0.0062	0.0072	0.0088	0.0136	0.0035	$4.03 \cdot 10^{-5}$

Table 3.6: Calibration results when assuming CF data follow a log-normal distribution. The calibration is run on a quarterly basis for the rolling window-adjusted observations on inflation forecasts.

Para-meter	Min	25^{th}centile	Median	75^{th}centile	Max	Obs. Median	Mean Error
Egypt							
μ_{opt}	0.0899	0.1029	0.1135	0.1321	0.2176	0.1057	$3.57 \cdot 10^{-4}$
σ_{opt}	0.0060	0.0107	0.0143	0.0209	0.0361	0.0134	$3.57 \cdot 10^{-4}$
Nigeria							
μ_{opt}	0.0763	0.1002	0.1162	0.1284	0.1519	0.1088	$1.41 \cdot 10^{-4}$
σ_{opt}	0.0004	0.0070	0.0099	0.0135	0.0269	0.0096	$1.41 \cdot 10^{-4}$
S. Africa							
μ_{opt}	0.0492	0.0547	0.0588	0.0632	0.0875	0.0571	$6.19 \cdot 10^{-5}$
σ_{opt}	0.0022	0.0030	0.0035	0.0047	0.0125	0.0035	$6.19 \cdot 10^{-5}$

Table 3.7: Calibration results when assuming CF data follow a inverted beta distribution. The calibration is run on a quarterly basis for the rolling window-adjusted observations on inflation forecasts.

The results deliver the same picture as for the US. The log-normal distribution generates lower error terms compared to the inverted beta distribution. However, all errors are relatively close to each other. Additionally, the median of μ_{opt} is quite close to the median of the observed variables. In the inverted beta distribution, μ_{opt} is not as good as in the log-normal distribution, but σ_{opt} is better fitted.[20]

Summarizing, none of the distributions are clearly better in fitting the CF data set. Due to the slightly better error term for the log-normal distribution in the US and other aspects, e.g., multivariate distributions, we focus on log-normal for further analysis. Due to the above results for four different countries, the baseline scenario in the next section consists of $\mu = 0.06$ and $\sigma = 0.01$ as fixed parameters.

[20]Similar results can be seen for the calibration of the GDP forecasts in the CF data set. This, and α and β for the distributions for both variables can be found in Appendices C.7 and C.8.

3.5 Monte Carlo Simulation

The simulation section takes up the calibration results and conducts several simple MC experiments. Thereby, expectation value and variance become stochastic, enabling us to check how this variability influences the findings of Section 3.3. We orientate at the following sequence.

1. Specify the parameters in Eq.(3.5): μ, σ, γ, and N (in the multivariate case also n, the number of variables, and ρ, the correlation).

2. Calculate the *bias*, also Eq.(3.5), by drawing N random variables, following a log-normal distribution. Repeat this 10^5 times to obtain a *bias*-distribution.

3. Alter one of the parameters and repeat step 2. As soon as the parameter has covered a certain range, jump to step 4.

4. Graphically show the results as boxplots in a x-y-diagram with the varying parameter on the x-axis and the *bias* on the y-axis.

There is little variation when the first moment takes different values with a change in *bias* significantly lower than 1bp.[21] Hence, μ is constantly set to 0.06, a happy medium regarding the calibrated means. We set N to 30 since this matches the typical number of firms participating in the CF survey. Increasing this number will not result in a substantial difference. However, we examine this in more detail in Appendix C.15. We use 10^5 repetitions to make sure the obtained distributions already converged.

The boxplots, which are uncommon in this context, depict the non-parametric characteristics of a distribution as described in Mcgill et al (1978). The lower (upper) hinge of the box presents the first (third) quartile, while the middle line presents the median, the second quartile. This gives a good impression concerning the distribution's skewness. The lines extending vertically from the boxes (whiskers) expand both hinges by the interquartile range, multiplied by 1.5. As an orientation, when using a normal distribution, outliers larger (smaller) than the upper (lower) extreme account for only 0.35% of the probability mass. This value will be somewhat larger since $bias > 0$ and, thus, the simulated distributions are likely to be asymmetric with the mean not equaling the median. Although outliers are excluded for graphical clearness in the following figures, we check for their share not being too large ($< 2\%$) as justification to use the standard boxplots.[22]

[21] See Appendix C.9 examining the derivative $\partial bias / \partial \mu$ in detail.

[22] This keeps the interpretation simple and is in line with Hubert and Vandervieren (2008, 5191). In their article, they propose adjusted boxplots accounting for skewed data when outliers exceed 5%.

Throughout this section, the following scheme is used to describe the results. The simulated distributions are analyzed in terms of the first three moments, the best fitting parametric distribution relating to outliers, and the relationship between the medians and the varying parameters. Regressing the median-*bias* on the parameters extents the analytical results and accounts for the approximation bias' immanent skewness.[23]

3.5.1 Standard Deviation

According to Eq.(3.12), we take the standard deviation, a measure for the data's uncertainty, as the first varying parameter, whereas γ is held to one. The calibrated σ's range from 0.001 to 0.032. We choose 20 values starting from nearly zero up to a maximum value of 0.04, which is larger than calibration suggests to account for the possible bias in long-term forecasts. In this extreme scenario, with $\mu = 0.06$, growth rates of 10% are quite realistic since the 68–95–99.7 rule applies approximately for the log-normal distribution.[24] Figure 3.4 shows the results.

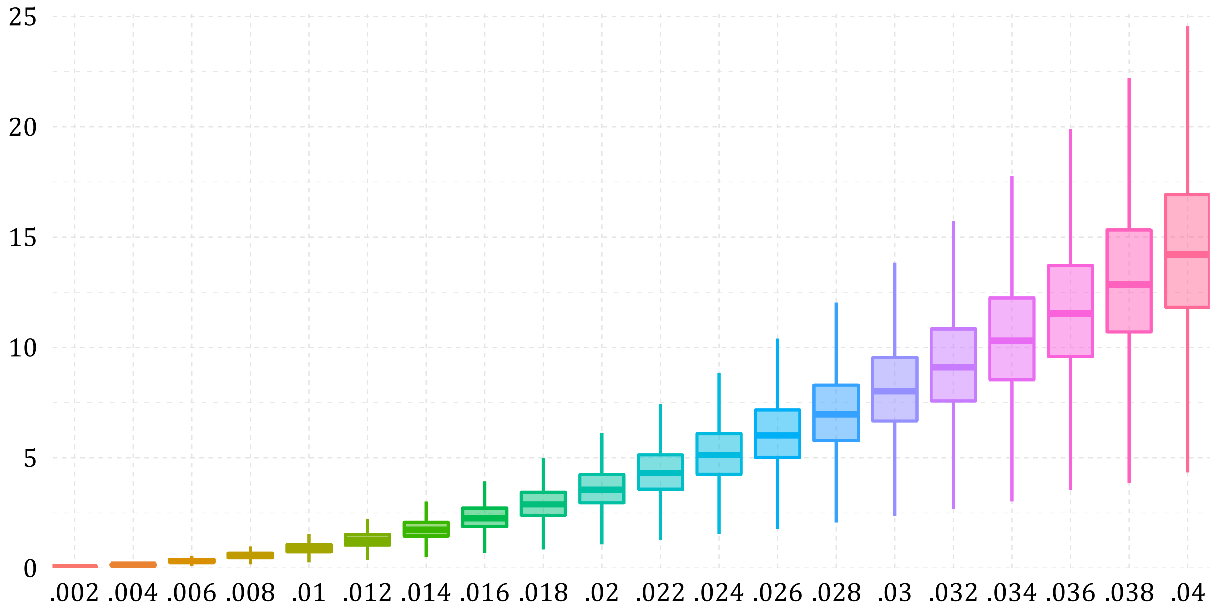

Figure 3.4: Simulations with 10^5 repetitions each (log-normal distribution with $\mu = 0.06$, $N = 30$, and a lower bound of -1). Resulting distributions of the approximation bias are shown as boxplots. Horizontal axis: Standard deviation (σ). Vertical axis: Growth rate difference in basis points (*bias*).

[23]To not overload Section 3.3, we include the median analysis in the simulation part only and, at the same time, using the advantage of the graphical analysis.

[24]Despite the distribution being truncated and skewed, this approximation holds very accurate, e.g., when $\sigma = 0.06$, the probability mass inside the 3σ-interval lowers by only 0.1pp to 99.6%.

The values originating from Eq.(3.12) are augmented by distributions for each σ, illustrating the sensitivity to small samples. The first twelve boxplots (including $\sigma = 0.024$) are of marginal relevance being strictly under 10bp. However, with a larger standard deviation the *bias* is increasing and averages 15bp for the extreme scenario, even reaching up to 25bp. Figure 3.4 also reveals that *bias*-predictions with increasing σ become more and more inaccurate (increasing interquartile range). Moreover, empirical analysis of the simulation data shows that the variance of the simulated distributions increases proportional to the σ's. The distributions' skewness is consistently positive with the deviation of mean and median located slightly over 2% (i.e., always less than one basis point).[25] Cullen and Frey (1999) analysis shows that the resulting distributions best fit to a gamma distribution.[26] This means, in turn, that for every σ there are theoretically around 1% outliers larger than the upper extreme. This also holds empirically. Most interesting, the relationship between σ and the approximation bias (median) is quadratic with an R^2 of almost 100% when running regression analysis. The detailed results are shown in Appendix C.10.[27]

The intuition behind the relationship can be outlined by a simple case where f from Eq.(3.2.1) is the convex function $f(X) = X^2$:

$$\mathrm{E}[X^2] = (\mathrm{E}[X])^2 + \mathrm{Var}[X] = (\mathrm{E}[X])^2 + \sigma_X^2. \tag{3.21}$$

Here, the residual (Δ_X) consists of the squared standard deviation.[28] For this example, in contrast to the analytical derivation, X does not necessarily follow a specific distribution. Nevertheless, we also check for the accuracy of a second-order Taylor expansion with regard to Eq.(3.12):

$$T_2^{bias}(\sigma \mid \sigma_0 = 0) = 10^4 \cdot \sigma^2/m. \tag{3.22}$$

The isolated quadratic part describes the relationship sufficiently enough up to $\sigma = 0.16$.[29]

[25] $\mathrm{E}[(mean - median)/median \mid \sigma] = 2.35\%$. In line with the our own calculations, the medcouple, a normalized or robust measure for the skewness reaching from -1 to 1, is only around 0.08.

[26] More comprehensive non-parametric tests (e.g., Kolmogorov–Smirnov) are avoided to keep the framework simple. The classification merely serves to check whether theoretical and empirical values are roughly the same.

[27] Also in Appendix C.10, we show similar results for the CARA function but hereinafter, for the lack of substantial difference, we stick to the CRRA function.

[28] With the binomial formula: $\mathrm{Var}[X] = \mathrm{E}[X^2] - \mathrm{E}[X]^2$. Note the close connection between Jensen's inequality and our model (Appendix C.2).

[29] Appendix C.11 shows this in more detail. See also Appendix C.12, further examining the approximation bias in terms of a ratio between the approximated and the un-biased term.

3.5.2 Curvature – Elasticity – Risk Aversion

The second varying parameter accounts for the degree of non-linearity of f from Eq.(3.3). In an attempt to interpret this property as general as possible, this can be described by the curvature, typically defined as the amount by which a curve deviates from being a straight line. By defining γ as curvature of $f(1+x)$, the relative risk aversion equals:

$$RRA_f = -(1+x) \cdot f''/f' = 1 + \gamma. \tag{3.23}$$

Concerning this interpretation of γ, Meyer and Meyer (2005) assemble slightly different versions of risk aversion to make them comparable and Chiappori and Paiella (2011) conduct an in-depth analysis of risk aversion using panel data.

As mentioned earlier, $f(1+x)$ is understood as the marginal utility, satisfying the economical situation. In this case, the inverse, γ^{-1}, can be interpreted as elasticity. Additionally, in a time-varying context, γ^{-1} stands for the EIS. For the sequence of γ, applied to the study, we orientate at Meyer and Meyer (2005, 260) by starting slightly above zero (0.25) and going up to 5 (i.e., $\gamma^{-1} \in [0.2, 4]$). Figure 3.5 shows the simulation results analogous to the previous subsection.[30]

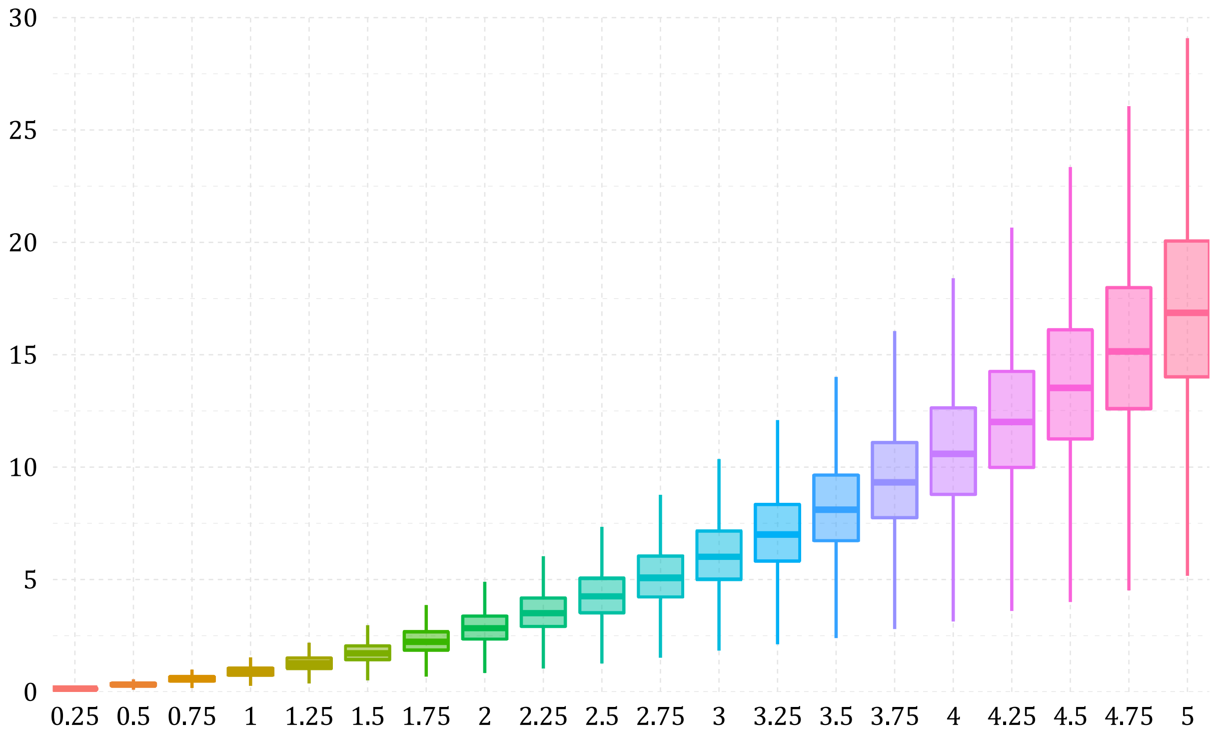

Figure 3.5: Horizontal axis: Curvature (γ). Vertical axis: Growth rate difference in basis points.

[30]From an economical point of view, the horizontal axis should increase with the EIS, which is shown in Appendix C.14.

Almost identical to Figure 3.4, boxplots one to twelve are hardly exceeding the 10bp line. The outcomes are breaking this line for an EIS of 1/3 and lower. The average bias is increasing over 15bp for a curvature of 5 (relative risk aversion of 6), with almost 30bp at the upper extreme. The interquartile range is increasing with larger curvature. Similarly, the variance is proportionate to the curvature. Investigating skewness and possible parametric distributions show the same results as with a varying σ. However, for the largest value of γ, outliers make up for almost 2%. The relationship of x and y is approximately $bias \sim \gamma^2$.[31] Also, in terms of pure elasticities, $\log(bias) \sim \log(\gamma)$, the regression's goodness-of-fit edges up to $R^2 = 0.99$. This allows for the interpretation of a %-change caused by a 1% increase. In this case, the system is relative elastic with a log-coefficient of around 1.67. Analogous to the σ-version but less accurately, the quadratic relationship can be described by a second-order Taylor expansion for $\gamma \leq 0.9$:

$$T_2^{bias}(\gamma \mid \gamma_0 = 0) = 10^4 \cdot \log(r/m)\Big[\log\Big(\mathrm{e}\sqrt{m^3/r}\Big)\gamma^2 + \gamma\Big]. \tag{3.24}$$

In contrast to Eq.(3.22), with the standard deviation as variable, Eq.(3.24) should only be used for a certain range of realistic values.[32] Overall, an exponential link is preferable when characterizing the relation between curvature and approximation bias.

3.5.3 Number of States – Sample Size

The parameter N, in terms of the simulation procedure, is the sample size per repetition. So far, N equaled 30 to represent the available number of forecasts in the CF data sets. Economically, N designates the number of possible future states. For the generic case of $N = 1$, there is only one outcome and, therefore, no uncertainty. This makes Jensen's inequality redundant. When N is approaching infinity, the approximation bias converges to the analytical finding. Since both scenarios are not reasonable, we vary N from 1 to 20 and examine how the result is driven by uncertainty regarding different prospective outcomes.[33]

When N is increasing, the variance in the repetitions vanishes. However, for small N, the variance is not exploding. Figure 3.6 depicts the baseline case ($\mu = 0.06$, $\sigma = 0.01$, $\gamma = 1$) for a sample size reaching from 1 to 20.

[31] See Appendix C.10 for more detail by using regression analysis.

[32] See Appendix C.13 for more detail.

[33] In a different context, for example, N can be seen as the number of political parties at an election. When N is small, the future outcome of their economic policies is still not clear but easier to anticipate.

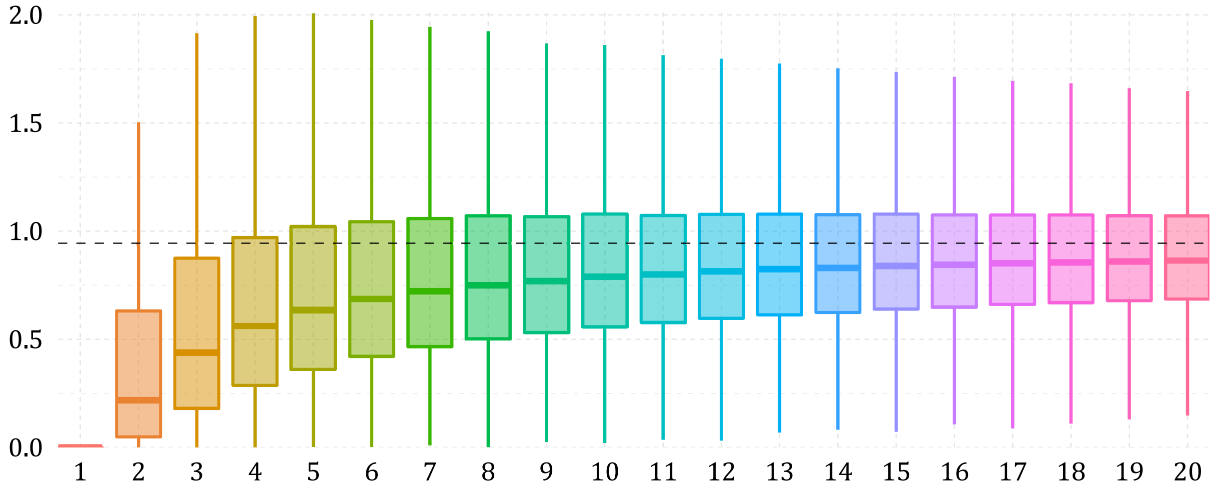

Figure 3.6: Baseline case. Dashed line depicts the theoretical mean value. Horizontal axis: Sample size (i.e., number of states N). Vertical axis: Growth rate difference in basis points.

With an increasing number of states, the distributions are contracting around the dashed line—the theoretical value—slightly below 1bp. For $N = 1$ there cannot be any difference, being in a situation with no uncertainty. Due to the zero lower bound, the distributions are initially heavily skewed. Graphically, this becomes apparent for $N = 2$, when the mean stays at 50% of the dashed line, while the median is only close to 25%. Interestingly, until four states are reached, the upper extreme is increasing and, thereupon, slowly decreasing. As to be expected, the magnitude is extremely small.

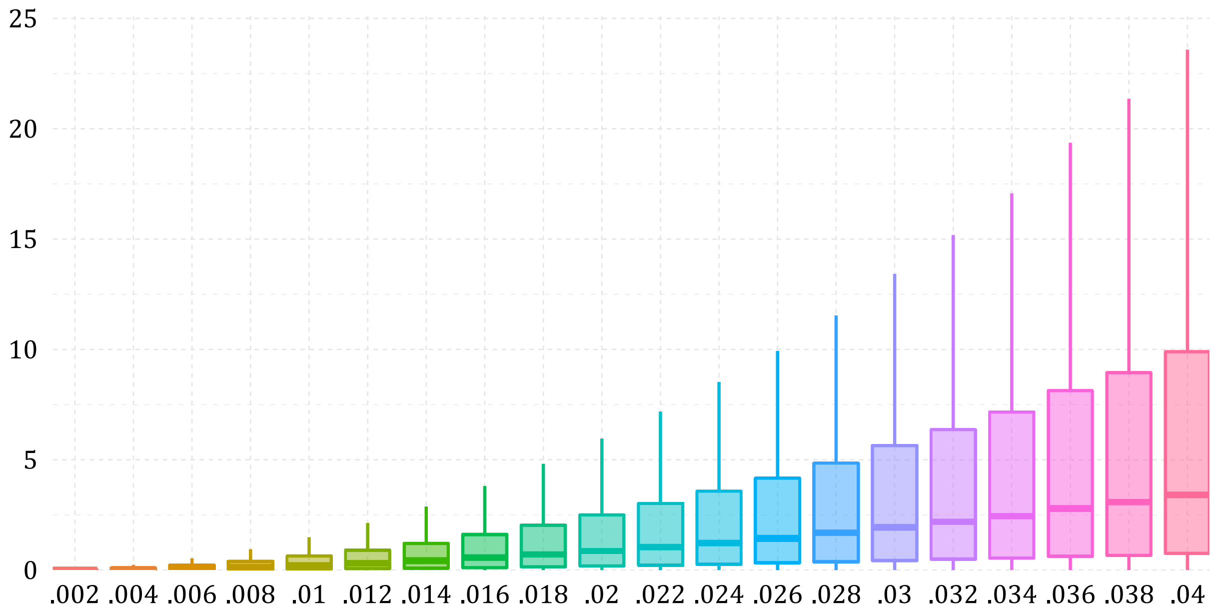

Figure 3.7: Baseline case with varying σ and two states, i.e. $N = 2$. Horizontal axis: Standard deviation (σ). Vertical axis: Growth rate difference in basis points.

Figure 3.7 replicates Figure 3.4 (varying σ) but only drawing two RV's, respectively. All distributions are skewed with a median-*bias* reaching only up to 3bp. An important question comes up, that is, which measure (mean or median) to choose when describing the approximation bias in a situation with few outcomes. On the one hand, most scenarios are negligible, on the other hand, (right-tail) outliers are still present. For $\sigma = 0.04$, the upper extreme is almost as large as in Figure 3.4.

In the model context, N is not interacting with other parameters or variables. Put differently, a parameter constellation other than the baseline case in Figure 3.6 does not alter the behavior for increasing N. In Appendix C.15, we explain in more detail how the convergence to the theoretical value solely depends on the sample size.

3.5.4 Multivariate Functions

To further exploit our model, we increase the number of variables (n), which also leads to the correlation (ρ) as an additional parameter. Simple Euler equations already include variables like consumption (growth) and price (growth). They should also (theoretically) contain information about how these variables are interacting (i.e., their co-movement).[34] Large-scale DSGE models like the ECB-Global, the IMF's Global Projection Model, and further adjusted versions can contain dozens of variables and hundreds of parameters.

For higher-order Taylor expansions, Collard and Juillard (2001) examine models of the form: $\mathrm{E}_t[f(x_{t+1}, y_{t+1}, ...)] = 0$, for non-linear f. Still, our approach focuses on Jensen's inequality.[35] Taking up on Eq.(3.5) for the baseline case ($\gamma = 1$) and multiplicatively expanding by another variable gives

$$bias(X,Y) = 10^4 \cdot \left(\mathrm{E}[1+X] \cdot \mathrm{E}[1+Y] - \mathrm{E}\left[(1+X)^{-1}(1+Y)^{-1}\right]^{-1}\right), \tag{3.25}$$

assuming that both X and Y are log-normal. Multiplying the new variable Y, instead of a different transformation, preserves the model's structure and replicates the way most (un-approximated) Euler equations work. The factor to produce growth rate differentials stays at 10^4 since multiplying centered growth rates results in a new growth rate, combining the others. This works analogously to adding level data in the same unit of measure. Figure 3.8 explores how the correlation between two variables affects the approximation bias.

[34]See, e.g., An and Schorfheide (2007, 118), including four variables in the context of a medium-scale DSGE model.

[35]See also Mitrinović et al (1993, 4), dealing with multivariate functions, $f(\mathbb{R}^n)$, in the context of Jensen's inequality.

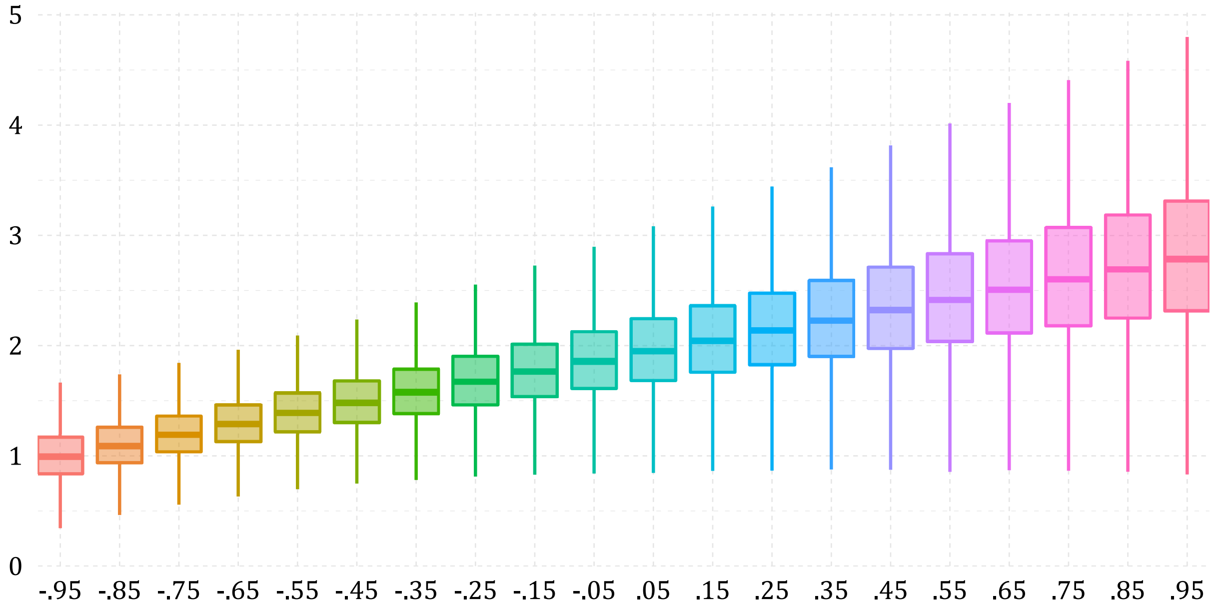

Figure 3.8: Baseline case with two variables. Horizontal axis: Correlation (ρ). Vertical axis: Growth rate difference in basis points. Technical note: The correlation between RV's $\sim \mathcal{N}(0,1)$ is preserved when transforming into the log-normal form. Also, when drawing from a $\mathcal{N}(0,1)$, the correlation equals the covariance.

The bias' magnitude is extremely small, reaching from 1 to 3. For negative correlation values up to -0.5, the standard deviation of the simulated distributions remains approximately the same, linearly increasing thereafter. The skewness is rather low with 0.46 on average. A gamma distribution can describe the individual results, however, with changing shape and scale parameters for different correlation values. Outliers account for approximately 1% in the case with maximum correlation. The relationship appears to be linear with negative correlation counteracting the bias.

Similar to Eq.(3.21), a special case can heuristically illustrate the rationale behind the linear relation. Again, take f from Eq.(3.2.1) to a bivariate environment: $f(X,Y) = X \cdot Y$.

$$\mathrm{E}[X \cdot Y] = \mathrm{E}[X] \cdot \mathrm{E}[Y] + \mathrm{Cov}[X,Y] = \mathrm{E}[X] \cdot \mathrm{E}[Y] + (\sigma_X \sigma_Y) \cdot \mathrm{Corr}[X,Y]. \tag{3.26}$$

In this case, the residual Δ_{XY} comprises the correlation times a coefficient (the standard deviations).[36]

[36] With the binomial formula: $\mathrm{Cov}[X,Y] = \mathrm{E}[X \cdot Y] + \mathrm{E}[X] \cdot \mathrm{E}[Y]$. Note that the correlation is the standardized covariance: $\mathrm{Corr}[X,Y] = \mathrm{Cov}[X,Y] / \left(\sqrt{\mathrm{Var}[X]} \cdot \sqrt{\mathrm{Var}[Y]}\right)$.

As a last step, pushing forward to a more comprehensive form, the quantity of variables ought to be reflected in the formula. Thus, modifying the model the same way as accomplished in Eq.(3.25) leads to

$$bias(X_1, \ldots, X_n) = 10^4 \cdot \left(\prod_{i=1}^{n} \mathrm{E}[1 + X_i] - \mathrm{E}\left[\prod_{i=1}^{n} (1 + X_i)^{-1} \right]^{-1} \right), \tag{3.27}$$

a generalized version with n variables. Specifying $n = 5$ and, for simplicity, assuming the same correlation between all these variables, Figure 3.9 reveals a similar pattern as in the bivariate case.[37]

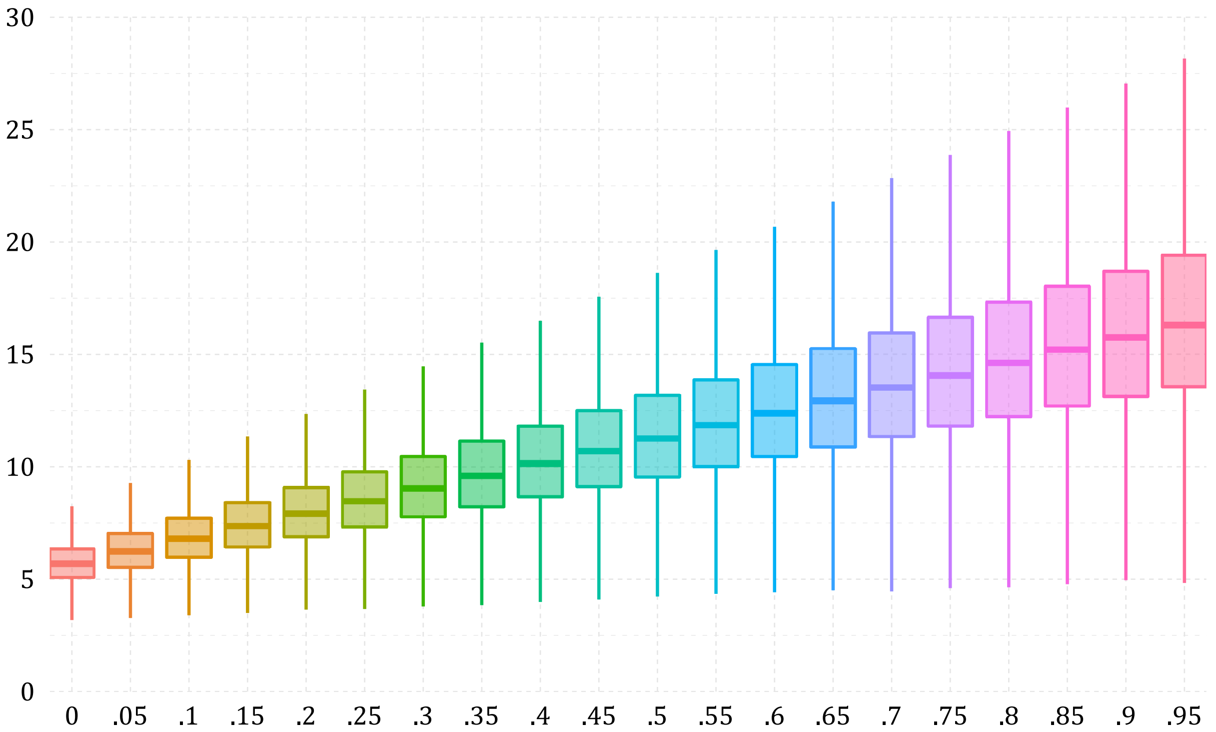

Figure 3.9: Baseline case with $n = 5$ variables. Horizontal axis: Correlation (ρ). Vertical axis: Growth rate difference in basis points.

The distribution indicators are similar and a nearly linear relationship reaches from the minimum to the maximum correlation value. For five highly correlated variables ($\rho = 0.95$), the bias roughly averages at 15bp, with outliers over 25bp. In this scenario, compared to Figure 3.8, the relationship is still linear, but the slope is larger (approximately 1.15bp per 0.1 ρ-step).

Finally, Figure 3.10 varies the number of variables while slightly deviating from the BL case. Since high growth rates for a large number of macroeconomic variables are

[37] It is interesting to note that in this case a covariance matrix cannot be positive definite, which is required. In other words, there is no combination of values possible where the overall correlation is always negative.

unrealistic, we switch to the calibrated mean for the US ($\mu = 2.5\%$).[38] As an additional assumption, the variables are mildly correlated ($\rho = 0.1$).

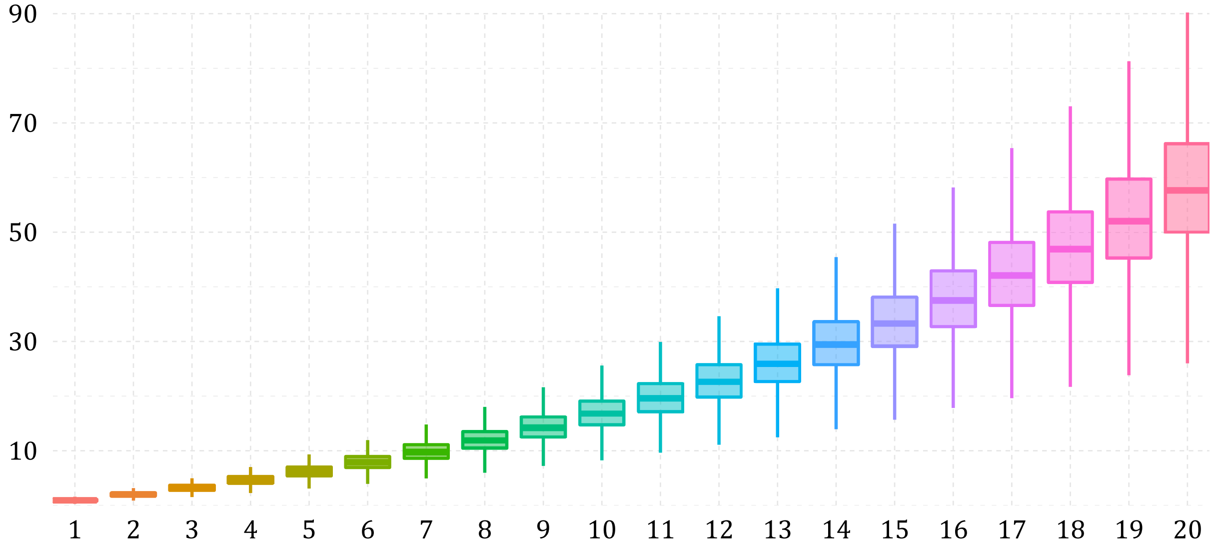

Figure 3.10: Baseline case with on overall correlation of $\rho = 0.1$. Horizontal axis: Number of variables (n). Vertical axis: Growth rate difference in basis points.

For ten or less variables, the average bias is not surpassing the 25bp mark. Thus, these situations can be compared to the extreme scenarios in Figures 3.4 and 3.5. For $n = 20$, an average bias of over 50bp is reached and outliers of almost 1pp are possible. The standard deviation increases over proportionately and the skewness stays at 0.5.[39] Distribution analysis, again, points towards gamma distributed residuals and outliers account for 1%. There is a predominant quadratic relationship since the exponential coefficient is significant but basically zero as shown in the regression table in Appendix C.10.

To recapitulate, Appendix C.16 provides a general overview of all figures shown in this section and the multiple-planes figure in Section 3.3.

[38]For $\mu = 6\%$, values of over 2pp will be reached.

[39]Medcouple averages at 0.08 and the %-deviation of mean and median averages at 2%.

3.6 Conclusions

This mostly theoretical paper explores a source of error in the context of macroeconomic models. Occurring in intertemporal Euler equations, Jensen's inequality is typically ignored when bringing the model to the data. Therefore, we set up an illustrative framework to compare the expected outcome of a non-linear function with the functional value of the expected argument consisting of growth rates. Being interested in the magnitude, this difference is constructed in a way that it can be measured in basis points, thereupon designated as approximation bias. Since, in the prevalent DSGE family, this bias is rather small, we evaluate parameter constellations in which the difference becomes apparent.

First, we derive analytical solutions with assumptions typical for DSGE models and growth rates, subsequently calibrating first and second moments for the US and emerging markets from forward-looking Consensus Forecasts data. Second, we test the variability in a simulation-based analysis and examine resulting distributions for a wide range of parameter values. Third, we further extend the model to check for the multivariate influence and, thus, correlation among variables. Throughout the article, we focus on translating model parameters into economical factors.

To generalize the results, we track down five separate factors, describing the functional relationship relative to the bias. The approximation bias increases (i) quadratically to uncertainty, (ii) exponentially to both the overall risk aversion and (iii) the model size, (iv) inversely proportional to the number of future states, and (v) linear to variables' co-movement. On the other hand, the first moments, mean and median, march to a different drummer by switching the sign of their influence depending on the curvature. However, this influence is negligible.

In absolute terms, when uncertainty is high, growth rates are overestimated up to 25 basis points. Consequently, a corresponding interest rate, adjustable by the central bank, should generally be lower when accounting for the approximation bias. Expecting a future scenario consisting of three possible states only, the bias' mean remains low, yet its distribution will be heavily skewed. Accordingly, when including only a few variables, the correlation among them will not be an issue, with negative values even counteracting the bias. Lastly, considering a large number of variables, overestimation mattered the most, with outliers even reaching one percentage point.

Our findings are important for large-scale model users like central banks in major economies where a possible error can add up and significantly bias the predictions. They also matter for institutions in emerging economies, which are more and more adopting DSGE models. We showed, in particular, that in situations with large uncertainty the bias cannot be ignored.

This groundwork provides a rich field for future research. To avoid the approximation when the bias is potentially large, examining density forecasts as in Rich and Tracy (2010) are of particular interest. Finally, putting all findings together, a Kalman-like filter to transform times series could be established to circumvent the issue. An expected difference to the actual values depending on the identified factors could be derived, including simulation-based confidence intervals.

Appendix C

Table of Contents

C.1 Approximating Jensen's Inequality by Quadratic Taylor Series

Since linearizing causes the inequality to vanish, we check for its relevance after conducting second-order (multivariate) Taylor expansion. In contrast to the first-order version, the function's curvature is not ignored. Our proof is presented for the convex version in an illustrative, special case with two real numbers a and b, where $a < b$:

$$\frac{f(a)+f(b)}{2} \geq f\left(\frac{a+b}{2}\right) \tag{C1}$$

We set $\mu(a,b) = (a+b)/2$ as the arithmetic mean and, therefore, $\mu_0(a_0,b_0)$ as the center point. The LHS is additive separable and can be piece-wise differentiated. Interpreting the RHS as a composite function $f(\mu(a,b))$ helps to keep track after the first step since cross-derivatives have to be considered. Carrying out a quadratic Taylor expansion on both sides of Eq.(C1), by using arguments a and b, yields:

$$T_2^{LHS}(\mu(a,b)) = \frac{1}{2}\Bigg[f(a_0) + f'(a_0)(a-a_0) + \frac{1}{2}f''(a_0)(a-a_0)^2$$

$$+f(b_0)+f'(b_0)(b-b_0)+\frac{1}{2}f''(b_0)(b-b_0)^2\Big] \tag{C2.1}$$

$$\begin{aligned} T_2^{RHS}(\mu(a,b)) =& f(\mu_0)+\mu'(a_0)\cdot f'(\mu_0)(a-a_0)+\mu'(b_0)\cdot f'(\mu_0)(b-b_0) \\ &+\frac{1}{2}(f\circ\mu)''_{aa}(\mu_0)(a-a_0)^2+\frac{1}{2}(f\circ\mu)''_{bb}(\mu_0)(b-b_0)^2 \\ &+(f\circ\mu)''_{ab}(\mu_0)(a-a_0)(b-b_0) \end{aligned} \tag{C2.2}$$

Without a loss of generality the approximation can be centered at the origin: $a_0 = b_0 = 0$ and $f(0) = 0$. Rearranging—by using the binomial theorem—and simplifying the expressions—by setting $f'(0) = f_0'$, $f''(0) = f_0''$, and $\mu(a,b) = \mu$ to save space—gives:

$$T_2^{LHS}(\mu(a,b)) = \frac{1}{2}\left[f_0'\cdot(a+b)+\frac{1}{2}f_0''\cdot(a^2+b^2)\right] = f_0'\cdot\mu+f_0''\cdot\mu-f_0''\frac{ab}{2} \tag{C3.1}$$

$$T_2^{RHS}(\mu(a,b)) = \frac{1}{2}f_0'\cdot a+\frac{1}{2}f_0'\cdot b+\frac{1}{8}f_0''\cdot a^2+\frac{1}{8}f_0''\cdot b^2+\frac{1}{4}f_0''\cdot ab = f_0'\cdot\mu+\frac{1}{2}f_0''\cdot\mu^2 \tag{C3.2}$$

Bringing back both expressions in the inequality form reveals the difference by means of the convexity property and the AM-GM inequality:

$$f_0'\cdot\mu+\frac{1}{2}f_0''\cdot\mu^2+\frac{1}{2}f_0''\underbrace{(\mu^2-ab)}_{>0} \geq f_0'\cdot\mu+\frac{1}{2}f_0''\cdot\mu^2. \tag{C4}$$

After a quadratic approximation on both sides, the inequality still holds.

C.2 Definition of the *Approximation Bias*

Modifying Eq.(3.2.2) will not fundamentally change the model's results but will lead to a clearer interpretation of Δ. The idea is to show the resemblance of (i) the difference of two growth rates and (ii) the reversed difference of their inverses. The latter can be approximated by first-order Taylor expansion to result in the actual difference. In the context of a DSGE model's first-order condition (i.e., the Euler equation) combined with the derivative of the CRRA function, we calculate the inverse of growth rates, weighted by the parameter γ:

$$\text{un-approximated:}\quad gr_w^{-1} = \mathrm{E}\left[\frac{1}{(1+X)^\gamma}\right];\quad \text{biased:}\quad gr_{w,b}^{-1} = \frac{1}{(1+\mathrm{E}[X])^\gamma} \tag{C5}$$

We use the indices w for *weighted* and b for *biased* in connection with growth rates gr. Additionally, gr is centered around one, representing negative (positive) growth for values smaller (larger) than one. Expressed as its magnitude, the plain Jensen's inequality gives a differential of inverted growth rates:

$$\widetilde{bias} = gr_w^{-1} - gr_{w,b}^{-1} = \frac{1}{gr_w \cdot gr_{w,b}}(gr_{w,b} - gr_w), \tag{C6}$$

which is positive for convex functions. Also, the first-order (multivariate) Taylor expansion of this expression is equivalent to the simple difference $gr_{w,b} - gr_w$:

$$T_1^{\widetilde{bias}}(gr_w, gr_{w,b}), \quad \text{at the center point:} \quad \mathbf{gr_0} = (1,1) \tag{C7.1}$$

$$\Rightarrow \quad \widetilde{bias}(1,1) + \widetilde{bias}'_{gr_w}(1,1) \cdot (gr_w - 1) + \widetilde{bias}'_{gr_{w,b}}(1,1) \cdot (gr_{w,b} - 1) = gr_{w,b} - gr_w. \tag{C7.2}$$

Therefore, we use these re-inverses directly for a cleaner interpretation. This changes Eq.(3.2.2) in a way that the plain difference is not only a linearized approximation but the actual research subject. To draw a closer connection, several numerical examples illustrate the similar outcome. Figure C1 reveals the discrepancies depending on the gr_w–level and an approximation bias of 10/25/50bp. The deviations, stemming from the fraction in Eq.(C6), are multiplied by 10^4, thus, being measured in bp.

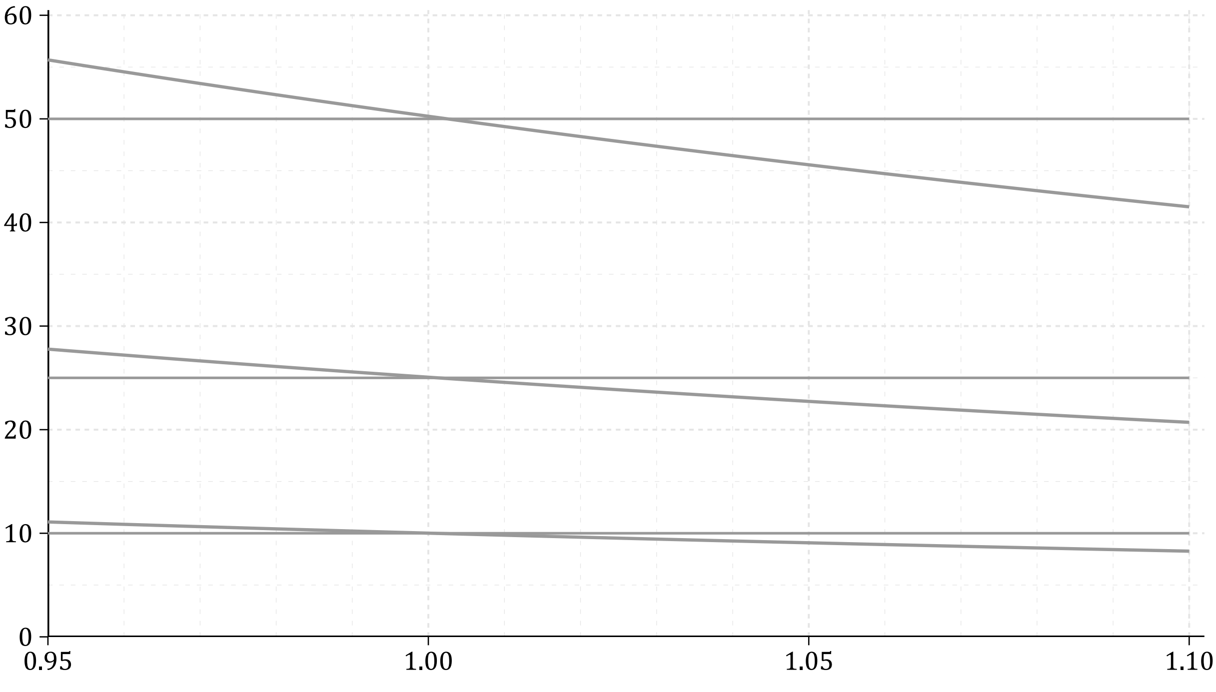

Figure C1: Comparing the difference ($gr_{w,b} - gr_w$) for 10/25/50bp and the corresponding bias in Eq.(C6) depending on the level of growth. Horizontal axis: Weighted growth rate gr_w. Vertical axis: Growth rate difference in basis points.

C.3 Moment Generating Function: Proof

Performing the critical step $\mathrm{E}[\exp(-\gamma\beta Z)] \Rightarrow \exp((\gamma\beta)^2/2)$ to drop the stochastic source, the moment generating function for the (standard) normal distribution is utilized:

$$M(t) = \mathrm{E}\left[e^{tZ}\right] = e^{t^2/2}, \quad Z \sim \mathcal{N}(0,1). \tag{C8}$$

To proof this relationship, the law of the unconscious statistician (LOTUS) is needed to write out the composition regarding the expectation value in terms of an integral:

$$\mathrm{E}\left[e^{tZ}\right] = \int_{\mathbb{R}} e^{tx} \cdot \frac{1}{\sqrt{2\pi}} e^{-x^2/2} dx = \frac{1}{\sqrt{2\pi}} \int_{\mathbb{R}} e^{-\frac{1}{2}(x^2-2tx)} dx. \tag{C9}$$

Expanding the exponent for a binomial formula and factoring out the constant gives

$$\mathrm{E}\left[e^{tZ}\right] = \frac{1}{\sqrt{2\pi}} \int_{\mathbb{R}} e^{-\frac{1}{2}(x^2-2tx+t^2-t^2)} dx = e^{t^2/2} \cdot \underbrace{\frac{1}{\sqrt{2\pi}} \int_{\mathbb{R}} e^{-\frac{1}{2}(x-t)^2} dx}_{=1}. \tag{C10}$$

Finally, since the area of a horizontally shifted (by t) standard normal distribution is still one, Eq.(C8) emerges.

C.4 Analytical Solution – Additional Inspection

To obtain a clearer picture of the auxiliary parameter r, the geometric approach in Figure C2 can help.

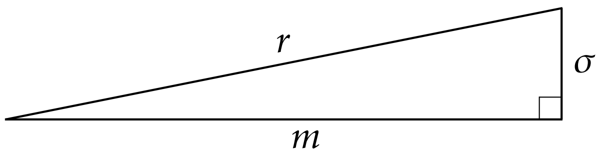

Figure C2: Graphical representation of the two moments and the auxiliary parameter r.

Without factoring out m^γ, the connection to the originating Eq.(3.6) becomes unmistakable. Simultaneously increasing the curvature,

$$\lim_{\gamma \to \infty} bias(\gamma \mid m > 1) = 10^4 \cdot \Big[\underbrace{m^\gamma}_{\to \infty} - \underbrace{m^\gamma \cdot (m/r)^{\gamma^2+\gamma}}_{\to 0} \Big], \tag{C11}$$

shows at the first underbrace the bias growing exponentially, whereas the second expression, after a maximum at $\gamma = \log(m^2/r)/\log(r^2/m^2)$, converges quadratic–exponentially towards zero. In a special case with $m = 1$ and therefore $\mu = 0$ and $r = \sqrt{1+\sigma^2}$, the average growth equals 0%. Here, the second term, stemming from the unbiased expression can be transformed into sums for $\sigma < 1$ and $\gamma \in \mathbb{N}$ by means of the geometric series and triangular numbers:

$$
\begin{aligned}
bias(\sigma,\gamma) &= 10^4 \cdot \left[1-(1/r)^{\gamma^2+\gamma}\right] && \text{(C12.1)}\\
&= 10^4 \cdot \left[1-\left(\frac{1}{1+\sigma^2}\right)^{\frac{\gamma(\gamma+1)}{2}}\right] && \text{(C12.2)}\\
&= 10^4 \cdot \left[1-\left(\sum_{i=0}^{\infty}(-1)^i\sigma^{2i}\right)^{\sum_{i=1}^{\gamma} i}\right]. && \text{(C12.3)}
\end{aligned}
$$

C.5 Algebraic Formula for the Variance

Typically shown by the binomial theorem, an alternative way to point out equality of the variance formula,

$$\mathrm{Var}[X] = \mathrm{E}[X^2] - (\mathrm{E}[X])^2, \tag{C13}$$

works analogously to the approach in Section 3.3. Inserting the distribution formula and its mean, μ, leads to

$$
\begin{aligned}
\mathrm{Var}[X] &= \mathrm{E}[\exp(\alpha+\beta Z)^2] - \mu^2 && \text{(C14.1)}\\
&= \exp(2\alpha)\cdot \mathrm{E}[\exp(2\beta Z)] - \mu^2 = \exp(2\alpha)\cdot\exp((4\beta^2)/2) - \mu^2 \\
&= \left(\frac{\mu}{\sqrt{1+(\sigma/\mu)^2}}\right)^2 \cdot \exp(\beta^2)^2 - \mu^2 = \left(\frac{\mu^2}{1+(\sigma/\mu)^2}\right)\cdot(1+(\sigma/\mu)^2)^2 - \mu^2 \\
&= \mu^2\cdot(1+(\sigma/\mu)^2) - \mu^2 = \sigma^2, && \text{(C14.2)}
\end{aligned}
$$

confirming the centered second moment for the log-normal distribution.

C.6 Inverted Beta-Distribution – Parameters

Similarly to Eqs.(3.7), log-normal case, we aim to solve for the parameters of the inverted beta (or beta prime) distribution. Being more unknown than the log-normal distribution, we show this in more detail. The moment-generating function (see, e.g., Keeping 1962, 84),

$$\mathrm{E}[X^\eta] = \prod_{i=1}^{\eta} \frac{\alpha+i-1}{\beta-i}, \quad \eta\in\mathbb{N} \text{ and } \eta<\beta, \tag{C15}$$

draws the connection between raw moments and parameters. The latter have to be written in terms of μ and σ to translate the grid in Eq.(3.18) into α and β. As claimed in Eq.(C15), η has to be smaller than β and, therefore, β has to be sufficiently large. Indeed, this is given in the calibration. For $\eta = 1$ and $\eta = 2$, the mean and the second central moment are

$$\mathrm{E}[X] = \mu = \frac{\alpha}{\beta - 1} \quad \text{and} \tag{C16.1}$$

$$\mathrm{E}[X^2] - \mathrm{E}[X]^2 = \sigma^2 = \frac{\alpha(\alpha + \beta - 1)}{(\beta - 2)(\beta - 1)^2}, \tag{C16.2}$$

respectively. First, replacing α in Eq.(C16.2) with Eq.(C16.1) and solving for β leads to

$$\sigma^2 = \frac{\mu(\beta - 1)(\mu(\beta - 1) + \beta - 1)}{(\beta - 2)(\beta - 1)^2} = \frac{\mu(\mu + 1)}{(\beta - 2)} \tag{C17.1}$$

$$\Leftrightarrow \quad \beta = 2 + \frac{\mu + 1}{\sigma^2}\mu. \tag{C17.2}$$

Second, solving Eq.(C16.1) for α and replacing β with Eq.(C17.2) leads to

$$\alpha = \mu\left(\frac{\mu(\mu + 1)}{\sigma^2} + 2 - 1\right) = \mu + \frac{\mu + 1}{\sigma^2}\mu^2. \tag{C18}$$

C.7 Parameter Results for US Inflation Forecasts

To obtain a better insight into the connection of the parameters, Table C1 displays the results of the calibration before conversion. The conversion of α and β is done by using Eqs.3.7 and Eqs.C16.

Parameter	Min	25^{th}centile	Median	75^{th}centile	Max
log-norm.					
α	−0.0032	0.0189	0.0243	0.0315	0.0411
β	0.0001	0.0001	0.0002	0.0007	0.0057
inv. beta					
α	0.1000	61.408	101.75	157.17	444.60
β	14.908	2301.5	3587.5	5372.9	18505.8

Table C1: Calibration results (US) when assuming CF data follow a log-normal and inverted beta distribution, respectively. The calibration is run on a monthly basis for the rolling window-adjusted observations on inflation forecasts.

For the log-normal distribution, the resulting values are close to the values after conversion. The α and β values for the inverted beta distribution are more widespread. This is a direct consequence of two characteristics of the distribution. The first one is that negative values are not drawn which can be overcome by a shift. The second—more crucial—point is the high probability mass at the left end of the distribution which can only be overcome by large values for α and β. A side effect of these values is a large spread of drawn variables which results in the higher error values compared to the log-normal distribution.

C.8 Calibration Results for US GDP Forecasts

The same tests and calibration as in Section 3.4 is run with the GDP growth forecast as observed variable. The time horizon is the same but the focus is only on the US and not on the frontier markets.

As before, we start with a normality test to check whether the log GDP forecast variables are normally distributed. The results can be seen in Table C2. In more than 75% of the observations, the J-B test cannot reject the H_0 of non-normally distributed variables.

Norm. Test	*p*-value Min	25^{th}centile	Median	75^{th}centile	Max
J-B	0	0.146	0.525	0.763	0.999
S-W	$6.99 \cdot 10^{-6}$	0.099	0.339	0.635	0.993
A-D	$4.95 \cdot 10^{-5}$	0.081	0.314	0.578	0.989
LF	$2.54 \cdot 10^{-4}$	0.085	0.334	0.641	0.994

Table C2: Normality test results for GDP growth forecasts (US).

As the results of the normality tests are sufficient, the calibration can be run. The results are presented in Table C3.

Parameter	Min	25$^{\text{th}}$centile	Median	75$^{\text{th}}$centile	Max	Obs. Median	Mean Error
log-norm.							
μ_{opt}	−0.0178	0.0192	0.0259	0.0320	0.0420	0.0260	$1.18{\cdot}10^{-5}$
σ_{opt}	0.0001	0.0001	0.0001	0.001	0.0022	0.0027	$1.18{\cdot}10^{-5}$
inv. beta							
μ_{opt}	0.0052	0.0255	0.0293	0.0329	0.2832	0.0260	$2.26{\cdot}10^{-4}$
σ_{opt}	0.0013	0.0022	0.0029	0.0039	0.1397	0.0027	$2.26{\cdot}10^{-4}$

Table C3: Calibration results (US) when assuming CF data follow a log-normal and inverted beta distribution, respectively. The calibration is run on a monthly basis for the rolling window-adjusted observations on GDP growth forecasts.

Compared to the results from the calibration of inflation forecasts, we can identify the same pattern. Whereas the log-normal distribution fits μ really good, the error in σ is larger. The inverted beta distribution shows a contrary picture with a good fit in σ and bad fit in μ. Nevertheless, the log-normal distribution again has a lower error. At last, the direct parameters resulting from the calibration before the conversion into μ and σ are presented in Table C4.

Parameter	Min	25$^{\text{th}}$centile	Median	75$^{\text{th}}$centile	Max
log-norm.					
α	−0.0179	0.0190	0.0256	0.0315	0.0411
β	0.0001	0.0001	0.0001	0.0001	0.0022
inv. beta					
α	0.1021	62.681	120.30	182.10	676.98
β	15.079	2117.6	3919.9	6210.9	19782.2

Table C4: Calibration results (US) when assuming CF data follow a log-normal and inverted beta distribution, respectively. The calibration is run on a monthly basis for the rolling window-adjusted observations on GDP growth forecasts.

The structure of the results is close to the one from the inflation forecasts. The resulting values from the log-normal distribution are close to the values after conversion and the α and β values for the inverted beta distribution are more widespread.

C.9 Impact of the Mean on the Approximation Bias

In the following, derivatives are used to evaluate the effect of μ on the approximation bias. Sticking to Eq.(3.11.3), the centered growth (m) is utilized. Nevertheless, the constant transformation, $m = 1 + \mu$, ensures equivalent derivatives:

$$\frac{\partial bias}{\partial \mu} \equiv \frac{\partial bias}{\partial m}. \tag{C19}$$

Since the absolute values of the approximation bias heavily depend on σ and γ (see Figure 3.3), it is difficult to draw conclusions concerning the impact of μ. We differentiate the *bias*-function to account for the change depending on a change in the mean growth rate. Using the product and chain rule, (...) refers to the part not changing:

$$\frac{\partial bias}{\partial m} = 10^4 \cdot \left[\gamma m^{\gamma-1}(...) + m^{\gamma}\left(\frac{\gamma(\gamma+1)}{2}\left(1+\frac{\sigma^2}{m^2}\right)^{-\frac{\gamma(\gamma+1)}{2}-1} \cdot (-2\sigma^2 m^{-3})\right)\right] \tag{C20.1}$$

$$= 10^4 \cdot \gamma m^{\gamma-1}\left[(...) - (\gamma+1)\left(1+\frac{\sigma^2}{m^2}\right)^{-\frac{\gamma(\gamma+1)}{2}-1} \cdot \frac{\sigma^2}{m^2}\right] \tag{C20.2}$$

$$= 10^4 \cdot \gamma m^{\gamma-1}\left[1 - \left(1+\sigma^2/m^2\right)^{-\frac{\gamma(\gamma+1)}{2}}\left(1+\frac{(1+\gamma)\sigma^2}{m^2+\sigma^2}\right)\right]. \tag{C20.3}$$

Testing the baseline scenario for extreme μ-values:

$$\frac{\partial bias}{\partial m}(\mu = -5\% \mid BL) \approx -1.2 \;\widehat{=}\; -0.012 bp/pp \tag{C21.1}$$

$$\frac{\partial bias}{\partial m}(\mu = 20\% \mid BL) \approx -0.8 \;\widehat{=}\; -0.008 bp/pp \tag{C21.2}$$

The interpretation is a change in basis point (e.g., an increase of the bias) caused by a 1pp increase of the mean growth. For the BL case, the change at the upper and lower bound is basically zero. Testing maximum values for σ and γ:

$$\frac{\partial bias}{\partial m}(\mu = -5\% \mid \sigma = 0.04, \gamma = 1) \approx -17.6 \;\widehat{=} -0.176 bp/pp \tag{C22.1}$$

$$\frac{\partial bias}{\partial m}(\mu = 20\% \mid \sigma = 0.04, \gamma = 1) \approx -11.1 \;\widehat{=} -0.111 bp/pp \tag{C22.2}$$

$$\frac{\partial bias}{\partial m}(\mu = -5\% \mid \sigma = 0.01, \gamma = 5) \approx \quad 40.6 \;\widehat{=}\quad 0.406 bp/pp \tag{C22.3}$$

$$\frac{\partial bias}{\partial m}(\mu = 20\% \mid \sigma = 0.01, \gamma = 5) \approx \quad 64.8 \;\widehat{=}\quad 0.648 bp/pp \tag{C22.4}$$

Even for the maximum values, the change is significantly under 1bp. This makes it uninteresting to further examine μ as a varying parameter in the simulations.

C.10 Regression Outputs

Accompanying the MC simulations in Section 3.5, we regress the median-*bias* on the varying parameters, respectively. Using the median instead of the mean is interesting when facing skewed data and since there are already theoretical solutions in some cases for the mean. Also, this goes hand in hand with Figures 3.4–3.10 which display the standard boxplots. However, despite the mean being always larger, there are no substantial differences. As a robustness check, we also present regression results—in the same vein—for both the CARA function and the inverted beta distribution. Starting with the main results, Table C5 shows five regressions for four parameters.

Term	$bias(\sigma)$	$bias(\gamma)$	$\log bias(\gamma)$	$bias(\rho)$	$\log bias(n)$
const.	−0.002 (0.004)	−0.265*** (0.062)	−0.121*** (0.002)	1.903*** (0.000)	−0.146*** (0.001)
linear	0.003 (0.004)	−0.109* (0.054)		0.009*** (0.000)	0.066*** (0.001)
quadr.	0.890*** (0.001)	0.679*** (0.010)		−0.000 (0.000)	−0.000*** (0.000)
log			1.575*** (0.002)		1.022*** (0.002)
log-quadr.			0.155*** (0.002)		
$\overline{R}^2$	1	0.99	1	1	1
Std.Err.	$5.46 \cdot 10^{-3}$	$8.31 \cdot 10^{-2}$	$6.39 \cdot 10^{-3}$	$1.18 \cdot 10^{-3}$	$1.05 \cdot 10^{-3}$
Obs.	20	20	20	20	20

Table C5: Second moment measures (σ and ρ) are multiplied by 100. ***/**/* denote significance at the 1%/5%/10% level.

Multiplying σ and ρ by 100 accounts for the typical step size when referring to one increment. Therefore, the first regression column predicts an increase in the *bias* by $2 \cdot 0.89 \times 100 \cdot \sigma_1$ when increasing the standard deviation by 0.01 at a level of σ_1. Since the other estimates are extremely small and insignificant, they are not absorbing explanatory power from the quadratic term. Also, explaining basically 100% of the dependent variable's variation confirms the (nearly) quadratic relationship discussed in Section 3.3.

The second column draws a different picture since the model artificially shifts the parabola's vertex to the forth quadrant. In addition, the quadratic term is smaller than in the σ-case, probably underestimating the effect for larger values. Alternatively, in the third column, estimating the elasticity (1.575) increases the explanatory power. However, the effect cannot be isolated and the relationship is still more complex, expressed by the significant squared log-coefficient. The intercept comes into play if $\gamma = 1$ (log-utility) and indicates a positive *bias* close to zero. Without the squared term, the elasticity would be somewhat larger (1.665), the intercept insignificant, and $\overline{R}^2 = 0.99$.

Column four confirms the linear relationship regarding the correlation between two variables. Staying at 1.9bp without any correlation, a 0.01-step results in a significant change that is basically zero. However, for more than two variables, Figure 3.9 points out an increase in the slope while preserving the linear connection. In the last column, a roughly unit elastic relationship emerges, reinforced by the linear term, which effects an increase of 6.6% for every additional variable. For $n = 1$, $\log bias = -0.08$, which perfectly matches the baseline result of just below 1bp visible in Figure 3.6.

As seen in Table C6, the above numbers are mostly confirmed in our robustness check. Therefore, for both the inverted beta (instead of log-normal) and the CARA (instead of CRRA) we renounce examining the multivariate part, which is non-trivial for the multivariate inverted beta-distribution. The first two columns are basically equal to column one and three in Table C5. In the CARA case, the quadratic coefficient is somewhat smaller (varying σ) and the elasticity is slightly larger (varying γ). Mathematically, in the log-utility case ($\gamma = 1$) and after applying the inversion $g(y)$, the marginal CRRA-function is only a first-order Taylor expansion of the CARA around zero: $1 + x \approx e^x$. However, the simpler CRRA-function better fits into our model assumptions and is used frequently in the literature.

Term	$bias_{\text{beta}}(\sigma)$	$\log bias_{\text{beta}}(\gamma)$	$bias_{\text{CARA}}(\sigma)$	$\log bias_{\text{CARA}}(\gamma)$
const.	−0.010	−0.120***	−0.002	−0.699***
	(0.007)	(0.002)	(0.004)	(0.003)
linear	0.019**		0.005	
	(0.008)		(0.004)	
quadr.	0.885***		0.499***	
	(0.002)		(0.001)	
log		1.575***		2.077***
		(0.002)		(0.003)
log-quadr.		0.156***		0.043***
		(0.002)		(0.003)
$\overline{R}^2$	1	1	1	1
Std.Err.	$9.91 \cdot 10^{-3}$	$5.97 \cdot 10^{-3}$	$5.16 \cdot 10^{-3}$	$8.51 \cdot 10^{-3}$
Obs.	20	20	20	20

Table C6: σ is multiplied by 100 to account for the typical step size. ***/**/* denote significance at the 1%/5%/10% level.

C.11 2[nd]-Order Taylor Series for Eq.(3.12)

In addition to the regression analysis, we check for accuracy whether the relationship can be titled "quadratic" for a realistic range of σ, from a theoretical point of view. Approximating around $\sigma_0 = 0$ is chosen for simplicity, although this is the smallest possible value, and therefore it cannot be the optimal center point. It turns out that this approximation is sufficient for eligible values. However, as an extension, we also choose center points larger than zero to check how the formula changes and to clarify the mechanics behind the Taylor series. The following function has to be constructed from Eq.(3.12):

$$T_2(\sigma \mid \sigma_0) = bias(\sigma_0) + bias'(\sigma_0)(\sigma - \sigma_0) + \frac{1}{2} bias''(\sigma_0)(\sigma - \sigma_0)^2. \tag{C23}$$

First and second derivatives are:

$$bias'(\sigma) = 10^4 \frac{2m^3\sigma}{(m^2+\sigma^2)^2} \quad \Rightarrow \quad bias'(0) = 0 \tag{C24.1}$$

$$bias''(\sigma) = 10^4 \frac{2m^3(m^2 - 3\sigma^2)}{(m^2+\sigma^2)^3} \quad \Rightarrow \quad bias''(0) = 10^4 \cdot 2m^{-1} \tag{C24.2}$$

This ends in a simple quadratic relationship corrected by m, the centered mean:

$$T_2(\sigma \mid \sigma_0 = 0) = 10^4 \cdot \sigma^2 / m \tag{C25}$$

Compared to the accurate solution, second-order Taylor expansion overestimates the bias when the standard deviation is increasing from the center point. Taking the classical log-linearizing of growth rates as a reference point, a growth rate of 5% leads to a deviation of almost 2.5%:[40]

$$\frac{5\%}{\log(1.05)} - 1 \approx 2.48\% \tag{C26}$$

Using this benchmark in terms of Eqs.(3.12) and (C25) gives

$$\frac{T_2(\sigma = 0.167)}{bias(\sigma = 0.167)} - 1 \approx 2.48\%. \tag{C27}$$

Since 0.167 is roughly four times larger than the maximum value chosen in the simulation, we can conclude that the quadratic approximation is sufficient. Nevertheless, as further extension, using a center points greater than zero, Table C7 gives an impression of how the accuracy changes over the σ's.

Center point	$-2.5\% <$ %-difference $< 2.5\%$		Difference at $\sigma = 0.01$
σ_0	min σ	max σ	Δbp
0.005	0.001	0.168	0
0.010	0.001	0.169	0
0.015	0.002	0.171	0
0.020	0.004	0.173	−0.001
0.025	0.005	0.176	−0.002
0.030	0.007	0.180	−0.007
0.035	0.009	0.184	−0.015
0.040	0.011	0.188	−0.029
0.045	0.014	0.192	−0.052
0.050	0.016	0.196	−0.085

Table C7: For σ values smaller (larger) than σ_0 the theoretical bias is underestimated (overestimated).

[40] 5% would be the approximation and log(1.05) the correct expression (in a non-linear equation). Therefore, the percentage deviation is standardized by the latter term.

With a larger center point, the maximum σ-value increases at which the approximation is sufficient. However, this gained accuracy does not compensate the simultaneously increasing minimum σ-value, with $\sigma_0 = 0.04$ already surpassing the baseline case. The latter is further examined in the last column, showing the absolute difference in basis points. This difference is still very small, not reaching a tenth of a basis point. Therefore, from a practical point of view, even when the center point is not optimal, the approximation error is negligible.

C.12 Jensen's Inequality as Ratio

Formulating the problem as a ratio gives the advantage of a simpler formula. Initially, the factor 10^4 gets redundant, cancelling out due to the fraction. Also, in this case, the function $g(y)$ only switches denominator and numerator, resulting in a ratio > 100%:

$$bias_r(m,\sigma,\gamma) = \frac{(1 + \mathrm{E}_t[growth_{t+1}])^\gamma}{\mathrm{E}_t[(1 + growth_{t+1})^{-\gamma}]^{-1}} = \frac{m^\gamma}{m^\gamma \cdot \left(\frac{m}{\sqrt{m^2+\sigma^2}}\right)^{\gamma(\gamma+1)}} \tag{C28.1}$$

$$= \left(\frac{m}{\sqrt{m^2+\sigma^2}}\right)^{-\gamma(\gamma+1)} = \left(\frac{\sqrt{m^2+\sigma^2}}{m}\right)^{\gamma(\gamma+1)} = \left(1 + \frac{\sigma^2}{m^2}\right)^{\frac{\gamma(\gamma+1)}{2}}. \tag{C28.2}$$

Additionally, the formula reduces to squared expressions for all parameters while the curvature remains in the exponent. Given positive integer values for γ, the formula can be written in a discrete form as

$$bias_r(m,\sigma,\gamma) = \left(1 + (\sigma/m)^2\right)^{\sum_{i=0}^{\gamma} i} = \prod_{i=1}^{\gamma} \left(1 + (\sigma/m)^2\right)^i, \tag{C29}$$

a product which factors only consist of 100% plus a squared coefficient of variation weighted by integer exponents. Figure C3 depicts Eq.(C29) for several curvature values, revealing a deviation, even for extreme scenarios, by only a few percent.

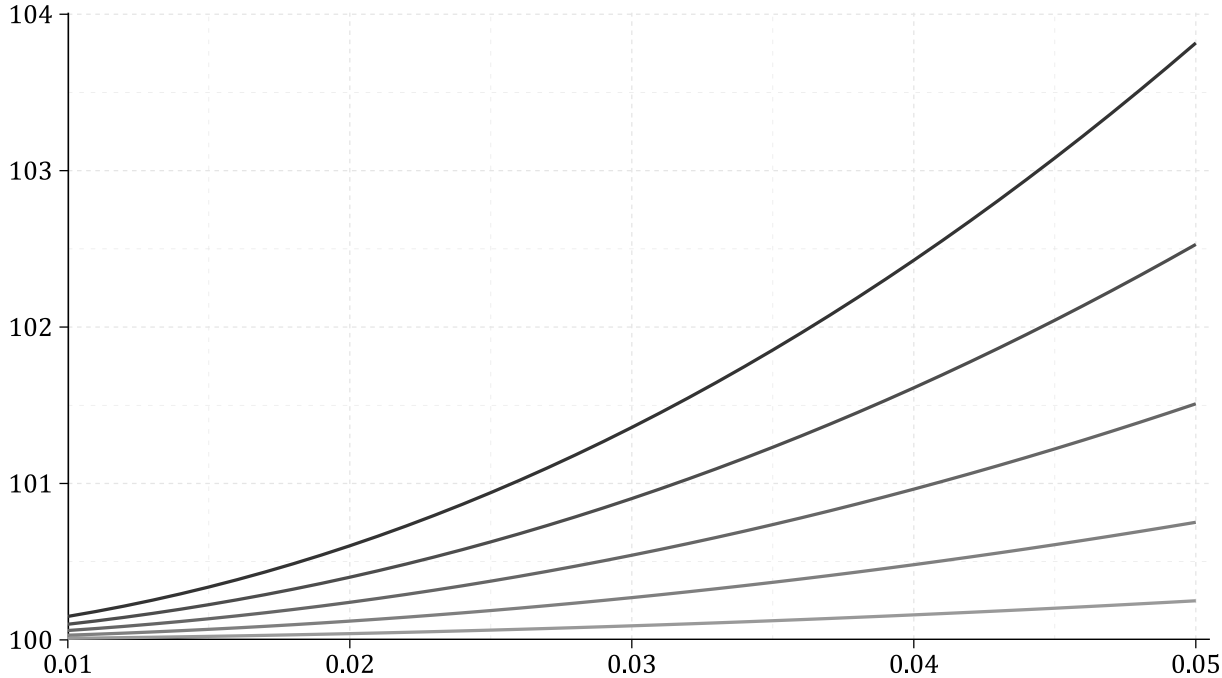

Figure C3: Comparing the Jensen ratios for $\gamma_i \in \{1, 2, 3, 4, 5\}$ and varying σ/m. Lines are ordered from lightgray ($\gamma = 1$) to darkgray ($\gamma = 5$). Horizontal axis: Coefficient of variation (σ/m). Vertical axis: Ratio of growth rates in %.

C.13 2nd-Order Taylor Series for Eq.(3.13)

The following function has to be constructed from Eq.(3.13):

$$T_2(\gamma \mid \gamma_0) = bias(\gamma_0) + bias'(\gamma_0)(\gamma - \gamma_0) + \frac{1}{2} bias''(\gamma_0)(\gamma - \gamma_0)^2. \tag{C30}$$

Analogous to Eq.(C25), the center point, γ_0, equals zero. The first derivative is calculated by the product rule, the chain rule, and the log-rule to switch the sign:

$$\begin{aligned} bias'(\gamma) &= 10^4 \Big[\log(m) m^\gamma \cdot \Big(1 - (m/r)^{\gamma(\gamma+1)}\Big) + m^\gamma \cdot (-\log(m/r))(m/r)^{\gamma(\gamma+1)}(2\gamma+1) \Big] \\ &= 10^4 \cdot m^\gamma \Big[\log(m) \cdot \Big(1 - (m/r)^{\gamma(\gamma+1)}\Big) + \log(r/m)(m/r)^{\gamma(\gamma+1)}(2\gamma+1) \Big] \\ &= 10^4 \cdot m^\gamma \Big[\log(m) + (m/r)^{\gamma(\gamma+1)} \cdot \Big(\log(r/m)(2\gamma+1) - \log(m)\Big) \Big] \qquad \text{(C31.1)} \\ \Rightarrow \quad bias'(0) &= 10^4 \cdot \log(r/m) \qquad \text{(C31.2)} \end{aligned}$$

Applying the product rule twice, with [...] and (...) for the parts not differentiated, gives

$$\begin{aligned} bias''(\gamma) = 10^4 \Big[& \log(m) m^\gamma \cdot [...] + \\ & m^\gamma \cdot \Big(\log(m/r)(m/r)^{\gamma(\gamma+1)}(2\gamma+1) \cdot (...) + (m/r)^{\gamma(\gamma+1)} \cdot 2\log(r/m) \Big) \Big] \\ = {} & 10^4 \cdot m^\gamma \Big[\log(m) \cdot [...] + \log(r/m)(m/r)^{\gamma(\gamma+1)}(2 - (2\gamma+1)(...)) \Big] \qquad \text{(C32.1)} \end{aligned}$$

$$
\begin{aligned}
\Rightarrow \quad bias''(0) &= 10^4 \cdot [\log(m)\cdot\log(r/m) + \log(r/m)\cdot(2-(\log(r/m)-\log(m)))] \\
&= 10^4 \cdot \log(r/m)\Big(2\log(m) + 2 - \log(r/m)\Big) \\
&= 10^4 \cdot \log(r/m)\Big(2\log(m) + 2\log(\mathrm{e}) + \log(m/r)\Big) \\
&= 10^4 \cdot 2\log(r/m)\log\left(m\mathrm{e}\sqrt{m/r}\right). \qquad \text{(C32.2)}
\end{aligned}
$$

Putting the derivatives together leads to a quadratic equation without intercept and similar coefficients for the linear and the quadratic term:

$$
T_2(\gamma \mid \gamma_0 = 0) = 10^4 \cdot \log(r/m)\Big[\log\left(\mathrm{e}\sqrt{m^3/r}\right)\gamma^2 + \gamma\Big] \qquad \text{(C33)}
$$

Compared to the accurate solution, second-order Taylor underestimates the bias when the curvature is increasing from the center point. Using the benchmark in Eq.(C26) in terms of Eqs.(3.13) and (C33) gives

$$
\left|\frac{T_2(\gamma = 0.9)}{bias(\gamma = 0.9)} - 1\right| \approx 2.49\%. \qquad \text{(C34)}
$$

This corresponds to a curvature up to 0.9 and, thus, slightly smaller than the baseline case. In terms of the economic interpretation, the quadratic Taylor-series is accurate enough for EIS-values larger than 1.1. Following the meta-study by Havranek et al (2015), this includes not even half of the scenarios. Hence, in contrast to the σ-version in Appendix C.11, we would not refer to this relationship as quadratic. For reasonable values, the relationship is exponential with approximately constant elasticities, $\partial\log(bias)/\partial\log(\gamma)$.

C.14 Simulation with the Elasticity of Intertemporal Substitution

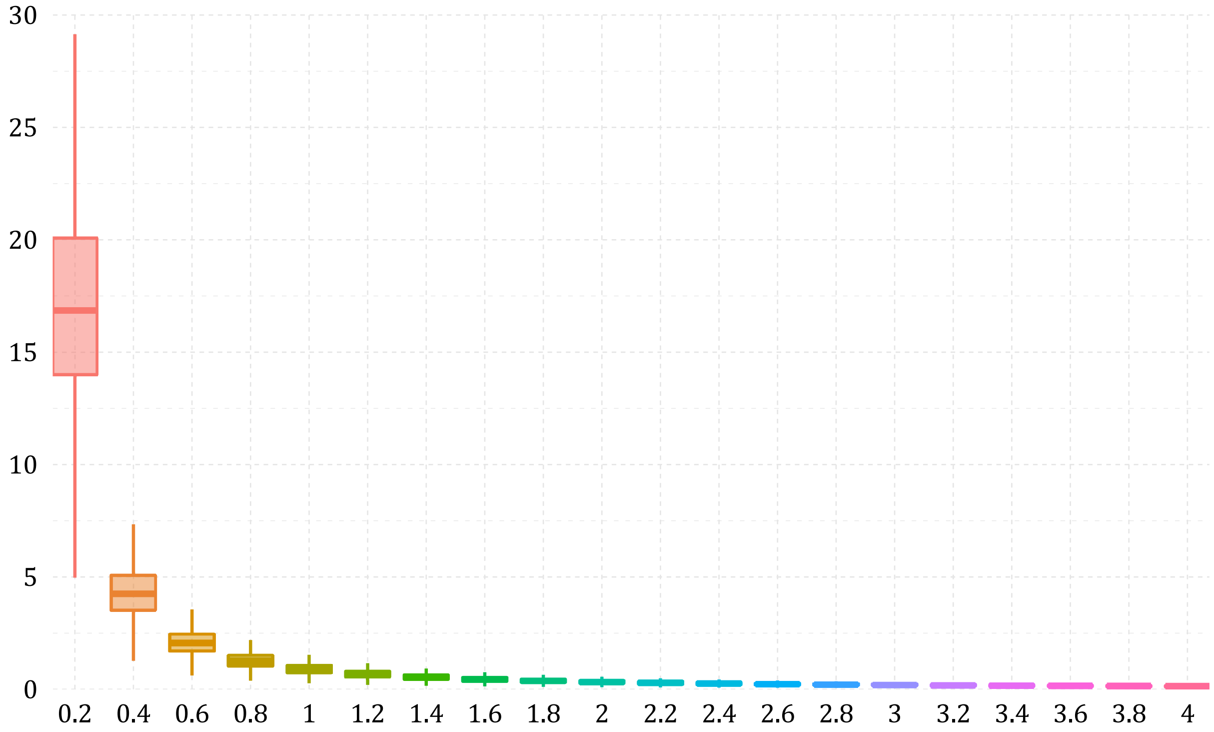

Figure C4: Horizontal axis: EIS (γ^{-1}). Vertical axis: Growth rate difference in basis points.

Appearing like the distorted mirror image of Figure 3.5, the graphic shows a significant impact for EIS = 0.2 only.

C.15 Convergence for Large Samples

We show how the empirical bias approaches the analytical bias by means of the variance formula, $\text{Var}[X] = E[X^2] - E[X]^2$, a special case of Jensen's inequality. This example is particularly traceable since the analytical bias consists of σ^2 only. Therefore, this case specifies the function f but shows the results being not dependent on the moments or the distribution, provided that the required moments are defined. The setup is as follows:

$$\lim_{N\to\infty} \mathrm{E}\left[\frac{1}{N}\sum_{i=1}^{N} x_i^2 - \left(\frac{1}{N}\sum_{i=1}^{N} x_i\right)^2\right] = \sigma^2, \quad x_i \sim i.i.d.(\mu, \sigma^2) \tag{C35}$$

We claim that the %-difference to σ^2 for finite N is always negative and approaches this value in the form of a hyperbola:

$$\frac{\mathrm{E}\left[\frac{1}{N}\sum_{i=1}^{N} x_i^2 - \left(\frac{1}{N}\sum_{i=1}^{N} x_i\right)^2\right] - \sigma^2}{\sigma^2} = -\frac{1}{N} \tag{C36}$$

The interpretation in percent is convenient since for $N = 1$ the value stays at -100% and approaches 0% for $N \to \infty$. Eq.(C36) can be simplified by using $\mathrm{E}[x_i \cdot x_j] = \mathrm{E}[x_i] \cdot \mathrm{E}[x_j] + \mathrm{Cov}[x_i, x_j]$ as the key step:

$$\Rightarrow \qquad \frac{1}{N}\sum_{i=1}^{N}\mathrm{E}[x_i^2] - \frac{1}{N^2}\mathrm{E}\left[\left(\sum_{i=1}^{N} x_i\right)^2\right] = \sigma^2 - \frac{\sigma^2}{N} \tag{C37.1}$$

$$\Leftrightarrow \qquad \mu^2 + \sigma^2 - \frac{1}{N^2}\mathrm{E}\left[(x_1 + \ldots + x_N)^2\right] = \sigma^2 - \frac{\sigma^2}{N} \tag{C37.2}$$

$$\Leftrightarrow \qquad N^2\mu^2 - \mathrm{E}\left[\sum_{i=1}^{N} x_i^2 + 2\sum_{i=1}^{N-1}\left(x_i \cdot \sum_{j=1+i}^{N} x_j\right)\right] = -N\sigma^2 \tag{C37.3}$$

$$\Leftrightarrow \quad N^2\mu^2 - N(\mu^2 + \sigma^2) - 2\mathrm{E}\Big[\underbrace{x_1x_2 + x_1x_3 + \cdots + x_1x_N}_{(N-1)\text{ terms}} + \underbrace{x_2x_3 + x_2x_4 + \cdots + x_2x_N}_{(N-2)\text{ terms}} + \cdots + \underbrace{x_{N-1}x_N}_{1\text{ term}}\Big] = -N\sigma^2 \tag{C37.4}$$

$$\Leftrightarrow \qquad N^2\mu^2 - N\mu^2 - 2\frac{N(N-1)}{2}\mu^2 = 0. \quad \blacksquare \tag{C37.5}$$

From Eq.(C37.4) to Eq.(C37.5), the *i.i.d.*-property ensures that $\mathrm{Cov}[x_i, x_j] = 0$. The fraction in the last step, $N(N-1)/2 = 1 + 2 + \ldots + (N-1)$, equals the total amount of terms x_ix_j.

Interpreting N as the amount of states, in which the future economy can be situated, the analytical bias has to be corrected downwards by $(N-1)/N$. E.g., for two possible states, the bias has only half the size as analytically derived.

C.16 Overview: Figures

Figure	μ	σ	γ	ρ	n	N	~max. Δbp
3.3	−5%-20%	0.001-0.04	1.5/2/2.5	–	1	∞	70
3.4	6%	0.002-0.04	1	–	1	30	25
3.5	6%	0.01	0.25-5	–	1	30	30
3.6	6%	0.01	1	–	1	1-20	2
3.7	6%	0.002-0.04	1	–	1	2	25
3.8	6%	0.01	1	−0.95-0.95	2	30	5
3.9	6%	0.01	1	0-0.95	5	30	30
3.10	2.5%	0.01	1	0.1	1-20	30	90

Table C8: Overview for all figures using varying parameters. μ ($= m-1$) and σ designate the growth rates' mean and standard deviation, respectively. γ reflects the non-linear function's curvature. ρ is the correlation between two or more variables. n counts the number of variables in the model. N stands for the sample size. The last column shows the maximum differences in basis points of the respective figure.

Bibliography

Ahir, H., Bloom, N. & Furceri, D. (2018): "The World Uncertainty Index," *SSRN* 3275033.
https://doi.org/10.2139/ssrn.3275033

An, S. & Schorfheide, F. (2007): "Bayesian Analysis of DSGE Models," *Econometric Reviews* 26, 113–172.
https://doi.org/10.1080/07474930701220071

Aruoba, S.B., Fernández-Villaverde, J. & Rubio-Ramírez, J.F. (2006): "Comparing Solution Methods for Dynamic Equilibrium Economies," *Journal of Economic Dynamics & Control* 30, 2477–2508.
https://doi.org/10.1016/j.jedc.2005.07.008

Attanasio, O.P. & Low, H. (2004): "Estimating Euler Equations," *Review of Economic Dynamics* 7, 406–435.
https://doi.org/10.1016/j.red.2003.09.003

Attanasio, O.P. & Weber, G. (1989): "Intertemporal Substitution, Risk Aversion and the Euler Equation for Consumption," *The Economic Journal* 99, 59–73.
https://doi.org/10.2307/2234070

Baker, S., Bloom, N. & Davis, S.J. (2016): "Measuring Economic Policy Uncertainty," *The Quarterly Journal of Economics* 131, 1593–1636.
https://doi.org/10.1093/qje/qjw024

Bassetto, M. (2004): "Negative Nominal Interest Rates," *American Economic Review* 94, 104–108.
https://doi.org/10.1257/0002828041302064

Bauer, C. & Neuenkirch, M. (2017): "Forecast Uncertainty and the Taylor Rule," *Journal of International Money and Finance* 77, 99–116.
https://doi.org/10.1016/j.jimonfin.2017.07.017

Beaudry, P. & van Wincoop, E. (1996): "The Intertemporal Elasticity of Substitution: An Exploration using a US Panel of State Data," *Economica* 63, 495–512.
https://doi.org/10.2307/2555019

Bernoulli, D. (1738): "Exposition of a New Theory on the Measurement of Risk," Translated by Louise Sommer (1954), *Econometrica* 22, 23–36.
https://doi.org/10.2307/1909829

Black, F. & Scholes M. (1973): "The Pricing of Options and Corporate Liabilities," *Journal of Political Economy* 81, 637–654.
https://doi.org/10.1086/260062

Blanchard, O.J. & Mankiw, N.G. (1988): "Consumption: Beyond Certainty Equivalence," *American Economic Review* 78, 173–177.
https://jstor.org/stable/1818118

Bollerslev, T., Gibson, M. & Zhou, H. (2011): "Dynamic Estimation of Volatility Risk Premia and Investor Risk Aversion from Option-Implied and Realized Volatilities," *Journal of Econometrics* 160, 235–245.
https://doi.org/10.1016/j.jeconom.2010.03.033

Boneva, L.M., Braun, R.A. & Waki, Y. (2016): "Some unpleasant Properties of Loglinearized Solutions when the Nominal Rate is Zero," *Journal of Monetary Economics* 84, 216–232.
https://doi.org/10.1016/j.jmoneco.2016.10.012

Branch, W.A. (2014): "Nowcasting and the Taylor Rule," *Journal of Money, Credit and Banking* 46, 1035–1055.
https://doi.org/10.1111/jmcb.12128

Calvo, G.A. (1983): "Staggered Prices in a Utility-Maximizing Framework," *Journal of Monetary Economics* 12, 383–398.
https://doi.org/10.1016/0304-3932(83)90060-0

Cantillon, R. (1755): "Essay on the Nature of Trade in General," Translated & Edited by A.E. Murphy (2015), *Liberty Fund*, Indianapolis.
https://libertyfund.org/books/essay-on-the-nature-of-trade-in-general

Carabenciov, I., Freedman, C., Garcia-Saltos, R., Laxton, D., Kamenik, O. & Manchev, P. (2013): "GPM6 - The Global Projection Model with 6 Regions," *IMF Working Paper* 13/87, 1–78.
https://books.google.de/books?id=F37uHGxjjo8C

Carroll, C.D. (2001): "Death to the Log-Linearized Consumption Euler Equation! (And Very Poor Health to the Second-Order Approximation)," *Advances in Macroeconomics* 1, Article 6.
https://doi.org/10.2202/1534-6013.1003

Carroll, C.D. & Kimball, M.S. (1996): "On the Concavity of the Consumption Function," *Econometrica* 64, 981–992.
https://doi.org/10.2307/2171853

Chetty, R. (2006): "A New Method of Estimating Risk Aversion," *American Economic Review* 96, 1821–1834.
https://doi.org/10.1257/aer.96.5.1821

Chiappori, P.-A. & Paiella, M. (2011): "Relative Risk Aversion is Constant: Evidence from Panel Data," *Journal of the European Economic Association* 9, 1021–1052.
https://doi.org/10.1111/j.1542-4774.2011.01046.x

Christiano, L.J., Trabandt, M. & Walentin, K. (2011): "DSGE Models for Monetary Policy Analysis," *Handbook of Monetary Economics* 3A, 285–367.
https://doi.org/10.1016/B978-0-444-53238-1.00007-7

Clarida, R., Galí, J. & Gertler, M. (1999): "The Science of Monetary Policy: A New Keynesian Perspective," *Journal of Economic Literature* 37, 1661–1707.
https://doi.org/10.1257/jel.37.4.1661

Clarida, R., Galí, J. & Gertler, M. (2000): "Monetary Policy Rules and Macroeconomic Stability: Evidence and Some Theory," *Quarterly Journal of Economics* 105, 147–180.
https://doi.org/10.1162/003355300554692

Collard, F. & Juillard, M. (2001): "A Higher-Order Taylor Expansion Approach to Simulation of Stochastic Forward-Looking Models with an Application to a Nonlinear Phillips Curve Model," *Computational Economics* 17, 125–139.
https://doi.org/10.1023/A:1011624124377

Cullen, A.C. & Frey, H.C. (1999): "Probabilistic Techniques in Exposure Assessment: A Handbook for Dealing with Variability and Uncertainty in Models and Inputs," *Springer US*.
https://books.google.de/books?id=P9l5q4RjcwcC

De Paoli, B. & Zabczyk, P. (2013): "Cyclical Risk Aversion, Precautionary Saving, and Monetary Policy," *Journal of Money, Credit and Banking* 45, 1–36.
https://doi.org/10.1111/j.1538-4616.2012.00560.x

Del Negro, M., Schorfheide, F., Smets, F. & Wouters, R. (2007): "On the Fit of New Keynesian Models," *Journal of Business & Economic Statistics* 25, 123–143.
https://doi.org/10.1198/073500107000000016

Dieppe, A., Georgiadis, G., Ricci, M., Van Robays, I. & van Roye, B. (2018): "ECB-Global: Introducing the ECB's Global Macroeconomic Model for Spillover Analysis," *Economic Modelling* 30, 1–21.
https://doi.org/10.1016/j.econmod.2018.01.007

Dixit, A.K. & Stiglitz, J.E. (1977): "Monopolistic Competition and Optimum Product Diversity," *American Economic Review* 67, 297–308.
https://doi.org/10.7916/D8S75S91

Dolado, J.J., María-Dolores, R. & Naveira, M. (2014): "Are Monetary–Policy Reaction Functions Asymmetric?: The Role of Nonlinearity in the Phillips Curve," *European Economic Review* 49, 485–503.
https://doi.org/10.1016/S0014-2921(03)00032-1

Epstein, L.G. & Zin, S.E. (1989): "Substitution, Risk Aversion, and the Temporal Behavior of Consumption and Asset," *Econometrica* 57, 937–969.
https://doi.org/10.2307/1913778

Fernández-Villaverde, J. (2010): "The Econometrics of DSGE Models," *SERIEs* 1, 3–49.
https://doi.org/10.1007/s13209-009-0014-7

Fernández-Villaverde, J., Guerrón-Quintana, P., Rubio-Ramírez, J.F. & Uribe, M. (2011): "Risk Matters: The Real Effects of Volatility Shocks," *American Economic Review* 101, 2530–2561.
https://doi.org/10.1257/aer.101.6.2530

Fernández-Villaverde, J., Rubio-Ramírez, J.F. & Schorfheide, F. (2016): "Solution and Estimation Methods for DSGE Models," *Handbook of Monetary Economics* 2A, 527–724.
https://doi.org/10.1016/bs.hesmac.2016.03.006

Galí, J. (2015): "Monetary Policy, Inflation, and the Business Cycle," 2nd Edition, *Princeton University Press*, Princeton, NJ.
https://press.princeton.edu/titles/10495.html

Galí, J. & Gertler, M. (1999): "Inflation Dynamics: A Structural Econometric Analysis," *Journal of Monetary Economics* 44, 195–222.
https://doi.org/10.1016/S0304-3932(99)00023-9

Galí, J. & Rabanal, P. (2004): "Technology Shocks and Aggregate Fluctuations: How Well Does the Real Business Cycle Model Fit Postwar U.S. Data?," *NBER Macroeconomics Annual* 19, 225–288.
https://jstor.org/stable/3585339

Gomez, F.A.R. & Paz, L.S. (2013): "Estimating the Elasticity of Intertemporal Substitution: Is the Aggregate Financial Return free from the Weak Instrument Problem?," *Journal of Macroeconomics* 36, 63–75.
https://doi.org/10.1016/j.jmacro.2013.01.005

Gürkaynak, R.S., Sack, B. & Wright, J.H. (2010): "The TIPS Yield Curve and Inflation Compensation," *American Economic Journal: Macroeconomics* 2, 70–92.
https://doi.org/10.1257/mac.2.1.70

Hall, R.E. (1978): "Stochastic Implications of the Life Cycle-Permanent Income Hypothesis: Theory and Evidence," *Journal of Political Economy* 86, 971–987.
https://jstor.org/stable/1840393

Hall, R.E. (1988): "Intertemporal Substitution in Consumption," *Journal of Political Economy* 96, 339–357.
https://jstor.org/stable/1833112

Hamilton, J.D., Harris, E.S., Hatzius, J. & West, K.D. (2016): "The Equilibrium Real Funds Rate: Past, Present, and Future," *IMF Economic Review* 64, 660–707.
https://doi.org/10.1057/s41308-016-0015-z

Havranek, T., Horvath, R., Irsova, Z. & Rusnak, M. (2015): "Cross-Country Heterogeneity in Intertemporal Substitution," *Journal of International Economics* 96, 100–118.
https://doi.org/10.1016/j.jinteco.2015.01.012

Hubert, M. & Vandervieren, E. (2008): "An Adjusted Boxplot for Skewed Distributions," *Computational Statistics and Data Analysis* 52, 5186–5201.
https://doi.org/10.1016/j.csda.2007.11.008

Ibragimov, M., Ibragimov, R. & Walden, J. (2015): "Heavy-Tailed Distributions and Robustness in Economics and Finance," *Lecture Notes in Statistics* 214, Springer International Publishing, Switzerland.
https://doi.org/10.1007/978-3-319-16877-7

Jensen, H. (2002): "Targeting Nominal Income Growth or Inflation?," *American Economic Review* 92, 928–956.
https://doi.org/10.1257/00028280260344533

Jensen, J.L.W.V. (1906): "Sur les Fonctions Convexes et les Inégalités Entre les Valeurs Moyennes," *Acta Mathematica* 30, 175–193.
https://doi.org/10.1007/BF02418571

Judd, K.L. (1998): "Numerical Methods in Economics," *MIT Press*, Cambridge, MA.
https://books.google.de/books?id=9Wxk_z9HskAC

Jurado, K., Ludvigon, S.C. & Ng, S. (2015): "Measuring Uncertainty," *American Economic Review* 105, 1177–1216.
https://doi.org/10.1257/aer.20131193

Keeping, E.S. (1962): "Introduction to Statistical Inference," *D. Van Nostrand Co.*, Princeton, NJ.
https://books.google.de/books?id=-G-094bPVIIC

Keynes, J.M. (1936): "The General Theory of Employment, Interest, and Money," 2018 Edition, *Palgrave Macmillan*, Cham, Switzerland.
https://doi.org/10.1007/978-3-319-70344-2

Kim, J., Kim, S., Schaumburg, E. & Sims, C.A. (2008): "Calculating and Using Second-Order Accurate Solutions of Discrete Time Dynamic Equilibrium Models," *Journal of Economic Dynamics & Control* 32, 3397-3414.
https://doi.org/10.1016/j.jedc.2008.02.003

Kydland, F.E. & Prescott, E.C. (1982): "Time to Build and Aggregate Fluctuations," *Econometrica* 50, 1345–1370.
https://doi.org/10.2307/1913386

Laubach, T. & Williams, J.C. (2003): "Measuring the Natural Rate of Interest," *The Review of Economics and Statistics* 85, 1063–1070.
https://jstor.org/stable/3211826

Lettau, M. & Ludvigson, S.C. (2009): "Euler Equation Errors," *Review of Economics Dynamics* 12, 255–283.
https://doi.org/10.1016/j.red.2008.11.004

Lindé, J. (2018): "DSGE Models: Still Useful in Policy Analysis?," *Oxford Review of Economic Policy* 34, 269–286.
https://doi.org/10.1093/oxrep/grx058

Ljungqvist, L. & Sargent, T.J. (2012): "Recursive Macroeconomic Theory," *MIT Press*, Cambridge, MA.
https://jstor.org/stable/j.ctt5vjq05

Lovell, M.C. (1986): "Tests of the Rational Expectations Hypothesis," *American Economic Review* 76, 110–124.
https://jstor.org/stable/1804130

Lucas, R.E. (1976): "Econometric Policy Evaluation: A Critique," *Carnegie-Rochester Conference Series on Public Policy* 1, 19–46.
https://doi.org/10.1016/S0167-2231(76)80003-6

Ludvigson, S.C. & Paxson, C.H. (2001): "Approximation Bias in Linearized Euler Equations," *Review of Economics and Statistics* 83, 242–256.
https://doi.org/10.1162/00346530151143789

McCallum, B.T. & Nelson, E. (2004): "Timeless Perspective vs. Discretionary Monetary Policy in Forward-Looking Models," *Federal Reserve Bank of St. Louis Review* 86, 43–56.
https://doi.org/10.20955/r.86.43-56

Mcgill, R., Tukey, J.W. & Larsen, W.A. (1978): "Variations of Box Plots," *The American Statistician* 32:1, 12–16.
https://doi.org/10.1080/00031305.1978.10479236

Merton, R.C. (1973): "Theory of Rational Option Pricing," *The Bell Journal of Economics and Management Science* 4, 141–183.
https://doi.org/10.2307/3003143

Meyer, D.J. & Meyer, J. (2005): "Relative Risk Aversion: What Do We Know?," *The Journal of Risk and Uncertainty* 31, 243–262.
https://doi.org/10.1007/s11166-005-5102-x

Mitrinović, D.S., Pečarić, J.E. & Fink, A.M. (1993): "Classical and New Inequalities in Analysis," *Kluwer Academic Publishers*, Dordrecht.
https://doi.org/10.1007/978-94-017-1043-5

Morin, R.A. & Suarez, A.F. (1983): "Risk Aversion Revisited," *The Journal of Finance* 38, 1201–1216.
https://doi.org/10.1111/j.1540-6261.1983.tb02291.x

Newey, W.K. & West K.D. (1987): "A Simple, Positive Semi-Definite, Heteroskedasticity and Autocorrelation Consistent Covariance Matrix," *Econometrica* 55, 703–708.
https://doi.org/10.2307/1913610

Nobay, A.R. & Peel, D.A. (2003): "Optimal Discretionary Monetary Policy in a Model with Asymmetric Central Bank Preferences," *The Economic Journal* 113, 657–665.
https://doi.org/10.1111/1468-0297.t01-1-00149

Pratt, J.W. (1964): "Risk Aversion in the Small and in the Large," *Econometrica* 32, 122–136.
https://doi.org/10.2307/1913738

Razali, N.M. & Wah, Y.B. (2011): "Power Comparisons of Shapiro-Wilk, Kolmogorov-Smirnov, Lilliefors and Anderson-Darling Tests," *Journal of Statistical Modeling and Analytics* 2, 21–33.
https://researchgate.net/publication/267205556

Rich, R. & Tracy, J. (2010): "The Relationship among Expected Inflation, Disagreement, and Uncertainty: Evidence from Matched Point and Density Forecasts," *The Review of Economics and Statistics* 92, 200–207.
https://doi.org/10.1162/rest.2009.11167

Roberts, J.M. (1995): "New Keynesian Economics and the Phillips Curve," *Journal of Money, Credit and Banking* 27, 975–984.
https://doi.org/10.2307/2077783

Rossi, B. & Sekhposyan, T. (2015): "Macroeconomic Uncertainty Indices Based on Nowcast and Forecast Error Distributions," *American Economic Review* 105, 650–655.
https://doi.org/10.1257/aer.p20151124

Rossi, B. & Sekhposyan, T. (2017): "Macroeconomic Uncertainty Indices for the Euro Area and its Individual Member Countries," *Empirical Economics* 53, 41–62.
https://doi.org/10.1007/s00181-017-1248-z

Rotemberg, J.J. & Woodford, M. (1997): "An Optimization-Based Econometric Framework for the Evaluation of Monetary Policy," *NBER Macroeconomics Annual* 12, 297–361.
https://doi.org/10.1086/654340

Rotemberg, J.J. & Woodford, M. (1999): "Interest Rules in an Estimated Sticky Price Model," in J.B. Taylor (Editor), Monetary Policy Rules, 57–119, *University of Chicago Press*, Chicago.
https://nber.org/chapters/c7414

Samuelson, P.A. (1965): "Rational Theory of Warranty Pricing," *Industrial Management Review* 6, 13–31.
https://doi.org/10.1007/978-3-319-22237-0_11

Sargent, T.J. (1987): "Dynamic Macroeconomic Theory," *Harvard University Press*, Cambridge, MA.
https://books.google.de/books?id=nVuyXF8ibeIC

Sbordone, A.M., Tambalotti, A., Rao, K. & Walsh, K.J. (2010): "Policy Analysis Using DSGE Models: An Introduction," *Economic Policy Review* 16, 23–43.
https://doi.org/10.2139/ssrn.1692896

Schaling, E. (2004): "The Nonlinear Phillips Curve and Inflation Forecast Targeting: Symmetric Versus Asymmetric Monetary Policy Rules," *Journal of Money, Credit and Banking* 36, 361–386.
https://jstor.org/stable/3838978

Schmitt-Grohé, S. & Uribe, M. (2004): "Solving Dynamic General Equilibrium Models Using a Second-Order Approximation to the Policy Function," *Journal of Economic Dynamics & Control* 28, 755–775.
https://doi.org/10.1016/S0165-1889(03)00043-5

Schorfheide, F. (2013): "Estimation and Evaluation of DSGE Models: Progress and Challenges," in D. Acemoglu, M. Arellano & E. Dekel (Editors), Advances in Economics and Econometrics, 184–230, *Cambridge University Press*, Cambridge, UK.
https://doi.org/10.1017/CBO9781139060035.006

Schumpeter, J.A. (1954): "History of Economic Analysis," Edited by E.B. Schumpeter, *Oxford University Press*, New York.
https://books.google.de/books/?id=pTylUAXE-toC

Shapiro, S.S. & Wilk, M.B. (1965): "An Analysis of Variance Test for Normality (Complete Samples)," *Biometrika* 52, 591–611.
https://doi.org/10.2307/2333709

Sims, E. (2011): "Notes on Medium Scale DSGE Models," *Graduate Macro Theory II*, University of Notre Dame.
https://nd.edu/~esims1/medium_scale_dsge.pdf

Smets, F. & Wouters, R. (2003): "An Estimated Dynamic Stochastic General Equilibrium Model of the Euro Area," *Journal of the European Economic Association* 1, 1123–1175.
https://doi.org/10.1162/154247603770383415

Smets, F. & Wouters, R. (2007): "Shocks and Frictions in US Business Cycles: A Bayesian DSGE Approach," *American Economic Review* 97, 586–606.
https://doi.org/10.1257/aer.97.3.586

Straub, L. & Ulbricht, R. (2019): "Endogenous Second Moments: A Unified Approach to Fluctuations in Risk, Dispersion, and Uncertainty," *Journal of Economic Theory* 183, 625–660.
https://doi.org/10.1016/j.jet.2019.07.007

Svensson, L.E.O. & Woodford, M. (2005): "Implementing Optimal Policy through Inflation-Forecast Targeting," in B.S. Bernanke & M. Woodford (Editors), The Inflation-Targeting Debate, 19–83, *University of Chicago Press*, Chicago.
https://nber.org/chapters/c9556

Taylor, J.B. (1999): "Staggered Price and Wage Setting in Macroeconomics," in J.B. Taylor & M. Woodford (Editors), Handbook of Macroeconomics, 1009–1050, *Elsevier*, New York.
https://doi.org/10.1016/S1574-0048(99)10023-5

Walsh, C.E. (2003): "Speed Limit Policies: The Output Gap and Optimal Monetary Policy," *American Economic Review* 93, 265–278.
https://doi.org/10.1257/000282803321455278

Walsh, C.E. (2010): "Monetary Policy and Theory," 3rd Edition, *MIT Press*, Cambridge, MA.
https://books.google.de/books?id=Zov6AQAAQBAJ

Woodford, M. (2003a): "Optimal Interest-Rate Smoothing," *Review of Economic Studies* 70, 861–886.
https://doi.org/10.1111/1467-937X.00270

Woodford, M. (2003b): "Interest and Prices," *Princeton University Press*, Princeton, NJ.
https://books.google.de/books?id=8AlrisNOOpYC

Wu, J.C. & Xia, F.D. (2016): "Measuring the Macroeconomic Impact of Monetary Policy at the Zero Lower Bound," *Journal of Money, Credit and Banking* 48, 253–291. https://doi.org/10.1111/jmcb.12300

Yun, T. (1996): "Nominal Price Rigidity, Money Supply Endogeneity, and Business Cycles," *Journal of Monetary Economics* 37, 345–370. https://doi.org/10.1016/S0304-3932(96)90040-9

Zeldes, S.P. (1989): "Optimal Consumption with Stochastic Income: Deviations from Certainty Equivalence," *The Quarterly Journal of Economics* 104, 275–298. https://doi.org/10.2307/2937848

List of Figures

List of Tables

Lists of Symbols and Acronyms

Symbol	Explanation
α	First parameter of distribution (log-normal and inverted beta)
β	Second parameter of distribution (log-normal and inverted beta)
β_i	Parameters ("bias" equation, $i \in \{0,1,2\}$)
$\gamma_{(\tau)}$	Curvature / reciprocal value of the EIS / risk aversion ($\tau \in \{1,2\}$)
δ	Weighting on output gap in loss function
Δ_i	Residuals of Jensen's inequality / growth rate differential ($i \in \{c,\pi,x\}$)
ε	Elasticity of substitution
$\varepsilon_t^{(i)}$	Error terms (Euler condition and "bias" equation, $i \in \{J, bias\}$)
ϵ_t	Error term of demand shock
ζ_t	Error term of cost shock
η	Exponent in examples
θ	Auxiliary parameter
κ	Slope of NKPC
κ_i	(Aggregated) GDP weights ($i \in \{1,\ldots,5\}$)
λ	Lagrange multiplier
λ_i	GDP weights on individual level ($i \in \{1,\ldots,5\}$)
$\mu_{(EA)}$	Mean
ν	Demand shock persistence
ξ	Cost shock persistence
π_t	Inflation
π^*	Inflation target
$\varrho_{(t)}$	Discount factor / time preference
ρ	Correlation
$\sigma_{(i)}$ / $\sigma_{(i)}^2$	Standard deviation / variance
τ	Firm index; time index (alternative)
υ_s	Lagrange multipliers
φ	Variable of integration
ϕ	Price stickiness
χ_i	Summarizing parameters ($i \in \{\psi, y, \pi, \xi, e, \sigma\}$)
ψ	Parameter in cost function
ω_s	Lagrange multipliers

Table 1: Greek Symbols $\alpha - \omega$. Note: Similar meanings are separated by "/".

Symbol	Explanation
a	Real number in proof
A	Auxiliary parameter
b	Real number in proof; index ("biased")
B	Auxiliary parameter
B_t	Bonds
c	Constants in cost function (c_{fix}, c_{var})
c_t	Consumption growth
C_0	Constant of integration
$C_{(t)}$	Consumption
e_t	Cost shock
$f(.)$	Non-linear function / marginal utility
$F(.)$	CRRA utility function
$g(.)$	Model transformation
$gr_{(i)}$	(Weighted) growth rate
i	Index variable
i_t	Nominal interest rate
j	Index variable
k	Cost parameter in Calvo pricing
$K(.)$	Cost function
m	Centered mean $(1 + \mu)$
M	Index of months
n	Number of variables / model size
N	Number of forecasters / number of draws / number of future states
N_i	Number of forecasters in a specific country ($i \in \{1, \ldots, 5\}$)
$p_{(t)}$	Log-linearized price around the steady state
P_i	Price / price level
q_t	Calvo price
r	Auxiliary parameter; index ("ratio")
$r_{(t)}$	Long-run real interest rate
R	Range (stock market uncertainty measure)
s	Index variable
t	Time index; argument of moment generating function
$T_i(.)$	i^{th}-order Taylor expansion

Table 2: Latin Symbols a – T. Note: Similar meanings are separated by "/".

Symbol	Explanation
u_t	Demand shock
$U(.)$	Utility function
$V(.)$	Value function (Bellman equation)
w	Index (“weighted”)
W_t	Wage
$x_{(i)}$	Variable or parameter in examples; growth rate forecasts
$\tilde{x}$	Risk premium
X	Random variable (log-normally distributed)
X_{t-1}	Data matrix (“bias” equation)
y	Argument of $g(.)$
$y_{(\tau)}$	Log-linearized output growth rate around the steady state
$\widehat{y_{(t)}}$	Growth rate of output gap around the steady state
$\widetilde{y_{(t)}}$	Output growth rate
Y	Random variable (log-normally distributed)
$Y_{(i)}$	Output
$\mathcal{Y}_{(i)}$	Data for weighting scheme
z	Growth rate of $\mathcal{Z}$ in log-linearization example
$\widehat{z}$	Growth rate around the steady state
z_t	Random variable / transformed CF data (tested for normality)
Z	Random variable (normally distributed)
$\mathcal{Z}_{(t)}$	Variable in Examples

Table 3: Latin Symbols $u - Z$.

Acronym	Explanation
A-D	Anderson-Darling (Test)
AD	Aggregated Demand
AIC	Akaike Information Criterion
AM	Arithmetic Mean
AR	Autoregressive
AS	Aggregated Supply
BIC	Bayesian Information Criterion
BL	Baseline
bp	Basis point(s)
CARA	Constant Absolute Risk Aversion
CES	Constant Elasticity of Substitution
CF	Consensus Forecasts
CISS	Composite Indicator of Systemic Stress
CLIFS	Country-Level Index of Financial Stress
CRRA	Constant Relative Risk Aversion
DSGE	Dynamic Stochastic General Equilibrium
EA	Euro Area
ECB	European Central Bank
EFFR	Effective Federal Funds Rate
EIS	Elasticity of Intertemporal Substitution
EONIA	Euro Overnight Index Average
EPU	Economic Policy Uncertainty
FSI	Financial Stability Indicator
FTSE	Financial Times Stock Exchange (Index)
G-7	Group of Seven
GDP	Gross Domestic Product
GM	Geometric Mean
GMM	Generalized Method of Moments
IMF	International Monetary Fund
IS	Investment/Saving
J-B	Jarque-Bera (Test)

Table 4: Acronyms A – J.

Acronym	Explanation
LF	Lilliefors (Test)
LHS	Left-hand side
LOTUS	Law of the Unconscious Statistician
MATLAB	Matrix Laboratory
MC	Monte Carlo (Simulation)
ML	Maximum Likelihood
MPU	Monetary Policy Uncertainty
MSCI	Morgan Stanley Capital International
NKM	New Keynesian Model
NKPC	New Keynesian Phillips Curve
pp	Percentage point(s)
Qi	Quarter, $i \in \{1,2,3,4\}$
RBC	Real Business Cycle
RHS	Right-hand side
RRA	Relative Risk Aversion
RV	Random Variable
S-W	Shapiro-Wilk (Test)
S&P	Standard & Poor's
SONIA	Sterling Overnight Index Average
ss	Steady state
UK	United Kingdom
US	United States
VFTSE	Volatility Financial Times Stock Exchange (Index)
VIX	Volatility Index
VSTOXX	Volatility (Euro) Stoxx (Index)
WTI	West Texas Intermediate (Oil price)
WUI	World Uncertainty Index

Table 5: Acronyms L – W.

Summary (Deutsche Zusammenfassung)

Die Dissertation "Uncertainty in Macroeconomic Models" ist kumulativ verfasst, bestehend aus drei einzelnen Fachartikeln. Der zentrale Begriff *Uncertainty* wird im Folgenden mit *Ungewissheit* übersetzt, da Unsicherheit im ökonomischen Kontext bereits in der mikroökonomischen Entscheidungstheorie eine Rolle spielt.[1]

Obwohl die Dissertationsschrift aus in sich abgeschlossenen Kapiteln zusammengesetzt ist, bauen diese thematisch aufeinander auf und werden zudem in der Einleitung (*Motivation*) miteinander verwoben. Das Hauptmotiv, die Approximation von Modellgleichungen, zieht sich als roter Faden durch die gesamte Arbeit. Es wird diskutiert, inwiefern sich Approximationsmethoden erweitern lassen, aber auch wie sich deren Folgen auswerten lassen. Der Diskussion folgt zum einen die theoretische Umsetzung mithilfe formaler Herleitungen und Simulationen (1. und 3. Kapitel), zum anderen die praktische Anwendung mithilfe von Regressionsanalysen (2. Kapitel). Die empirische Grundlage bilden Prognosedaten der *Consensus Forecasts* (*CF*) und eine Vielzahl von Ungewissheitsmaßen.

1. Quadratische Approximierung

Der erste Artikel "Calibrating the Equilibrium Condition of a New Keynesian Model with Uncertainty" behandelt die Kalibrierung der Gleichgewichtsbedingung in einem um Ungewissheit erweiterten Neu-Keynesianischen Modell (*NKM*). Das grundlegende Modell, bestehend aus drei Gleichungen, wird zunächst detailliert hergeleitet und um Ungewissheit erweitert. Es wird ausführlich auf die essenziellen Teile eines dynamisch-stochastischen allgemeinen Gleichgewichtsmodells (*DSGE*) eingegangen, da es sich hier um den Überbegriff eines NKMs handelt. Dieser Modellklasse liegt ein mikroökonomisches Fundament zugrunde, da die Gleichungen jeweils per Optimierungskalkül hergeleitet werden. Dies berücksichtigt implizit die Anpassung der Wirtschaftssubjekte an eine Veränderung der makroökonomischen Variablen, z.B. durch Wirtschaftspolitik, letztlich um der Lucas-Kritik Genüge zu leisten.

Die nächsten Abschnitte fassen die Herleitung zusammen und betrachten nacheinander Unternehmen, private Haushalte sowie die Zentralbank, welche zusammen einen vollständigen Wirtschaftskreislauf bilden.

[1] Bei der Entscheidung unter Unsicherheit spielen auch psychologische Faktoren eine Rolle. Inwiefern dies auch auf die Makroökonomie übertragen werden kann, ist nicht Gegenstand dieser Arbeit. Um die Unterscheidung zu gewährleisten, wird dementsprechend der Begriff Ungewissheit verwendet.

Die erste Gleichung stellt eine Verbindung zwischen Preisentwicklung und Wirtschaftswachstum her. Im Zusammenspiel von monopolistischem Angebot und zeitlich verzögerter Preisanpassung seitens der Unternehmen wird die Neu-Keynesianische Phillipskurve (*NKPC*) hergeleitet. Diese beiden Marktfriktionen bilden den Kern des NKMs. Die NKPC folgt im Allgemeinen der Standardherleitung und bildet den linearen Zusammenhang zwischen Produktionslücke ($\widehat{y_t}$) und Inflation (π_t) zum Zeitpunkt t ab:[2]

$$\pi_t = \varrho \mathrm{E}_t \pi_{t+1} + \kappa \widehat{y_t}. \tag{1}$$

Mithilfe des Diskontfaktors (ϱ) wird die Inflationserwartung gewichtet. Der positive Sammelparameter κ setzt sich zusammen aus ϱ, der Substitutionselastizität bzgl. der Konsumgüter, der langfristigen Kostenelastizität der Unternehmen und einem Parameter bzgl. *Calvo Pricing*, dem Anteil der Unternehmen, die ihre Preise nur verzögert anpassen können. Ausgehend von der Annahme, dass Produktionswachstum und Arbeitslosenquote negativ miteinander korreliert sind, bildet Gl.(1) mit einem $\kappa > 0$ den Zusammenhang analog zur klassischen Phillipskurve ab.

Die Herleitung der zweiten Gleichung, der IS-Kurve, stellt die eigentliche Erweiterung des Modells dar. Ausgehend von einer intertemporalen Optimierung der Haushalte unter Berücksichtigung einer Budgetbeschränkung ergibt sich die Euler-Gleichung hinsichtlich des Konsums. Eine ausführlich beschriebene und mit Graphiken verdeutlichte Taylor-Approximation zweiten Grades sorgt dafür, dass die Komponente der Ungewissheit in der Modellgleichung erhalten bleibt. Konkret findet sich die bedingte Varianz der zukünftigen Produktionslücke und der Inflation additiv in der nun quadratischen IS-Kurve wieder:[3]

$$\widehat{y_t} = \mathrm{E}_t \widehat{y_{t+1}} - \frac{1}{\gamma}(i_t - r - \mathrm{E}_t \pi_{t+1}) - \frac{1}{2}\mathrm{Var}_t \widehat{y_{t+1}} - \frac{1}{2\gamma}\mathrm{Var}_t \pi_{t+1} + \ldots \tag{2}$$

Die Produktionslücke zum heutigen Zeitpunkt entspricht der erwarteten Version, korrigiert um die gewichtete Differenz der Fischer-Gleichung ($i_t \approx r + \mathrm{E}_t \pi_{t+1}$) und den Einfluss der Ungewissheit. Der Parameter γ, welcher eine Schlüsselrolle in der gesamten Dissertation spielt, bezeichnet den Kehrwert der intertemporalen Substitutionselastizität und steht in enger Verbindung mit der Krümmung der aggregierten Nutzenfunktion. Die beiden Varianzen in Gl.(2) stellen somit einen zusätzlichen negativen Einfluss auf $\widehat{y_t}$ dar.

[2]Die Variable $\widehat{y_t}$ ist definiert als die prozentuale Abweichung vom effizienten Produktionsniveau, welches zur Markträumung bzgl. Angebot und Nachfrage führt. Insbesondere drückt $\widehat{y_t} > 0$ einen Nachfrageüberschuss aus.

[3]Zur anschaulichen Zwecken weicht die Formel geringfügig von der Darstellung im eigentlichen Artikel ab.

Die dritte Gleichung schließt das Modell und folgt aus einem simplen Optimierungsverhalten der Zentralbank, welches zu einem angestrebten Verhältnis von $\widehat{y_t}$ und π_t führt:

$$\delta\widehat{y_t} = -\kappa\pi_t. \tag{3}$$

Die Zielvorgabe richtet sich hier nach Inflation und Produktion, während sie den bereits erwähnten Sammelparameter κ und den Gewichtungsfaktor δ beherbergt. Als einen Spezialfall von Gl.(3) sei die Gleichheit $\widehat{y_t} = \pi_t = 0$ hervorzuheben, welche verdeutlicht, dass eine Stabilisierung der Wirtschaft im Vordergrund steht.[4]

Das Zusammenfügen der drei Gleichungen ergibt eine Taylor-Regel (erweitert um Ungewissheit), welche, nach dem Zinssatz aufgelöst, der Zentralbank eine konkrete Handlungsanweisung geben kann. Ziel ist es jedoch, eine gesamtwirtschaftliche Gleichgewichtsbedingung abzuleiten. Aus diesem Grund werden NKPC und IS-Kurve zunächst um ein stochastisches Element erweitert, und zwar einem Kosten- bzw. einem Nachfrageschock (e_t bzw. u_t). Um eine gewisse Persistenz abzubilden, werden beide Schocks als AR(1)-Prozess modelliert.[5] Durch geeignetes Umformen können nun die makroökonomischen Variablen ($\widehat{y_t}$ und π_t) und deren bedingte Momente im statischen, langfristigen Gleichgewicht durch Parameter und Schocks dargestellt werden. Es ergibt sich schließlich eine Gleichung, welche den nominalen Zinssatz beschreibt:

$$i_t = r + \chi_\xi e_t - \frac{1}{2}\left(\chi_e e_t^2 + \chi_\gamma \sigma_e^2\right) + \gamma u_t. \tag{4}$$

Realer (r) und nominaler (i_t) Zinssatz werden hier in eine direkte Beziehung gesetzt, korrigiert um den Einfluss der Schocks. Wiederum bilden die χ_i positive Sammelparameter, bestehend aus den bereits eingeführten Größen. Der Einfluss der Ungewissheit findet sich in den quadratischen Termen wieder, dem quadrierten Kostenschock und deren Varianz σ_e^2. Eine Zentralbank, welche den Nominalzins unmittelbar setzen könnte, würde Kosten- und Nachfrageschocks zunächst mit höheren Zinsen beantworten, um den Inflationsdruck auszugleichen. Zusätzlich kommt allerdings ein negativer Effekt hinzu, welcher aus e_t^2 und der unbedingten Varianz besteht. Eine Version von Gl.(4) mit dem unbedingten Erwartungswert verdeutlicht diese Verbindung:[6]

$$\mathrm{E}[i_t] = r - \frac{\chi_e + \chi_\gamma}{2}\sigma_e^2. \tag{5}$$

Somit liegt $\mathrm{E}[i_t]$ im Gleichgewicht (geringfügig) unterhalb von r, wobei $\mathrm{E}_t\pi_{t+1} = 0$.

[4] Zudem wird der Fall mit einem Inflationsziel größer Null diskutiert, mit dem Ergebnis, dass sich die grundlegende Aussage nicht ändert.

[5] Der stochastische Anteil ist standardmäßig *i.i.d.* $\mathcal{N}(0, \sigma^2)$.

[6] Mit der binomischen Formel gilt: $\mathrm{Var}[e_t] = \mathrm{E}[e_t^2] - \mathrm{E}[e_t]^2$.

Die Herleitung der Gleichgewichtsbedingung Gl.(4) dient im Weiteren als Ausgangspunkt für einen Vergleich mit der Modellversion ohne Ungewissheit. Das Ziel ist es, die Differenz für ein breites Spektrum an Parameterkonstellationen zu quantifizieren. Die Kalibrierung erfolgt mithilfe einer umfassenden Literaturrecherche, bestehend aus jeweils mehreren Quellen pro Parameter inklusive einer Meta-Analyse bzgl. γ. Hieraus formt sich ein Baseline-Szenario und mögliche Bandbreiten an realistischen Werten.[7] Der Kostenschock nimmt eine Sonderstellung ein, da für das Hauptergebnis sowohl die Stärke $[-0.005, 0.025]$ als auch die Persistenz $[0.6, 0.8]$ variabel gehalten werden, um seinen Einfluss als Ebene (Abbildung 1) zu visualisieren.[8] In Bereichen geringer Schockstärke bzw. -persistenz macht die Differenz nur ungefähr 10 Basispunkte aus. Bei einer gleichzeitigen Annäherung an die Maximalwerte werden Unterschiede von über 50 Basispunkten erreicht.

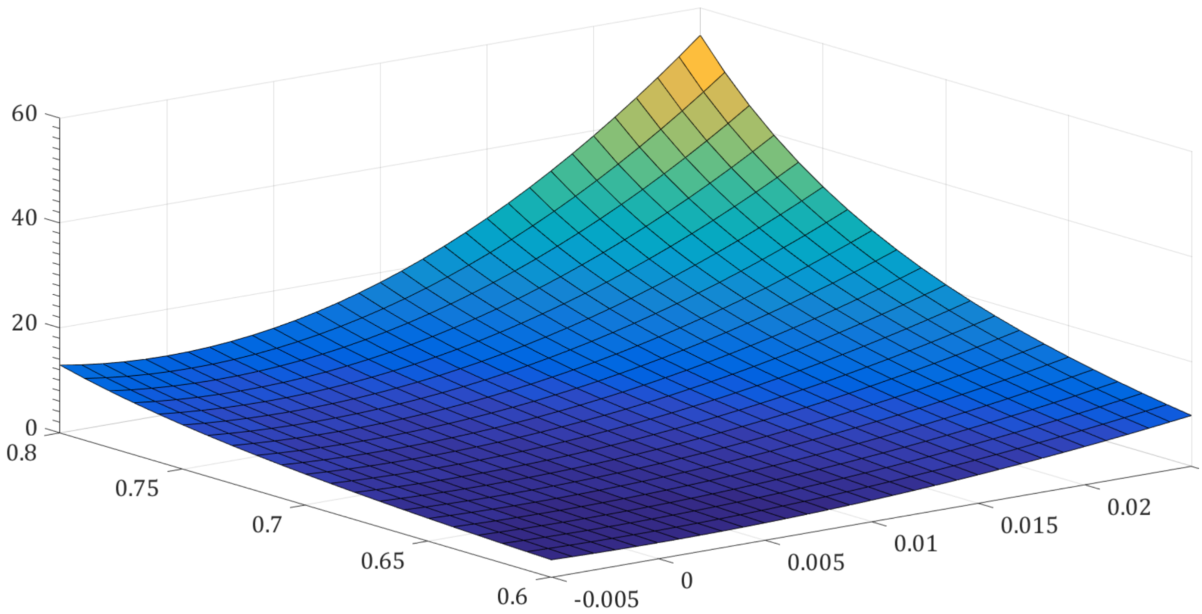

Abbildung 1: Differenz der Gleichgewichtsbedingung zwischen beiden Modellversionen (mit und ohne Ungewissheit). Horizontale Achsen: Persistenz und Kostenschock. Vertikale Achse: Differenz des Zinssatzes i_t in Basispunkten.

Neben weiteren numerischen Untersuchungen auf statischer Basis, zeigen Impuls-Antwort-Analysen den Effekt der Ungewissheit über die Zeit. Dabei werden nach einem Kostenschock ($e_t = 0.01$) sowohl die Auswirkungen auf die (erwarteten) Makrovariablen als auch die Modelldifferenz bei extremen Parametereinstellungen, z.B. eine flache und eine steile NKPC, verglichen. Letzteres Beispiel zeigt, dass eine steilere NKPC die Auswirkung von Ungewissheit verringert.

[7] Das Baseline-Szenario besteht aus: $\gamma = 1$, $\delta = 0.25$, $\kappa = 0.04$, $\rho = 0.99$, $\sigma_e^2 = 10^{-4}$. Bspw. entspricht demnach der negative Term in Gl.(5), der absolute Anteil der Ungewissheit, ungefähr 10 Basispunkten.

[8] Es zeigt sich, dass der Nachfrageschock in der Differenz keine Rolle spielt.

Zusammenfassend lässt sich sagen, dass Zinssätze unter Berücksichtigung der Ungewissheit im Allgemeinen niedriger sind. Obwohl das Ausmaß entscheidend vom Grad der Persistenz abhängt, hat dies numerisch, bei durchschnittlicher Parameterkonstellation, eine Auswirkung von ungefähr 25 Basispunkten. Die theoretische Analyse bestätigt zudem die Ergebnisse der empirischen Literatur.[9] Schließlich bleibt festzuhalten, dass, trotz langwieriger Herleitung, die Intuition hinter dem Ergebnis eine einfache ist. Die konkave Krümmung der aggregierten Nutzenfunktion, deren Grad durch γ bestimmt wird, sorgt für risikoaverse Haushalte. In Zeiten großer Ungewissheit braucht es einen Ausgleich für den resultierenden Disnutzen. In diesem simplen Neu-Keynesianischen Modell nimmt der Nominalzins diese Rolle ein.

2. Interne und Externe Ungewissheit

Der zweite Artikel "Non-Linearities and the Euler Equation: Does Uncertainty have an Effect on the Approximation Quality?" betrachtet eine nicht-lineare Euler-Gleichung und untersucht den Effekt von Ungewissheit auf die Approximationsgüte. Anknüpfend an den ersten Teil der Dissertation, wird die Herleitung der Euler-Gleichung nochmals im Detail aufgegriffen. Der grundlegende Unterschied ist jedoch der vollständige Verzicht auf Taylor-Approximationen.[10] Es wird gezeigt, dass selbst die nichtlineare Version die Intention der Herleitung nicht in Gänze widerspiegeln muss. Dieser Unterschied wird berechnet und im Anschluss als abhängige Variable per Regressionsanalyse untersucht. Dabei dienen interne Ungewissheit (die Standardabweichung der Variablen) und eine Reihe von externen Ungewissheitsmaßen als Regressoren.

Die Herleitung mündet zunächst in der unverzerrten Version der Euler-Gleichung hinsichtlich des Konsums, welche im darauffolgenden Schritt approximiert wird:

$$\frac{1+r_t}{1+i_t} = \mathrm{E}_t\left[(1+c_{t+1})^{-\gamma} \cdot (1+\pi_{t+1})^{-1}\right] \approx (1+\mathrm{E}_t c_{t+1})^{-\gamma} \cdot (1+\mathrm{E}_t \pi_{t+1})^{-1}. \tag{6}$$

Das Verhältnis der um Eins zentrierten (realen und nominalen) Zinssätze entspricht einem bedingten Erwartungswert über transformierte Wachstumsraten. Darin findet sich der marginale Nutzen abhängig vom zukünftigen Konsumwachstum (c_{t+1}), multipliziert mit dem Kehrwert der um Eins zentrierten zukünftigen Inflation.[11] Durch das Verschieben des Erwartungswertes direkt vor die Wachstumsrate, um beispielsweise

[9] Siehe auch Bauer and Neuenkirch (2017).

[10] Die Gleichung wird somit nicht als Polynom dargestellt, sondern in ihrer ursprünglichen nichtlinearen Form belassen.

[11] Es wurde die flexible isoelastische Nutzenfunktion (CRRA) genutzt. Außerdem wurden Konsum und Preisniveau aus den Perioden t und $t+1$ jeweils in Wachstumsraten umgeformt.

subsequent geeignete Prognosedaten ($E_t c_{t+1}$ und $E_t \pi_{t+1}$) zu verwenden, wird die Gleichung auf zwei Arten verändert. Zunächst wird die Kovarianz der transformierten Zufallsvariablen, c_{t+1} und π_{t+1}, übergangen.[12] Des Weiteren wird durch das Vertauschen von Erwartungswert und nicht-linearer Transformation Jensen's Ungleichung ignoriert. In makroökonomischen Modellen kommt dies vor allem vor, wenn in der dynamischen Betrachtungsweise von einer Periode zur nächsten der bedingte Erwartungswert nicht-lineare Variablentransformationen überspannt, wie z.B. $E_t[U(C_{t+1})]$. Gemeint ist hier der erwartete Nutzen zum Zeitpunkt t abhängig vom zukünftigen Konsum. Anhand des zweiten Faktors im Erwartungswert in Gl.(6), welcher die Inflationsrate beinhaltet, wird die Problematik verdeutlicht: $E_t[(1+\pi_{t+1})^{-1}] \geq (1+E_t\pi_{t+1})^{-1}$. Abbildung 2 zeigt, inwiefern sich die Differenz Δ_π anhand von zwei Werten errechnen bzw. darstellen lässt.

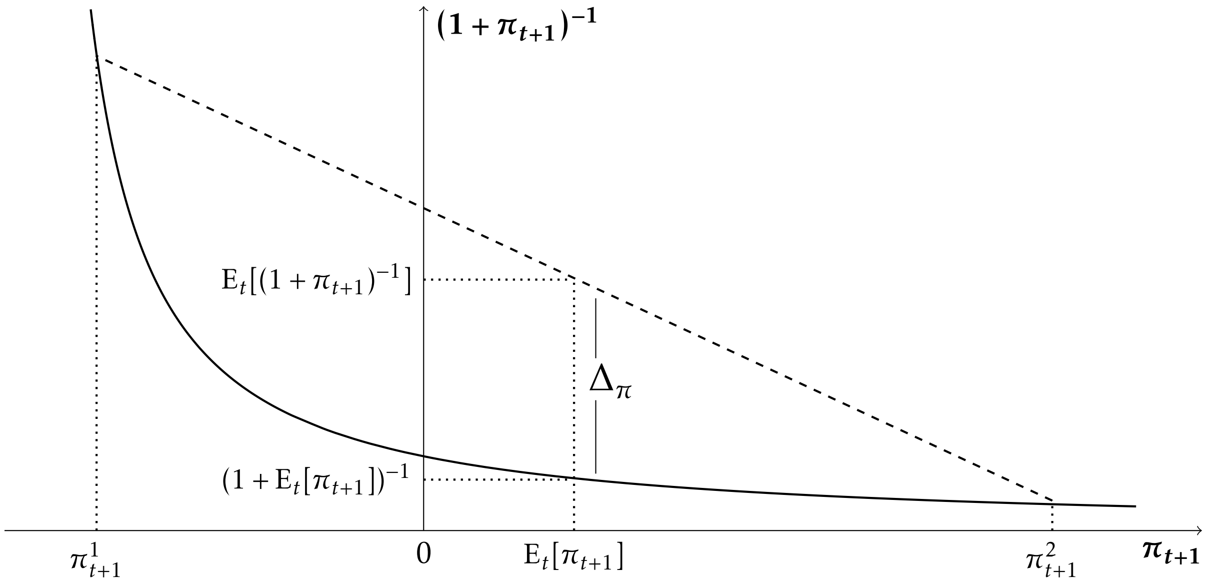

Abbildung 2: Schematische Darstellung von Jensen's Ungleichung anhand der konvexen Funktion $(1+\pi_{t+1})^{-1}$.

Durch die Beschaffenheit der monatlichen CF Daten, welche Individualprognosen für eine Reihe von Instituten, vorwiegend aus dem Finanzsektor, bereitstellt, wird versucht dieses Problem zu umgehen. Diese Querschnittsdaten dienen jeweils als Grundlage für die zukünftigen Werte c_{t+1} und π_{t+1}. Somit bleibt die funktionale Form bei der Verwendung von Daten in der theoretischen Modellgleichung vollständig erhalten. Wenn nun Daten als Proxy-Variablen für i_t, r_t, $E_t c_{t+1}$ und $E_t \pi_{t+1}$ verwendet werden, um wiederum die Gleichung zu identifizieren, ergibt sich eine weitere approximierte Form. Die Differenz dieser beiden Euler-Versionen wird untersucht, indem versucht

[12] Allerdings wird auf die (transformierte) Kovarianz kontrolliert. Die Werte werden verwendet, sind allerdings sehr klein ($\approx 10^{-6}$) und spielen im Weiteren keine Rolle.

wird, sie durch interne Ungewissheit (die Standardabweichung der Variablen) und eine Reihe von externen Ungewissheitsmaßen zu erklären.

Um die Zentrierung über eine länderspezifische Problematik hinaus zu gewährleisten, werden mit den USA, Großbritannien und der Euro-Zone parallel Daten drei großer Volkswirtschaften verwendet. In den Datensätzen sind erwartete Wachstumsraten für das aktuelle und das folgende Jahr vorhanden. Die zusätzliche Gewichtung der Prognosedaten erfolgt monatsweise, damit sich der Erwartungswert jeweils über ein Jahr erstreckt:

$$\mathrm{E}_t[growth_{t+1}|M] = \frac{13-M}{12} \cdot \mathrm{E}_{t,M}[growth_t] + \frac{M-1}{12} \cdot \mathrm{E}_{t,M}[growth_{t+1}]. \tag{7}$$

Der aktuelle Monat wird mit M bezeichnet und dient ausschließlich der Gewichtung.

Die Nominalzinsdaten für die drei Regionen setzen sich aus den kurzfristigen Zinsen auf dem Interbankenmarkt zusammen, welche zwar eine gewisse Variabilität aufweisen, allerdings maßgeblich von der Geldpolitik der Zentralbanken getrieben werden. Die Renditen von inflationsindexierten Anleihen werden jeweils als Proxy-Variable für die schwer zu messende langfristige, reale Zinsrate angenommen. Damit ist es möglich Gl.(6) auf Datenbasis zu beschreiben.

Nach der Identifizierung der Euler-Gleichung wird γ geschätzt, indem für eine Bandbreite an möglichen Werten die Residuen der Euler-Gleichung auf Normalität getestet werden. Die Nullhypothese der Tests entspricht der Normalverteilung. Dementsprechend ist es günstig, die Hypothese nicht abzulehnen, was wiederum eine schwächere Aussage impliziert. Da hohe p-Werte trotzdem ein deutlicher Indikator sind, wird jener γ-Wert, welcher das Maximum generiert, als der Wahrscheinlichste angenommen, analog zur Maximum-Likelihood-Methode.

Die nun resultierenden Approximationsfehler sind relativ klein (bis zu 10 Basispunkte), sollen jedoch mittels Ungewissheit erklärt werden. Das sind zum einen die internen Ungewissheitsmaße, bestehend aus der Standardabweichung der genutzten Variablen und der des Produktionswachstums in den CF Datensätzen.[13] Die externen Ungewissheitsmaße dagegen setzen sich zusammen aus Maßen bzgl. der Börse (z.B. Volatilitätsindex), makroökonomischer Unsicherheit (z.B. *Economic Policy Uncertainty*) oder der Finanzstabilität (z.B. *Composite Indicator of Systemic Stress*). Für alle drei Regionen werden insgesamt 25 verschiedene Zeitreihen verwendet.[14]

[13] Aufgrund eines etwaigen Simultanitätsproblems sei darauf hingewiesen, dass diese hauptsächlich zur Kontrolle der theoretischen Überlegung dienen.

[14] Alle Zeitreihen wurden zunächst auf Monatsbasis konvertiert. Im Falle von höheren Frequenzen wurden die Werte zum Ende des Monats genommen, um sich den Umfragezeiträumen der CF anzupassen. Zeitreihen mit geringerer Frequenz wurden interpoliert.

Die Regressionsergebnisse zeigen signifikante Ergebnisse für die meisten internen Ungewissheitsmaße. Diese nehmen eine vorherrschende Rolle ein und übersteigen die Erklärungskraft der externen Daten. In dieser Gruppe zeigen der Weltunsicherheitsindex und die Ölpreisvolatilität (beide für die USA), der Indikator für die Finanzstabilität der EZB (Großbritannien) und ein Unsicherheitsindex bzgl. des Bruttoinlandsprodukts (Euro-Zone) einen signifikanten, positiven Einfluss. Die letztgenannten Ergebnisse können sich jedoch auch auf die Prioritäten der befragten Institute bei der Durchführung der CF Umfragen beziehen. Letztlich zeigt sich, dass selbst in den geringfügigen Approximationfehlern noch ein gewisser Erklärungsgehalt steckt. Eine sich anschließende Frage ist, unter welchen Bedingungen diese Fehler größere Ausmaße annehmen können.

3. Das Ausmaß von Jensen's Ungleichung

Der abschließende Teil "Evaluating the Approximation Bias in Forward-Looking DSGE Models" behandelt die Evaluation des Approximationsfehlers in, um Erwartungen erweiterten, DSGE Modellen. Zunächst wird die Relevanz von DSGE Modellen erörtert, mit der Schlussfolgerung, dass diese aufgrund der großen Bekanntheit und relativ kostengünstigen Implementierung, insbesondere für kleinere bis mittelgroße Institutionen oder generell für Entwicklungsländer, interessant sein können.

Thematisch schließt sich dieser Artikel dem zweiten Teil an, erweitert den methodischen Ansatz allerdings an zwei Punkten. Erstens werden die Ergebnisse nicht durch den Einsatz von Wachstumsprognosen aus den CF Datensätzen gespeist. Viel-

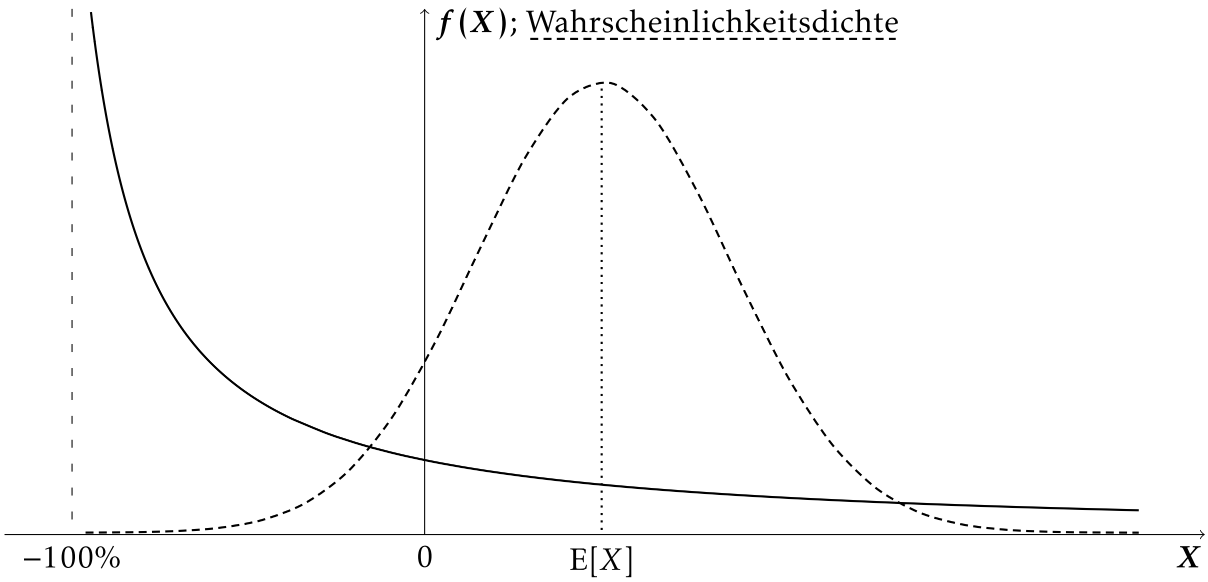

Abbildung 3: Grenznutzen und Verteilungsfunktion.

mehr dienen die Daten zur Kalibrierung von Verteilungen, die genutzt werden um allgemeinere Aussagen zu generieren. Abbildung 3 stellt diese Vorgehensweise schematisch dar. Mithilfe der Verteilungsfunktion werden Wahrscheinlichkeiten generiert um als Argument der nicht-linearen Funktion $\boldsymbol{f(X)}$ zu dienen. Zweitens wird die Definition des Approximationsfehlers zwar beibehalten, die Ausgestaltung des Modells wird jedoch genauer beschrieben. Statt der Euler-Gleichung als Ganzes wird der entscheidende Teil isoliert und leicht variiert. Dies ist mit dem Ziel verbunden, in der letztlichen Auswertung eine Fehler-Differenz zu messen, welche konkret als Differenz von Wachstumsraten interpretiert werden kann. Wie zuvor werden die Ergebnisse in Basispunkten dargestellt. Die zentrale Formel, ein illustratives Modell, hergeleitet aus Jensen's Ungleichung in Verbindung mit einer intertemporalen Verhaltensgleichung, beschreibt den Approximationsfehler

$$bias(X) = 10^4 \cdot \left((\mathrm{E}[1+X])^{\gamma} - \mathrm{E}[(1+X)^{-\gamma}]^{-1} \right), \quad (1+X) \sim \log \mathcal{N}\left(\mu, \sigma^2\right), \tag{8}$$

bestehend aus der Differenz von gewichteten Wachstumsraten und einer angenommenen Verteilung der Argumente X. Damit ist X explizit eine Zufallsvariable, welche einer Log-Normalverteilung folgt. Die verwendete Funktion folgt aus der Ableitung der isoelastischen Nutzenfunktion (CRRA) und generiert somit einen marginalen Nutzen, ausgehend von den Wachstumsprognosen.[15] In diesem Modell spielen drei Parameter eine Rolle: Die Krümmung der nicht-linearen Funktion, ausgedrückt durch γ und die beiden zentralen Momente der Verteilung, μ und σ^2.

Bezogen auf die vorhandene Literatur ist die Wahl der Verteilung naheliegend. Generell ist es allerdings nicht offensichtlich, eine passende Verteilung zu finden. Da es sich bei X um Wachstumsraten handelt, muss diese Verteilung um Null zentriert sein, eine untere Grenze aufweisen und eine gewisse Schiefe zulassen. Außerdem darf die Verschiebung der Wahrscheinlichkeitsmasse nicht zu unerwünschten Nebeneffekten führen, wie einer zu großen Standardabweichung. Hier gilt es zudem die Balance zu halten zwischen einer geringen Anzahl an Parametern und einer zu hohen Komplexität.[16]

Um das Ausmaß der Differenz in Gl.(8) zu bestimmen, wird sowohl ein mathematischer, als auch ein statistischer Ansatz gewählt, welche sich beidseitig ergänzen. In der analytischen Lösung wird zunächst der Erwartungswert der transformierten Zu-

[15] Dies ist weit verbreitet in der Fachliteratur, allerdings wird im Appendix auch mit einer Alternative, der CARA-Nutzenfunktion gearbeitet.

[16] Aufgrund der Definition auf einem halboffenen Intervall, analog zur Log-Normalverteilung, wird die invertierte Beta-Verteilung als Alternative herangezogen und im Kalibrierungskapital ausführlich diskutiert.

fallsvariablen bestimmt. Es stellt sich heraus, dass die stochastischen Einflüsse in der Gleichung vermieden werden können und ein deterministisches Ergebnis erzielt wird:

$$bias(\mu,\sigma,\gamma) = 10^4 \cdot (1+\mu)^{\gamma} \cdot \left(1 - \left(\frac{1+\mu}{\sqrt{(1+\mu)^2+\sigma^2}}\right)^{\gamma(\gamma+1)}\right). \tag{9}$$

In Gl.(9) zeigt sich, dass der Approximationsfehler in einem verketteten quadratischen bzw. exponentiellen Zusammenhang zu den bereits erwähnten Parametern steht. Beispielsweise bei dem vereinfachten Fall von $\gamma = 1$, wirkt sich die Standardabweichung näherungsweise quadratisch auf den Fehler aus, da $1+\mu \gg \sigma$ gilt:

$$bias(\mu,\sigma \mid \gamma = 1) = 10^4 \cdot \frac{(1+\mu)\cdot\sigma^2}{(1+\mu)^2+\sigma^2}. \tag{10}$$

Eine konkrete Einordnung dieser funktionalen Zusammenhänge wird im Appendix ausführlich diskutiert und berechnet. Exemplarisch sei an dieser Stelle eine Taylor-Approximierung zweiten Grades bezogen auf σ hervorgehoben, welche nach exakt definierten Kriterien eine hinreichende Genauigkeit bis $\sigma = 0.16$ bietet. Das anschließende Kapitel, welches die Kalibrierung der Momente ausgehend von Prognosedaten behandelt, zeigt, dass dieser Wert in jedem Fall eine nicht zu überschreitende Höchstgrenze darstellt.

Die verwendeten, länderspezifischen Daten aus den CF Prognosen beziehen sich zum einen auf die USA, da hier die beste Verfügbarkeit gewährleistet ist, und werden monatsweise getestet. Dies entspricht gleichzeitig der Veröffentlichungsfrequenz der CF. Damit außerdem die Situation in Schwellen- bzw. führenden Entwicklungsländern (*frontier markets*) berücksichtigt wird, werden die im gleichen Datensatz verfügbaren Staaten Ägypten, Nigeria und Südafrika hinzugenommen. Wegen der geringeren Anzahl an Prognosen erfolgt die Verwendung der Querschnitte quartalsweise. Im Vergleich zu den USA, mit einem gesamten Zeithorizont von 30 Jahren, stehen nun etwa 10 bis 20 Jahre zur Verfügung.

Um die Annahme von log-normalverteilten Zufallsvariablen zu untermauern, werden die Werte zunächst logarithmiert und schließlich auf Normalität geprüft. Dabei erfolgt die Umwandlung in erwartete Wachstumsraten, welche sich konstant über einen einjährigen Zeithorizont erstrecken, analog zu Gl.(7) im vorherigen Artikel. Es zeigt sich, dass im Schnitt bei einem Anteil von ungefähr 80% der Fälle (bzw. Querschnitte) die Nullhypothese von nicht-normalverteilten Zufallsvariablen beibehalten wird. Unserer Meinung nach untermauert dies die Annahme der Log-Normalverteilung in einer Weise, dass die Verwendung zumindest nicht abgelehnt werden kann. Zudem bewegt sich die Größe der einzelnen Querschnitte teilweise im einstelligen Bereich. Typischerweise werden jedoch ca. 20 bis 30 Prognosen pro Monat bzw. Quartal erreicht. Die kalibrierten Werte der Standardabweichung, als Maß für Ungewissheit, reichen von knapp über Null bis knapp unter 0.04. Dementsprechend wird ein Wert von $\sigma = 0.01$ für das Baseline-Szenario und eine Bandbreite von 0.002 bis 0.04 für die folgenden Simulationen bestimmt. Der Mittelwert schwankt stark in Abhängigkeit vom betrachteten Land. In den USA können die Raten leicht im negativen Bereich liegen, während in den anderen Ländern im Maximum über 20% erreicht werden können. Wir entscheiden uns hier für einen Kompromiss von $\mu = 6\%$, allerdings zeigt sich, dass die Höhe des Erwartungswertes kaum einen Einfluss auf den Approximationsfehler hat. Dies wird anhand von numerischen Beispielen ausführlich erläutert.

Die Simulationen überprüfen schließlich zum einen die analytischen Ergebnisse mithilfe der kalibrierten Werten auf ihre Variabilität und zum anderen kann das Modell leicht erweitert werden, selbst wenn sich eine analytische Lösung als nicht praktikabel erweist. Konkret werden weitere Variablen dem Modell hinzugefügt. Selbst wenn eine analytische Herleitung theoretisch möglich wäre, erfolgt lediglich die numerische Auswertung, da diese Erweiterung starke Annahmen an das Modell hinzufügt und nur einen Ausblick geben soll. Diese Annahmen beziehen sich vor allem auf die multiplikative Erweiterung, dargestellt für den Fall mit zwei Variablen:

$$bias(X, Y \mid \gamma = 1) = 10^4 \cdot \left(\mathrm{E}[1+X] \cdot \mathrm{E}[1+Y] - \mathrm{E}\left[(1+X)^{-1}(1+Y)^{-1} \right]^{-1} \right). \tag{11}$$

Der entscheidende Vorteil ist jedoch die Analyse der Approximationsfehler als Verteilung abhängig von den jeweiligen Parameterwerten. Hier zeigt sich, dass eine gewisse Schiefe vorherrscht, die intuitiv mit der unteren Grenze von Null erklärt werden kann. Abbildung 4 zeigt den Fall einer variable Standardabweichung (als Proxy-Variable für Ungewissheit), wobei für große Werte eine mittlere Differenz von ca. 15 Basispunkten erreicht wird. Die Variation von γ (0.25 – 5) führt zu ähnlichen Ergebnissen.

Zusammenfassend lässt sich festhalten, dass der Approximationsfehler linear auf die Varianz und die Korrelation mehrerer Wachstumsvariablen reagiert und exponentiell auf die Krümmung und die Größe des Modells. Trotz des unterschiedlichen funktionalen Zusammenhangs kann bei den angenommenen Maximalwerten von σ und γ jeweils mit Approximationsfehlern von ca. 25 Basispunkten gerechnet werden. Im gesamten Kontext zeigt sich jedoch, dass die verwendeten Daten eine geringere Rolle spielen als letztlich die Ausgestaltung bzw. die Größe des Modells. Der Artikel schließt mit dem Vorschlag eines Daten-Filters, welcher parameterabhängig die Nutzung von

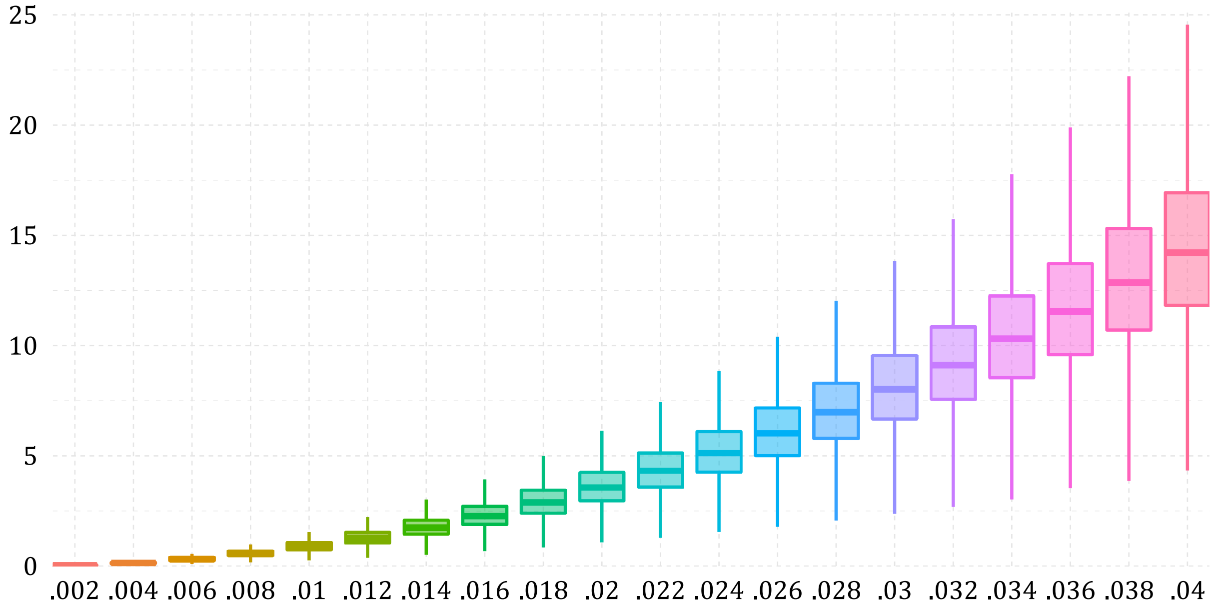

Abbildung 4: Simulation mit 100.000 Wiederholungen pro Parameterausprägung. Abszisse: Standardabweichung. Ordinate: Differenz der Wachstumsraten in Basispunkten.

Erwartungswerten korrigieren könnte, um einer Verzerrung der Ergebnisse entgegenzuwirken.

Resümierend bleibt die Frage offen, ob die exakte Interpretation von Modellgleichungen in der Makroökonomie eine Rolle spielen sollte. Falls diese Frage positiv beantwortet wird, so zeigt diese Arbeit, inwiefern der praktische Einsatz die Resultate verzerren kann.

La perfection est atteinte, non pas lorsqu'il n'y a plus rien à ajouter, mais

retirer.

— Antoine de Saint-Exupéry